Title

APPLICATION OF POWERFUL OXIDIZERS IN THE SYNTHESIS OF NEW HIGH-OXIDATION STATE ACTINIDE AND RELATED SPECIES

Author

Yeh, S.M.

Publication Date

1984-11-01

Lawrence Berkeley Laboratory
UNIVERSITY OF CALIFORNIA

Materials & Molecular Research Division

APPLICATION OF POWERFUL OXIDIZERS IN THE SYNTHESIS OF NEW HIGH-OXIDATION STATE ACTINIDE AND RELATED SPECIES

S.M. Yeh
(Ph.D. Thesis)

November 1984

Prepared for the U.S. Department of Energy under Contract DE-AC03-76SF00098

DISCLAIMER

LBL-13346

APPLICATION OF POWERFUL OXIDIZERS IN THE SYNTHESIS OF NEW HIGH-OXIDATION STATE ACTINIDE AND RELATED SPECIES

Sam Ming-jave Yeh

Materials and Molecular Research Division, Lawrence Berkeley Laboratory
and Department of Chemistry, University of California,
Berkeley, California 94720

This work was supported by the Director, Office of Energy Research, Office of Basic Energy Sciences, Chemical Sciences Division of the U. S. Department of Energy under Contract No. DE-AC03-76SF00098.

Table of Contents

APPLICATION OF POWERFUL OXIDIZERS IN THE SYNTHESIS OF NEW HIGH-OXIDATION STATE ACTINIDE AND RELATED SPECIES

Sam Ming-jave Yeh

Materials and Molecular Research Division, Lawrence Berkeley Laboratory
and Department of Chemistry, University of California,
Berkeley, California 94720

ABSTRACT

The fluorinating and oxide scavenging ability of XeF_6 have been studied by bringing XeF_6 into interaction with oxide-fluoride compounds of the third-transition-series elements (W, Re and Os) and uranium, in their highest oxidation states. $A^+MOF_5^-$ and $A^+M_2O_2F_9^-$ (A = K or Cs, M = W or U) were converted to $A^+MF_7^-$ by XeF_6, but the rhenium and osmium compounds, $K^+ReO_2F_4^-$ and $XeF_5^+OsO_3F_3^-$, resisted interaction with XeF_6. This latter resistance to exchange of oxygen for fluorine is attributed to the tightly packed ligand array in the pseudo-octahedral anions.

Strong interactions between XeF_2 or KrF_2 and the solvent have been observed for their solutions in anhydrous HF. Raman spectroscopic data have revealed three different types of fluorine environment associated with XeF_2 in the HF solution. Similar studies have established only one environment for KrF_2. Both XeF_2 and KrF_2 are seen to be effective in breaking up the polymeric $(HF)_n$ chains. Only weak interactions occur between cations and anions of $KrF^+AuF_6^-$ and $Kr_2F_3^+AuF_6^-$ in HF solution. The AuF_6^- anions, in each case, are slightly distorted

from O_h symmetry. $Kr_2F_3^+$ cations in HF solution have been shown to have the same dissymmetric V-shape which occurs in crystalline salts.

A low-temperature orthorhombic form, β-$ReF_6^+SbF_6^-$, a high-temperature rhombohedral form, α-$ReF_6^+SbF_6^-$, and a $ReF_6^+AuF_6^-$ have been prepared and characterized by Raman spectroscopic and X-ray powder diffraction data. These compounds possess only kinetic stability at ambient temperature and at ~20°C are best represented as $ReF_6^+ReF_7MF_6^-MF_5$. It is proposed that these materials involved ordered arrangements of the complexes ions (ReF_6^+ and MF_6^-) and the neutral species ReF_7 and monomeric MF_5. Thermochemical energy evaluations indicate that the ionization potential of ReF_6 is 261 kcal $mole^{-1}$ and that the fluoride-ion affinity of ReF_6^+ is -214 kcal $mole^{-1}$. This is more exothermal than the corresponding process for IF_6^+ (-208 kcal $mole^{-1}$). In contrast, $ReOF_5$ is shown to be a better fluoro-base than IOF_5 and also is a better base than ReF_7. $ReOF_4^+MF_6^-$ (M = Sb, Au and As) salts are of higher thermal stability than their $ReF_6^+MF_6^-$ analogues.

The powerful oxidizer KrF^+ in interaction with orange-yellow NpF_6 has yielded a colorless solution which probably contains Np(VII) species. NpF_6^+ salts were not formed, however, and this failure to stabilize NpF_6^+ indicates that the ionization potential of NpF_6 is > 291 kcal $mole^{-1}$.

CHAPTER 1

GENERAL INTRODUCTION AND EXPERIMENTAL PROCEDURES

I. General introduction

The work of this thesis deals with the application of powerful oxidizers to the synthesis of new compounds. The studies include: the characterization of fluoro-compounds of xenon and krypton employed as powerful oxidizers; evaluation of solvents and reaction conditions to utilize those oxidizers most effectively and the preparation and characterization of new rhenium (VII) compounds.

Chapter 1 gives a general description of the apparatus and the techniques used in preparing, manipulating and characterizing the materials essential to these studies. In Chapter 2 the oxide scavenging properties of XeF_6 are explored and the possibility of using XeF_6 as a solvent in extremely strong oxidizing reactions is considered.

In Chapter 3, Raman spectroscopic studies of XeF_2, KrF_2 and KrF_2 salts of AuF_5, as solids and in anhydrous HF solutions, are reported and discussed. These studies provide insight into the nature of the bonding in KrF_2 and XeF_2, the nature of the solvations of these molecules in HF and the nature of the HF solvent itself.

Chapter 4 composes the main body of this thesis. It includes the preparation of new ReF_6^+ salts and related chemistry. The $ReF_6^+MF_6^-$ salts are relatives of halogen cation salts (IF_6^+, etc.) but are the only known compounds containing a hexafluorometallate cation. An evaluation of the enthalpy for the process: $ReF_{7(g)} \longrightarrow ReF_{6(g)}^+ + F_{(g)}^-$ has been made. Chapter 5 describes the preparation of the $ReOF_4^+$ salts and the fluoro-basicities of ReF_7 and $ReOF_5$ are compared.

In Chapter 6, preliminary experimental results on the electron-oxidation of NpF_6 are presented and the prospects of preparing new neptunium (VII) and chlorine (VII) compounds are discussed.

II. Apparatus and material handling

The high energy oxidizers encountered in this research are generally moisture unstable so that handling of these chemicals requires special consideration. Methods for handling air-sensitive materials have been described by Shriver.[1] The preparations and characterizations used in this work involved the following: a vacuum line for transference of volatile reagents in and out of reaction vessels, an inert atmosphere glove box to handle less volatile solids and liquids, and various structural methods. The latter involved X-ray diffraction techniques for powders and single crystals, and Raman and infrared spectroscopy for solid, liquids solutions and gases.

A. Vacuum lines. Several vacuum lines were constructed during the period of the research. A general scheme is given below: The vacuum line manifold was equipped with a mechanic rough pump and usually with a silicone oil diffusion pump coupled with a large-bore manifold for high vacuum capability. A thermocouple gauge was used to monitor the pressure below 1 torr and a helicoid gauge was used to measure the pressure in the range of 1 to 1500 torr. The vacuum line was constructed of Autoclave Engineering high pressure fittings (30,000 psi) close to the F_2 cylinder. A Monel Bourdon gauge (0-500 psi) of Helicoid type was used to monitor the F_2 pressure. This high pressure region was used for the controlled delivery of F_2 into the

reaction system. A soda-lime tower was used, in a by-pass arrangement, ahead of or beyond the cold trap, to consume oxidizing chemicals and prevent them from damaging the mechanic pump. For the preparation and handling of the KrF_2 compounds, a scrupulously clean and prefluorinated vacuum line was used. An all Monel manifold was used which incorporated Hoke diaphragm valves (4618.N4M, HOKE Inc., Cresskill, N.J.) and unions and pipes, using Swagelok connections with Teflon TFE ferrules (Oakland Valve Co., CA). Two cold traps were used in the rough pump system, a metal one was ahead of the soda lime tower and a regular

glass trap was beyond the soda-lime tower. A metal cold trap was also employed ahead of the diffusion pump to achieve good vacuum and prevent back diffusion.

A newly assembled vacuum line was always leak tested using a quadrupole mass spectrometer helium leak detector (Consolidated Electrodynamic Corp., Monrovia, CA).

B. Reaction vessels. Different reaction vessels were used depending on the required reaction conditions. For the reactions involved KrF_2 or its derivatives, teflon FEP tubes (Chemplast Inc., Wayne, N.J.) heat-sealed at one end or sapphire tubing (Sapphikon, Milford, NH) fused-plugged at one end were used. For other systems, a wide variety of reaction vessels was used. These included Pyrex or quartz glass, Kel-F tubes (obtained from the Argonne National Laboratory), teflon FEP tubing and tubes of fused sapphire. The reaction tubes were connected to the Whitney valves (M-1KS4 or SS-1KS4, Oakland Valves Co., Oakland, CA) via Swagelok fittings with teflon TFE ferrules. The reaction vessels were always helium leak tested before use.

C. Dry boxes. The Dri-Labs (Vacuum Atmosphere Corp., North Hollywood, CA) used to handle extremely moisture sensitive materials were equipped with a circulating drying train, including an oxygen scavenger and a molecular sieve water scrubber. Nitrogen was routinely used as the circulating gas. The drying train was routinely regenerated to maintain the Dri-Labs but the atmosphere was monitored continuously for presence of moisture by running an incandescent filament in the atmosphere of the box.

For the X-ray powder diffraction and Raman spectroscopic studies, finely powdered solid samples were loaded into thin-walled quartz capillaries (Charles Supper Co., Natick, MS), temporarily plugged with Kel-F grease in the dry-box, and sealed using a microtorch outside the dry-box.

III. Chemical reagents

A. F_2. Fluorine gas was obtained from Matheson Gas Products (East Ruthford, New Jersey). The gas taken directly from the cylinder contained impurities such as N_2, O_2, HF, CF_4...etc. The oxygen was troublesome in the synthesis of KrF_2 because it led to O_2^+ salt formation. The purification of F_2 was done as follows: Several milliliters of liquid F_2 were condensed into a reaction vessel (teflon, sapphire or quartz) and kept at -196°C. The F_2 was photolized using a high pressure mercury UV lamp (1000 watt, General Electric Co., Cleveland, Ohio) for about 1 hour. The fluorine was then evaporated from the reaction vessel at liquid air temperature (~ - 188°C) into a one liter Monel storage bulb at liquid nitrogen temperature. Impurities such as O_2F_2 (from O_2), OF_2, HF and CF_4 were discarded from the least volatile fraction.

B. HF. HF was purchased from Matheson Gas Products. It was purified by trap to trap distillations (~ - 40°C) several times in an all-Kel-F vacuum line. The valves used in this vacuum line were as described by O'Donnell.[2] Anhydrous HF was stored in a Kel-F tube containing K_2NiF_6 until it was needed.

C. Kr and Xe. Research grade krypton and xenon gases were used as supplied by Airco Co. (Murray Hill, New Jersey).

D. Metals. The metals (rhenium, osmium, iridium, platinum and gold) used in the preparation of binary fluorides were purchased from Engelhard Industries (Union, N.J.). All metals were specified at least 99.99 percent pure and were used without further treatment.

E. Binary fluorides. The binary fluorides of the noble gases and the transition metals listed below were prepared according to the known methods cited in the references. The purity of the compounds was checked by vibrational spectroscopy.

Compounds	References
XeF_2	Week,[3] Falconer and Sunder[4]
XeF_6	Malm[5]
KrF_2	Zuchner[6]
ReF_7	Malm and Selig[7]
ReF_6	Malm and Selig[7]
OsF_6	Wienstock and Malm[8]
IrF_6	Ruff and Fisher[9]
PtF_6	Malm, Wienstock and Weaver[10]

F. Actinide fluorides. UF_6 and NpO_2 were used as supplied from Oak Ridge National Laboratory. Anhydrous NpF_4 was prepared as described by Banks.[11] NpF_6[12] was prepared by heating NpF_4 in a fluorine atmosphere in a Monel reactor to > 600°C. It was collected on a cold surface of the reactor at -78°C.

IV. Characterization of materials

A. Infrared spectroscopy. Infrared spectra were recorded using Perkin-Elmer model 183 or model 597 spectrometers. The accuracy of the peak assignments is believed to be within 3 cm^{-1}. Gas phase spectra were obtained using either a Monel bodied cell or one of Kel-F, both having a 10 cm path length. The cells were fitted with silver chloride windows cut from 1 mm sheet (Harshaw chemical Co., Cleveland, Ohio) provided with Teflon gaskets compressed to be leak-tight. Solid phase infrared spectra were taken by spreading the finely powdered sample between two AgCl sheets held and compressed within a Kel-F frame. The AgCl windows were routinely cleaned using dilute NH_4OH solution, and polished with a silver coated stainless steel burnister.

B. Raman spectroscopy. Raman spectra were obtained using a Jobin-Yvon Ramanor HG-2S spectrometer with double monochrometer. Four excitation wavelengths were used. Red light of 647 nm, was obtained using a krypton ion laser (Spectra-Physics Co., Model 165). Three excitation colors (514.5 nm, 488 nm and 457.9 nm) were obtained using an argon ion laser (Coherence Radiation Co., Model CR-2, which was later up-graded to a CR-4 model).

Spectra were usually obtained with samples contained in quartz capillaries, teflon FEP tubes or sapphire tubes. Raman spectra were routinely obtained with samples at low temperature because of the low thermal stability of the compounds involved. A low temperature sample holder as described by Biagioni[13] was used. The sample was cooled with a stream of cold nitrogen, shrouded by a stream of nitrogen at ambient temperature. This prevented moisture from condensing on the sample tube. The temperature was changed by adjusting the flow rate of the cold nitrogen. A temperature of -50°C was obtained with ease.

C. X-ray powder diffraction photography. X-ray powder patterns were obtained using either a North American Philips Co. precision powder camera of 450 mm circumference or a 114 mm Debye-Scherer camera, both using Ni filtered Cu K_α-radiation. Films were measured using a Norelco measuring device. The indexing of the powder diffraction data was aided by comparing the X-ray diffraction photograph of samples with those of related compounds of known lattice parameters. No refinement for absorption error effects was carried out. The accuracy of the derived lattice parameters is believed to be better than ±2%.

V. Special equipment and techniques

Because of the radiation hazard of neptunium, special facilities were required for handling the radioactive compounds. For such work each vacuum line was housed in an isolating box. The latter was either a Dri-Lab or a large box constructed of Lucite and fitted with leak free neoprene gloves. The isolating boxes were well vented through a filtered exhausting system and anything transferred in and out the

boxes was closely monitored by Geiger counter. Such work was done in the presence of a supervisor from the Health and Safety Department of the Lawrence Berkeley Laboratory. To minimize the possibility of escape of radioactive material into the laboratory the boxes always operated with an internal pressure lower than that of the laboratory.

Special equipment and techniques will be described in the appropriate chapters.

REFERENCES

1. D. F. Schriver, "The Manpulation of Air-Sensitive Compounds", McGraw-Hill, New York, 1969.
2. T. A. O'Donnell in "Comprehensive Inorganic Chemistry", ed. H. J. Emeleus et al., Pergamon Press, New York, 1973, p. 1018.
3. J. L. Weeks, C. L. Cernick and M. S. Matheson, J. Amer. Chem. Soc., 84 4612 (1962).
4. W. E. Falconer and W. A. Sunder, J. Inorg. Nucl. Chem., 29 (1967) 1980).
5. C. L. Chernick, J. G. Malm and S. M. Williamson, in "Inorganic Synthesis", H. F. Holtzclaw, Jr. ed., Vol. VIII, McGraw-Hill, New York, 1966, p. 258.
6. K. Zuchner, Ph. D. Thesis, University of Gottingen, West Germany, 1979.
7. J. G. Malm and H. Selig, J. Inorg. Nucl. Chem., 20 189 (1961).
8. B. Wienstock and J. G. Malm, J. Amer. Chem. Soc., 80 (1958) 4466.
9. O. Ruff and J. Fisher, Z. Anorg. Allgem. Chem., 179 161 (1929).
10. B. Wienstock, J. G. Malm and E. E. Weaver, J. Amer. Chem. Soc., 83 4310 (1961).
11. R. H. Banks, Ph.D. Thesis, University of California, Berkeley 1979.
12. G. T. Seaborg and H. S. Brown, U. S. Patent 2982 604 (1961).
13. R. N. Biagioni, Ph. D. Thesis, University of California, Berkeley, 1980.

CHAPTER 2

XeF_6, A FLUORINATOR AND AN OXIDE SCAVENGER

I. Introduction

An interest in the possible synthesis of neptunium (VII) compounds (see Chapter 6) led us to a series of investigations involving related uranium, tungsten and rhenium compounds. The finding are given in this chapter.

Since the prospective work on Np(VII) would involve the exploitation of the non-oxidizable ionizing solvent XeF_6 (in combination with KrF_2), the novel chemistry was related to the use of that solvent.[1] One of the most attractive possibilities for Np(VII) was the oxyfluoride $NpOF_5$, synthetic schemes for which involved the synthesis of an $NpOF_5^-$ precursor. In the uranium and tungsten studies much attention was therefore given to the preparation and characterization of analogues of that anion. The main purpose was to provide a vibrational spectroscopic and crystallographic basis for the easy characterization of the hazardous $NpOF_5^-$ species, but the pattern of oxide and oxyfluoride interaction with XeF_6 was also of interest.

Studies in this laboratory by Richardson[2] had already shown that XeF_6, although a well known scavenger of oxygen by formation of $XeOF_4$:

$$XeF_6 + O^{2-} \longrightarrow XeOF_4 + 2F^-$$

was not capable of completely fluorinating OsO_4:

$$3XeF_6 + OsO_4 \longrightarrow XeF_5^+ OsO_3F_3^- + 2XeOF_4$$

This provided for the possibility that other high oxidation state oxyfluorides might be stable in XeF_6. The present investigation revealed that UOF_5^-, $U_2O_2F_9^-$, WOF_5^- and $W_2O_2F_9^-$ salts were all carried to MF_7^- salts in XeF_6 but in the rhenium system, $K^+ReO_4^-$ yielded $K^+ReO_2F_4^-$.

II. Experiments

A. Special apparatus. General techniques for handling and characterizing materials have been described in Chapter 1. For the transference of XeF_6 and its derivatives, a readily demountable vacuum line was constructed as a supplement to the regular vacuum manifold. One-quarter inch O.D. stainless steel (SS316) tubing and Whitey valves (SS-3KS4) with Teflon ferrules were used in this short vacuum line. A Kel-F trap provided for the collection of volatile products in a dynamic vacuum. Pieces of Teflon FEP tubing (1/4" O.D.) flame-sealed at one end, and each fitted with a Whitey valve, were used as reaction vessels. Precautions were taken to prevent XeO_3 formation and any part of the vacuum line which had been exposed to the air was thoroughly passivated with ~1500 Torr of F_2 overnight then the vacuum line was pumped down, using a diffusion pump, to a hard vacuum prior to the transference of volatiles.

B. Preparation of the oxide tetrafluoride of uranium and tungsten and their alkali metal fluoride salts. Uranium oxide tetrafluoride was prepared from the reaction of uranium hexafluoride and quartz wool in anhydrous liquid HF as described by Paine[3] et al. High quality UOF_4 was obtained in this controlled hydrolysis as indicated by vibrational spectroscopy and its X-ray powder pattern. WOF_4 obtained from

such hydrolysis usually contained some WO_2F_2 but was purified by sublimation under vacuum at 70°C. Vibrational spectroscopy and an X-ray powder pattern then showed it to be of high purity.

Stoichiometric amounts of KF (or CsF) and MOF_4 were mixed in anhydrous liquid HF at room temperature to prepare the complex salts. A typical preparation of $K^+UOF_5^-$ proceeded as follows:

In the dry-box, UOF_4 and KF (powdered from single crystals) were mixed in a Kel-F reaction tube (Argonne tube) fitted with a Whitey valve. The anhydrous HF was distilled into the tube and the mixture was allowed to react at room temperature overnight with vigorous stirring using a spin bar. The HF was distilled off under vacuum and the yellow solid remained was dried under dynamic vacuum at room temperature for more than one hour. The solid was handled in the dry-box. The vibrational spectroscopic data and the powder pattern were consistent with the report of Joubert and Bougon.[4] The infrared and Raman spectra are shown in Fig. 1a and Fig. 2a respectively and the X-ray crystallographic data is given in Table I.

A similar procedure was followed in the preparation of $Cs^+UOF_5^-$, its infrared and Raman spectra are shown in Fig. 1b and Fig. 2b. The X-ray powder pattern was shown to be rhombohedral and the indexing is given in Table II.

In the preparation of $A^+UOF_5^-$ (A = K or Cs), small amount of $A^+U_2O_2F_5^-$ impurities, together with AHF_2 bifluoride, were observed in the Raman spectra (see Figure 2-a,b) although $A^+UOF_5^-$ was the dominant product. X-ray diffraction data did not reveal the presence of KHF_2 or $CsHF_2$, probably due to their low concentration and their weaker diffraction ability.

For the preparation of the complex salts of alkali metal fluorides with tungsten oxide tetrafluoride, the stoichiometric amounts of KF (or CsF) and WOF_4 were mixed in a 1/4" O.D. FEP reaction tube fitted with a Whitey valve, about 1 ml of anhydrous HF was distilled into the tube and the solution was refluxed at ~50°C for about 2 hours. The mixture formed a clear solution at this temperature and a solid crystallized as the solution was cooled slowly. Removal of HF by vacuum distillation yielded a white powder which was dried at room temperature under dynamic vacuum. In the case of KF with WOF_4, the Raman spectroscopic data (see Fig. 3c and Table III) showed the main product to be $K^+W_2O_2F_9^-$. For the Cs salt, the product is a nearly equal mixture of 1:1 and 1:2 adducts, i.e., $Cs^+WOF_5^-$ and $Cs^+W_2O_2F_9^-$. Their vibrational spectra are shown in Fig. 3-a,b and Table III (Raman) and Table IV (infrared).

C. Reactions with XeF_6. Typical reaction conditions and procedures were as follows: Excess XeF_6 was transferred into a FEP reaction tube containing the solid to be fluorinated. The mixture was warmed up to $\geq$50°C in a hot water bath to melt the XeF_6 and was kept molten for a few minutes. Interaction occurred quickly, a solution of XeF_6 dissolved in liquid $XeOF_4$ was formed. The reaction tube was cooled to room temperature and was kept for several hours to ensure the completion of the reaction. The $XeF_6/XeOF_4$ solution also contained UF_6 and WF_6 when UOF_4 and WOF_4 was used as reactants, as checked by Raman spectroscopy. The solid product always precipitated from the solution. The volatile compounds were removed into a collection tube under static vacuum at room temperature and were identified by either their Raman

spectra or their gas phase infrared spectra. The solid products were dried at room temperature under dynamic vacuum and were handled in the dry-box and were characterized by their vibrational spectra and their powder diffraction patterns. The following table summarizes the results of several such studies.

reactants + XeF_6 ---→ products + $XeOF_4$

reactants	products
UOF_4	UF_6
$K^+UOF_5^-$	$K^+UF_7^-$
$Cs^+UOF_5^-$	$Cs^+UF_7^-$
WOF_4	WF_6
$K^+W_2O_2F_9^-$	$K^+WF_7^-$
$Cs^+WOF_5^-/Cs^+W_2O_2F_9^-$	$Cs^+WF_7^-$
$K^+ReO_4^-$	$K^+ReO_2F_4^-$
OsO_4	$XeF_5^+OsO_3F_3^-$ *

*reference 2.

The Raman spectra of $A^+UF_7^-$ (A = K and Cs) are illustrated in Fig. 4, and $A^+ WF_7^-$ (A = K or Cs) in Fig. 5. The vibrational spectra (Raman and infrared) for $K^+ReO_2F_4^-$ and $XeF_5^+OsO_3F_3^-$ are shown in Fig. 6 and Fig. 7 respectively. The X-ray powder diffraction data for $A^+MF_7^-$ (A = K and Cs, M = U and W) are summarized in table I. The indexing of $K^+WF_7^-$, $Cs^+WF_7^-$ and $K^+UF_7^-$ are given in Table V, VI and VII.

D. Reactions with $XeOF_4$. $XeOF_4$ was used to react with two compounds, $K^+UOF_5^-$ and UOF_4, in the separated experiments, no reaction was observed.

III. Discussion

Some alkali salts $K^+UOF_5^-$ and $A^+WOF_5^-$ (A = K or Cs) had been prepared previously.[4,5,6] Usually these salts were impure and were generally in admixtures with $A^+M_2O_2F_9^-$ salts. The synthetic approach used in this work differed from those used previously and employed the interaction of the oxide fluoride with alkali fluoride in anhydrous liquid hydrogen fluoride. As in the previous synthetic work, however, the products usually involved a mixture of $A^+MOF_5^-$ and $A^+M_2O_2F_9^-$ salts.

The $A^+MOF_5^-$ salts, where $Cs^+UOF_5^-$ is new, were easily identified by their simple X-ray powder patterns, which were based either on a primitive rhombohedral cell or a small distortion of such a cell (see Table I). The $A^+M_2O_2F_9^-$ powder data were in all cases complex, and were not indexed. Nevertheless, the X-ray powder data clearly showed what the $A^+MOF_5^-$ and $A^+M_2O_2F_9^-$ mixture is, and provided a semiquantitative estimate of the relative abundance of each complex salt in the mixture. This information was crucial to the assignment of the Raman spectra. The latter provided for convenient identification of the species MOF_5^- and $M_2O_2F_9^-$.

Spectra of WOF_5^- and $W_2O_2F_9^-$ salts are tabulated in Table III (Raman) and Table IV (IR) and representative spectra are displayed in fig. 3. There are small variation in the vibrational spectra with cations but the WOF_5^- is readily identified by its strong Raman band of W-O stretch (ν_{W-O}) at ~980 cm^{-1}, plus its medium intensity band of W-F stretch (ν_{W-F}) at ~680 cm^{-1} (see Table VIII). Curiously there is only one band in the W-O stretch region (~1030 cm^{-1}) in the Raman spectra of $W_2O_2F_9^-$ salts. This suggests that one oxygen atom could have a bridging role, so the anion

might be

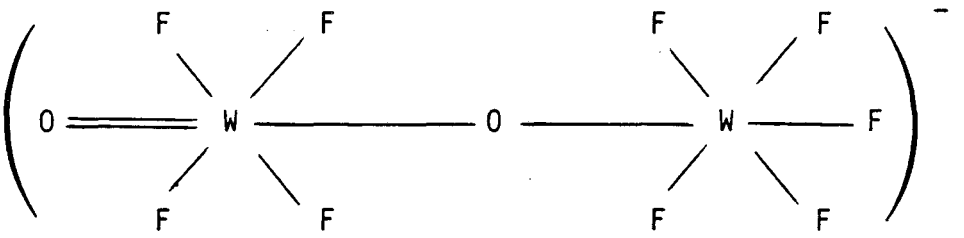

There can be no certainty of this without more data. In WOF_4 itself the combination[7] of X-ray single crystal data and vibrational data show that the $W_4O_4F_{16}$ structural unit is μ-fluoro bridged and the oxygen ligands uniquely associated with each W atom. The W-O stretch in the Raman spectrum is represented by a single band data 1055 cm^{-1}, in spite of the tetrameric structural unit. Therefore the μ-fluoro bridge formula is also a possibility for $W_2O_2F_9^-$

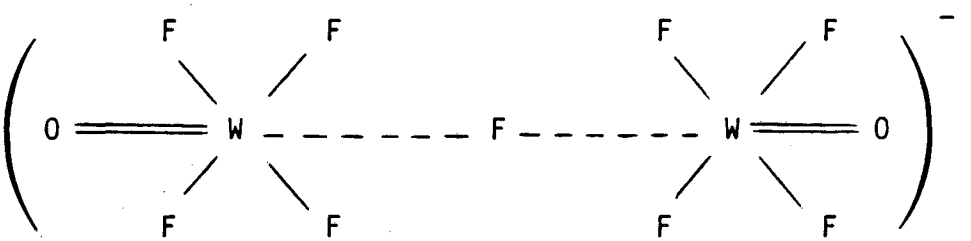

The greater symmetry of the latter formulation is in harmony with the simple Raman spectra of $W_2O_2F_9^-$ salts (see Fig.3c).

The uranium salts are similar crystallographically and vibrationally to their tungsten relatives. Again, the M-O stretch for the MOF_5^- salt is significantly lower (see Table VIII and Fig. 2) than in the oxide tetrafluoride (~73 cm^{-1} in both the tungsten and the uranium cases). The ν_{U-O} stretch in $U_2O_2F_9^-$ is closer to the value in the oxide tetrafluoride itself and makes for easy distinction of $A^+UOF_5^-$ and $A^+U_2O_2F_9^-$ salts. The lower stretching frequency ν_{M-O} in the anion

MOF_5^- (compared with MOF_4) may be simply correlated with the lower electronegativity of M in the more electron rich anion.

The observation that the $A^+MOF_5^-$ salts (both M = U and M = W) interact with XeF_6 according to the equation:

$$A^+MOF_5^- + XeF_6 \longrightarrow A^+MF_7^- + XeOF_4$$

is not surprising in view of the previous observation[8] of complete fluorination of UO_2F_2 by XeF_6:

$$UO_2F_2 + 2XeF_6 \longrightarrow UF_6 + 2XeOF_4.$$

The reaction does provide however for synthesis of $A^+MF_7^-$ salts which have not been reported hitherto because of the failure of conventional approaches[9,10] (see e.g. $K^+UF_7^-$[10]).

The $A^+MF_7^-$ unit cells are simple (see Table I) and indicative of monomeric MF_7^- anions, which, in the primitive cubic cases, must be randomly arranged or undergoing intramolecular rearrangement. The Raman spectra of the simple MF_7^- salts are characterized by a very strong sharp band (which must represent the totally symmetric M–F stretching mode) at ~710 cm^{-1} in the WF_7^- case (see Fig. 5) and at ~625 cm^{-1} for UF_7^- (see Fig. 4) which are similar to observations made previously[11,12]. These features provide for the ready identification of such salts. As in the oxyfluoride case, there is a notable decrease in stretching frequency from the neutral molecule UF_6 (ν_1 = 667 cm^{-1}) to single charged[11] UF_7^- (ν_1 ~ 622 cm^{-1}) and to double charged[11] UF_8^{2-} (ν_1 ~ 583 cm^{-1}).

This is also the case for their tungsten analogues. The W-F stretching frequencies[12] (ν_1) for WF_6, WF_7^- and WF_8^{2-} are 771, ~710 and 660 cm^{-1} respectively (see Table VIII).

The observation of Richardson[2] on the interaction of XeF_6 with OsO_4:

$$3XeF_6 + OsO_4 \longrightarrow XeF_5^+ OsO_3F_3^- + 2XeOF_4$$

indicates that the small pseudo-octahedral anion $OsO_3F_3^-$ is resistant to further oxygen exchange for fluorine. The molecule OsO_2F_4, which would be pseudo-octahedral, is not found even when the salt $XeF_5^+ OsO_3F_3^-$ is pyrolyzed. This gives some basis for believing that the higher actinide neptunium species $NpOF_5^-$ could be resistant to XeF_6 attack. The interaction of $K^+ReO_4^-$ with XeF_6 gives further evidence that the smaller transition element atoms can provide M-O bonds which are stable to XeF_6. Thus $K^+ReO_4^-$ yields $K^+ReO_2F_4^-$:

$$K^+ReO_4^- + 2XeF_6 \longrightarrow K^+ReO_2F_4^- + 2XeOF_4$$

The resistance of $ReO_2F_4^-$ and $OsO_3F_3^-$ to further attack by XeF_6 is probably due to a kinetic effect, the ligands about the small highly oxidized central atoms being in a tightly packed arrangement.

The salt $K^+ReO_2F_4^-$ can have two isomeric forms for $ReO_2F_4^-$ (cis and trans) and this may be the reason for the presence of at least three bands in the Re-O stretching region of the Raman spectrum (see Fig. 6). The X-ray powder diffraction pattern is also somewhat complex, perhaps because there are two structures represented, and was not indexed. The

Raman and X-ray data were indistinguishable from that obtained from samples of $K^+ReO_2F_4^-$ prepared as previously described.[13]

IV. Conclusion

The ability of XeF_6 to exchange fluorine for oxygen is well illustrated by its conversion of $A^+MOF_5^-$ and $A^+M_2O_2F_9^-$ salts (M = W or U, A = K or Cs) to $A^+MF_7^-$ salts but the resistance of $K^+ReO_2F_4^-$ and XeF_5^+ $OsO_3F_3^-$ to further exchange indicates that when the central atom is sufficiently small and the ligand environment a tightly packed one, the oxyfluoride can be stable in XeF_6.

REFERENCES

1. N. Bartlett and K. Leary, J. Chem. Soc., Chem. Comm., 903 (1972).
2. T. Richardson, unpublished results.
3. R. T. Paine, R. K. Ryan and L. B. Asprey, Inorg. Chem., 14 1113 (1975).
4. M. M. P. Joubert and R. Bougon, C. R. Acad. Sc. Paris, Series C 280 193 (1975).
5. Von. A. Benter and W. Sawodny, Z. Anorg. Allg. Chem., 427 37 (1976).
6. B. Hargreaves and R. D. Peacock, J. Chem. Soc., 2170 (1958).
7. M. J. Bennett, T. E. Haas and J. T. Purdham, Inorg. Chem., 11 207 (1972).
8. M. Bohinc and B. Felec, J. Inorg. Nucl. Chem., 34 2942 (1972).
9. N. S. Nikolaev and V. F. Sukhoverkov, Dokl. Akad. Naus. SSSR, 136 2938 (1972).
10. J. G. Malm, H. Selig and S. Siegel, Inorg. Chem., 5 130 (1966).
11. R. Bougon, R. M. Costes, J. P. Desmoalin, J. Michel and J. L. Person, J. Inorg. Nucl. Chem. H. H. Hyman Memorial volume, ed. J. J. Katz and I. Sheft, 1976.
12. W. A. Saunder, A. L. Wayda, D. Distefano, W. E. Falconer and J. E. Griffiths, J. Fluorine Chem., 14 299 (1979).
13. R. D. Peacock, J. Chem. Soc., 602 (1955).
14. L. B. Asprey, F. H. Kruse, A. Rosenzweig and R. A. Penneman, Inorg. Chem., 5 659 (1966).
15. G. B. Hargreaves and R. D. Peacock, J. Chem. Soc., 4212 (1957).
16. A. Rosenzuweig and D. T. Cromer, Acta. Cryst., 23 865 (1967).

17. A. T. Sadikova, G. G. Sadikov and N. S. Nikolaev, Soviet. At. Eng., 26 283 (1969).

18. J. R. Geichman, E. A. Smith and P. R. Ogle, Inorg. Chem., 2 1012 (1963).

19. S. T. Beaton, Ph.D. Thesis, University of British Columbia, Vancouver, Canada 1963.

20. J. H. Holloway, G. J. Schrobilgen and P. Taylor, J. Chem. Soc. Chem. Comm., 40 (1975).

21. R. Bougon, T. Bui Huy and P. Chappin, Inorg. Chem., 14, 1822 (1975).

22. J. A. A. Katelaar, C. Haas and J. Van Der Elsken, J. Chem. Phys., 24 624 (1956).

23. J. J. Rush and A. J. Melveger and L. W. Schroeder, J. Chem. Phys., 56 2793 (1972).

24. K. Nakamoto, "Infared spectra of inorganic and coordination compounds" 3rd ed., John Wiley and Sons, New York, London.

Table Contents

Table I.
Summary of X-ray powder diffraction data.

Compounds	a	b	c	α	z	$V_{formula}$	Reference
$KUOF_5$	8.07*	11.36	5.59		4	128+	This work
$KUOF_5$	8.02	11.25	5.55		4	125	(4)
KUF_6	7.96	11.46	5.61		4	128	(14)
$(NH_4)UOF_5$	8.01	11.56	5.62		4	132	(4)
$(NH_4)UF_6$	8.03	11.89	5.83		4	139	(14)
$CsWF_6$	5.31			95.3°	1	148	(15)
$CsWOF_5$	5.31			95.5°	1	148	(6)
$CsUOF_5$	5.39			95.5°	1	154	This work
$CsUF_6$	5.417			95.5°	1	157	(16)
$CsUF_7$	5.53				1	169	This work
$CsUF_7$	5.51				1	167	(17)
$CsWF_7$	5.41				1	158	This work
$NOUF_7$	5.29				1	148	(18)
$NOWF_7$	5.20				1	141	(19)
KWF_7	10.20				8	133	This work
KUF_7	10.79	10.51	10.22		8	145	This work

*in Å +in $Å^3$

Table II.

X-ray powder data for $Cs^{+}UOF_5^{-}$

Intensity	$1/d^2$ obs.	$1/d^2$ calc.	hkl
vw	0.0356	0.0350	100
s	0.0630	0.0629	T10
m^{+}	0.0782	0.0771	110
w	0.1408	0.1400	200
w^{+}	0.1879	0.1887	$\bar{2}11$
m	0.2020	0.2029	$2\bar{1}1$
m^{-}	0.2503	0.2516	$\bar{2}20$
vw	0.3090	0.3084	220
w	0.3265	0.3287	$3\bar{1}0$
		0.3713	310
w	0.3723		
		0.3718	211

s = strong, m = medium, w = weak, v = very

Rhombohedral cell.

$\underline{a} = 5.30\text{Å}$

$\alpha = 95.5^{\circ}$

$V = 154\text{Å}^3$

$z = 1$

Table III.

Raman spectroscopic data of $AF.(WOF_4)_n$ n = 1 or 2

Bridging Adducts		Ionic Adducts					
		$AF:WOF_4$ = 1:2			$AF:WOF_4$ = 1:1		
$XeF_2 \cdot 2WOF_4$ (a)	$XeF_2 \cdot WOF_4$ (a)	$A=K^+$ (*)	NO^+ (b)	Cs^+ (*)	$A=NO^+$ (b)	Cs^+ (c)	Cs^+ (*)
1052(49)[d]							
1044(24)	1044(14)	1044(10)	1040(10)				
	1033(56)			1031(s)			
					1001(10)	989(vs)	982(vs)
		700(6)	699(6)	795(m)			
					684(3.5)	689(m)	680(m)
		603(10)	594(0.5)	608(vw)			
					591(0.4)	594(vw)	588(vw)
585(100)							
	577(13)						
	573(100)						
541(1)							
	458(8)						
	439(11)						
409(5)		342(0.2sh)					
		324(4)	318(5.8)	317(m)	327(5.9)	331(m)	328(m)
		314(4)					
					292(sh)	287(vw)	292(vw)
		216(0.5)		215(vw)			
		208(0.5)	210(0.7)				
					200(sh)		
154(9)		153(4)			163(11)		152(vw)
144(5)							

s = strong, m = medium, w = weak, v = very

*This work
(a) Ref. 20
(b) Ref. 21
(c) Ref. 5
(d) in cm^{-1}, intensities in parenthesis

Table IV.

Infrared spectroscopic data of $AF \cdot (WOF_4)_n$ n = 1 or 2

$AF \cdot WOF_4$ = 1:2		$AF \cdot WOF_4$ = 1:1				
$A=NO^+$ (a)	Cs^+ (*)	$A=NO^+$ (a)	K^+ (b)	Rb^+ (b)	Cs^+ (b)	CS^+ (*)
1040(s)(c)		1034(s)				
		1003(vs)	996(vs)	989(vs)	987(vs)	980(vs)
703(sh)	705(m)					
		685(sh)	689(w)	688(w)	686(w)	676(w)
635(vs,br)	640(vs,br)					
		610(vs)	615(vs)	610(vs)	608(vs)	605(vs)
598(sh)	596(sh)					
			508(m)	507(m)	507(m)	500(m)
		455(ms)				
435(m)	435(m)					
			330(w)	329(w)	329(w)	
			284(vw)	286(m)	286(m)	
			242(s)	242(s)	242(s)	

s = strong m = medium w = weak br = broad sh = shoulder v = very

*This Work

(a) Ref. 21

(b) Ref. 5

(c) in cm^{-1}, relative intensities in parenthesis

Table V.

X-ray powder data for $K^+WF_7^-$

Intensity	$1/d^2$ obs.	$1/d^2$ calc.	hkl
vvw	0.0316	0.0288	111
vs	0.0387	0.0384	200
s	0.0480	0.4080	210
vvw	0.0557	0.5760	211
vvw	0.0619	---	---
vw	0.0767	0.0768	220
s	0.0861	0.0864	300
s	0.1154	0.1152	222
w	0.1245	0.1248	320
w	0.1337	0.1344	321
m	0.1537	0.1536	400
w	0.1636	0.1632	322
w^+	0.1922	0.1920	420
m^+	0.2019	0.2016	421
s	0.2316	0.2304	422
w^+	0.2408	0.2400	500
w^+	0.2505	0.2497	510
m	0.2785	0.2785	520
w	0.2880	0.2801	521
w^+	0.3075	0.3073	440
w^+	0.3164	0.3169	522
vvw	0.3260	0.3265	433
w	0.3470	0.3457	600
w	0.3564	0.3553	610
w^+	0.3859	0.3841	620
m	0.3947	0.3937	621

(continued)

Table V (continued)

Intensity	$1/d^2$ obs.	$1/d^2$ calc.	hkl
w^+	0.4034	0.4033	541
w	0.4327	0.4321	630
w^-	0.4425	0.4609	444
w	0.4706	0.4705	632
w^-	0.4803	0.4801	710
w^-	0.5187	0.5186	721
w	0.5379	0.5378	642
w^-	0.5470	0.5474	544
w^-	0.5862	0.5858	650
w^-	0.5955	0.5954	732
w	0.6240	0.6242	810
w^-	0.6327	0.6338	811
w	0.6608	0.6626	821
vvw	0.6710	0.6722	653

s = strong, m = medium, w = weak, v = very.

Cubic

$\underline{a} = 10.20$ Å

$V = 1061$ Å^3

$z = 8$

$V_{formula} = 132.6$ Å^3

Table VI.

X-ray powder data for $Cs^+WF_7^-$

Intensity	$1/d^2$ obs.	$1/d^2$ calc.	hkl
w	0.0349	0.0341	100
vs	0.0685	0.0682	110
m	0.1375	0.1368	200
s	0.2052	0.2048	211
m-w	0.2739	0.2730	220
m	0.3412	0.3412	310
vw	0.4095	0.4094	222
ms	0.4763	0.4776	321
vvw	0.5429	0.5458	400
w	0.6099	0.6140	330,411
vw	0.6772	0.6822	420
vvw	0.7451	0.7504	332
vvw	0.8137	0.8186	422
w	0.8826	0.8868	510

s = strong, m = medium, w = weak, v = very

Cubic

$\underline{a} = 5.41$ Å

$V = 158.3$ Å^3

$z = 1$

Table VII.
X-ray powder data for $K^+UF_7^-$

Intensity	$1/d^2$ obs.	$1/d^2$ calc.	hkl
W	0.0353	0.0343	200
S^+	0.0370	0.0362	020
S^-	0.0387	0.0382	002
W	0.0455	0.0458	021
CW	0.0546	0.0544	121
S	0.0705	0.0706	220
S	0.0732	0.0726	202
S	0.0756	0.0745	022
S^-	0.0794	0.0801	221
vw	0.0889	0.0901	130
vw	0.0917	0.0911	031
m	0.1069	0.1088	222
m^-	0.1159	0.1159	230
vw	0.1282	0.1283	132
vw	0.1326	0.1309	123
m^-	0.1455	0.1449	040
m^-	0.1547	0.1545	041
W^+	0.1746	0.1737	420
W^+	0.1829	0.1832	042
W^+	0.1009	0.1018	142
vw	0.1968	0.1965	214
vw	0.2006	0.1997	323
m^-	0.2100	0.2120	422
m	0.2168	0.2178	242
m^-	0.2270	0.2264	050
m^-	0.2366	0.2360	051
wv	0.2495	0.2482	015
vw	0.2566	0.2568	115

(continued)

Table VII (continued)

Intensity	$1/d^2$ obs.	$1/d^2$ calc.	hkl
w⁻	0.2692	0.2689	234
w⁻	0.2748	0.2753	025
w	0.2908	0.2906	404
w	0.3000	0.2996	414
vw	0.3096	0.3094	600
vw	0.3162	0.3165	305
w	0.3263	0.3261	060
vw	0.3347	0.3347	531
wv	0.3444	0.3443	006
wv	0.3643	0.3644	062
wv	0.3669	0.3679	504
vw	0.3828	0.3825	533
vw	0.3877	0.3978	216
vw	0.3911	0.3910	630
vw	0.4055	0.4046	613
wv	0.4255	0.4259	036
vw	0.4318	0.4318	623

s = strong, m = medium, w = weak, v = very

Orthorhombic

$\underline{a}$ = 10.79 Å

$\underline{b}$ = 10.51 Å

$\underline{c}$ = 10.22 Å

V = 1159 $Å^3$

z = 8

$V_{formula}$ = 145 $Å^3$

Table VIII.
Raman spectroscopic data

Compounds	ν(M=O)	ν(M-F)	Reference
UF_6		667	(3)
KUF_7		626	This work
$NOUF_7$		627	(11)
$CsUF_7$		622	(11)
$CsUF_7$		622	This work
$(NO)_2UF_8$		590	(11)
Cs_2UF_8		583	(11)
UOF_4	895 891 885	667 658 647	(3)
$KUOF_5$	815	592	This work
$CsUOF_5$	818	593	This work
WF_6		771	(24)
$NOWF_7$		715	(12)
KWF_7		714	This work
$CsWF_7$		707	This work
$(NO)_2WF_8$		660	(12)
WOF_4	1055	733	(21)
$(NO)(W_2O_2F_9)$	1041	699	(21)
$KW_2O_2F_9$	1044	700	This work
$CsW_2O_2F_9$	1031	695	This work
$(NO)WOF_5$	1001	689	(21)
$CsWOF_5$	989	689	(5)
$CsWOF_5$	982	680	This work
$(NO)_2WOF_6$	978	607	(21)

Figure Captions

Fig. 1. Infrared spectra of a) $K^+UOF_5^-$ and b) $Cs^+UOF_5^-$

Fig. 2. Raman spectra of a) $K^+UOF_5^-$ and b) $Cs^+UOF_5^-$. Peaks at 598 and 610 cm^{-1} are attributed to KHF_2 and $CsHF_2$ respectively.

Fig. 3. a) infrared spectrum of $Cs^+W_2O_2F_9^-$ and $Cs^+WOF_5^-$

b) Raman spectrum of $Cs^+W_2O_2F_9^-$ and $Cs^+WOF_5^-$

c) Raman spectrum of $K^+W_2O_2F_9^-$

Fig. 4. Raman spectra of a) $Cs^+UF_7^-$ and b) $K^+UF_7^-$

Fig. 5. Raman spectra of a) $K^+WF_7^-$ and b) $Cs^+WF_7^-$

Fig. 6. Infrared spectrum (a) and Raman spectrum (b) of $K^+ReO_2F_4^-$

Fig. 7. Infrared spectrum (a) and Raman spectrum (b) of XeF_5^+ $OsO_3F_3^-$

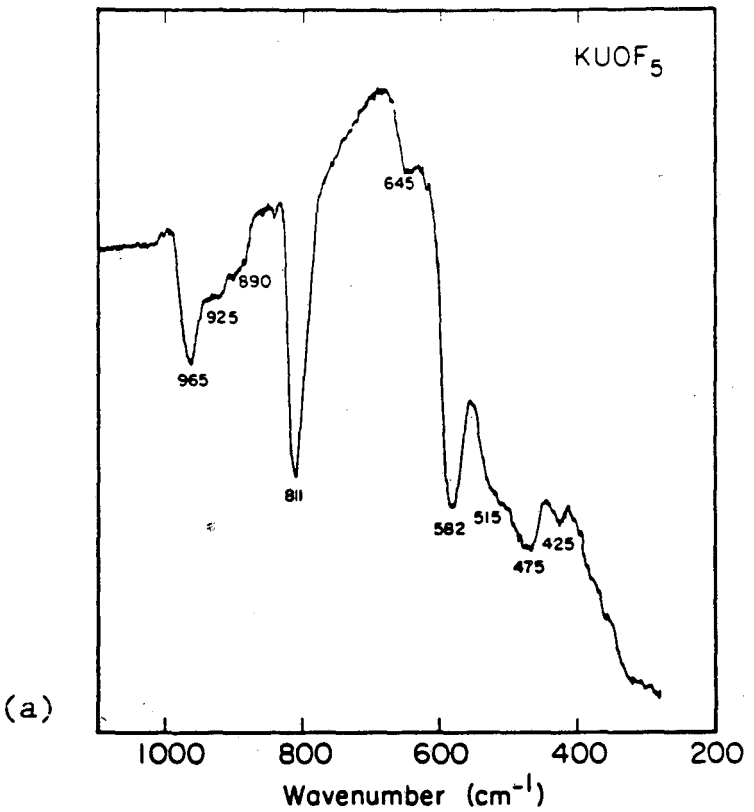
KUOF5
645
890
925
965
811
582
515
425
475
1000
800
600
400
200
Wavenumber (cm-1)

(a)

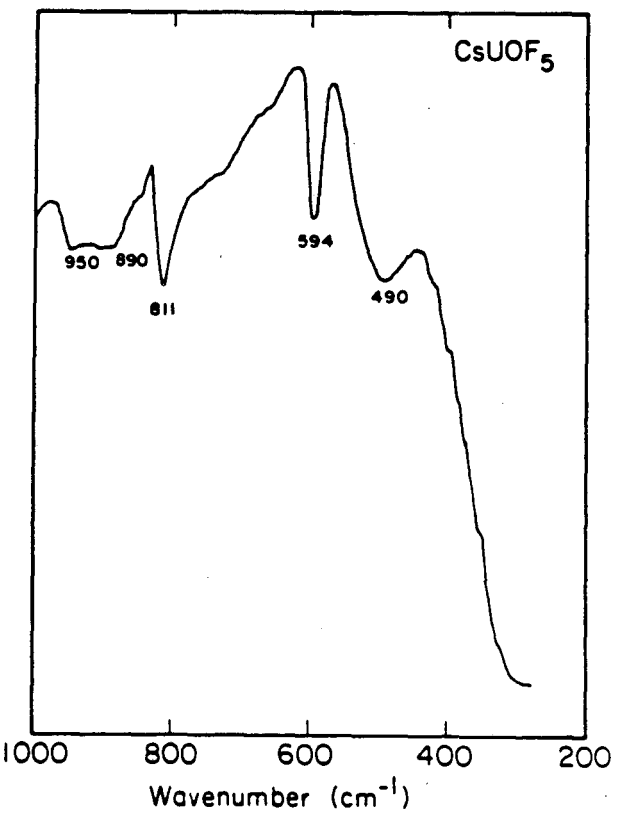
CsUOF5
950
890
811
594
490
1000
800
600
400
200
Wavenumber (cm-1)

(b)

Fig. 1

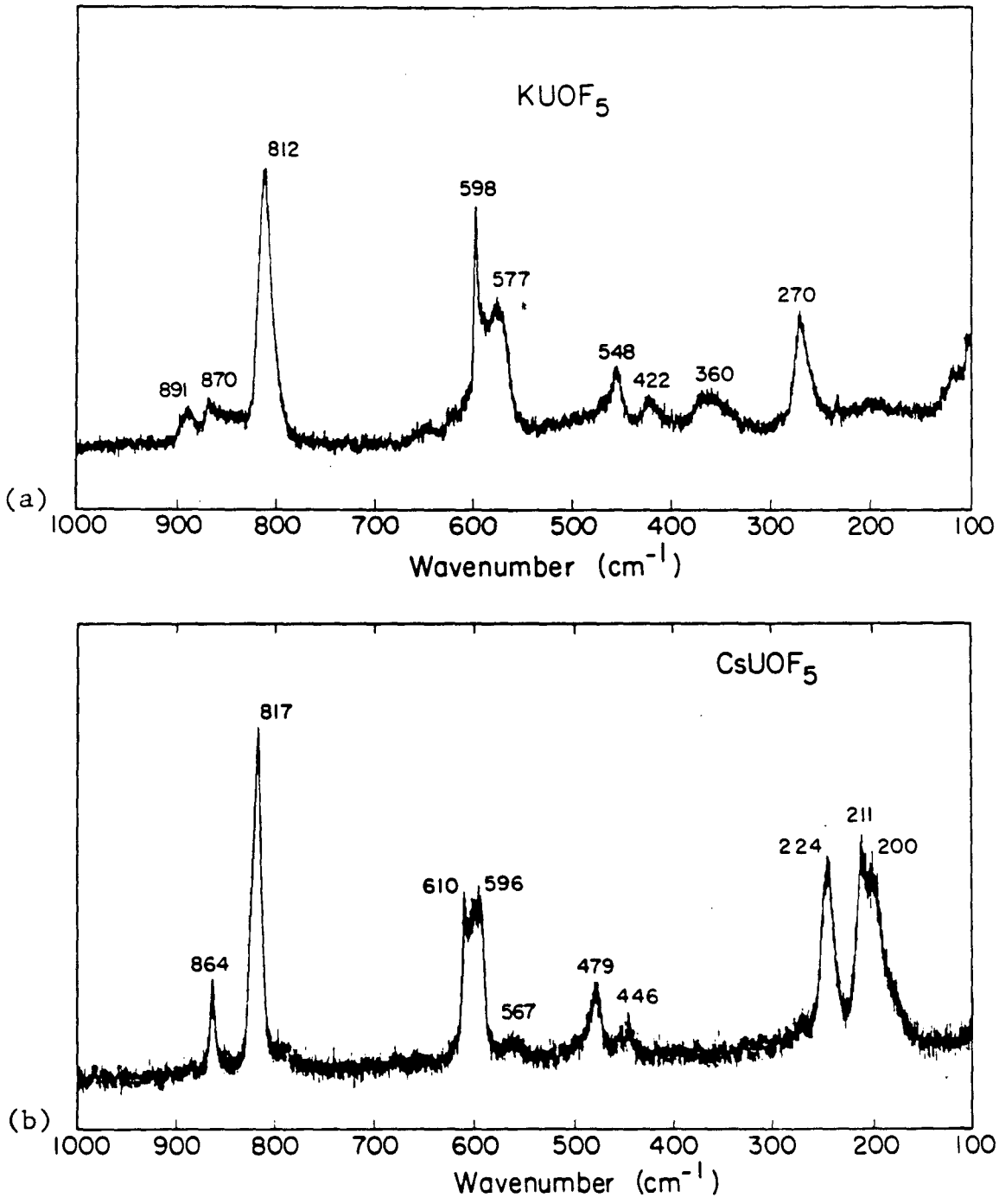
KUOF5
812
598
577
270
548
422
360
891
870
(a)
1000 900 800 700 600 500 400 300 200 100
Wavenumber (cm-1)
CsUOF5
817
211
224
200
610
596
864
479
446
567
(b)
1000 900 800 700 600 500 400 300 200 100
Wavenumber (cm-1)

Fig. 2

(a)

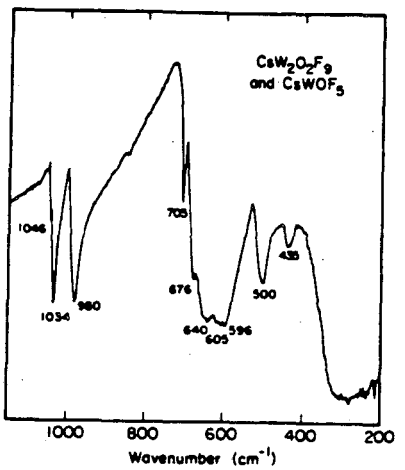

(b)

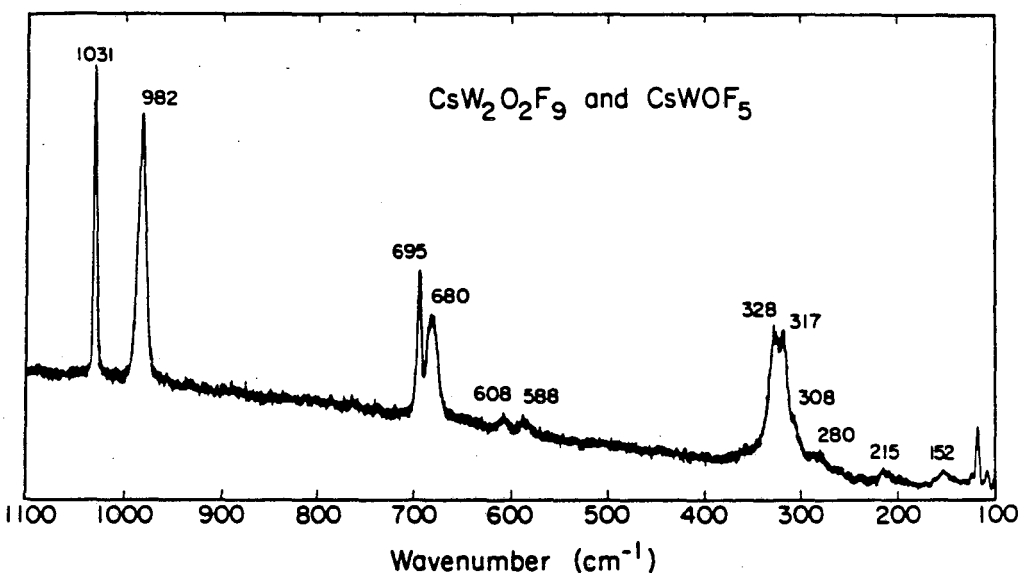

(c)

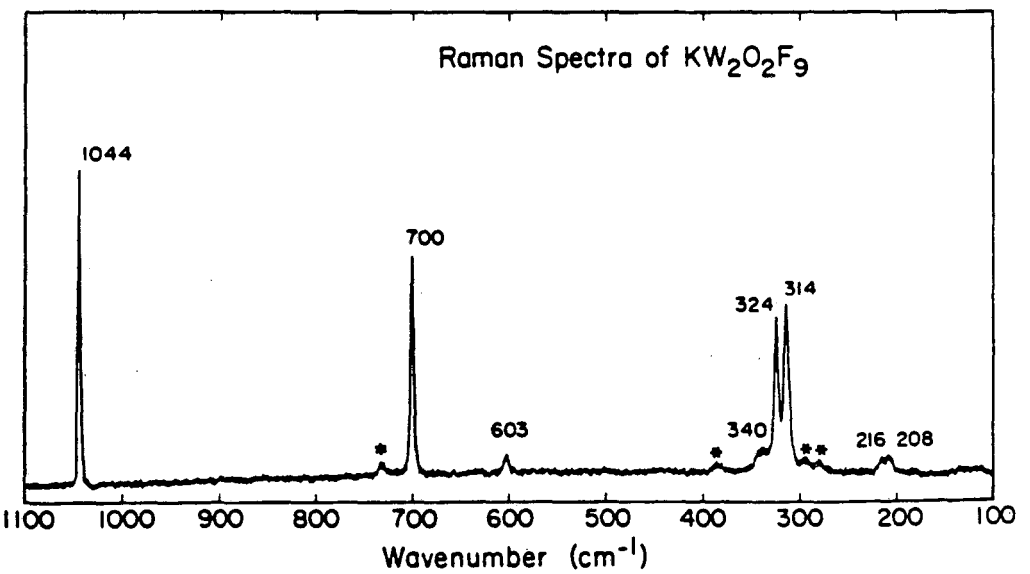

*FEP signals

Fig. 3

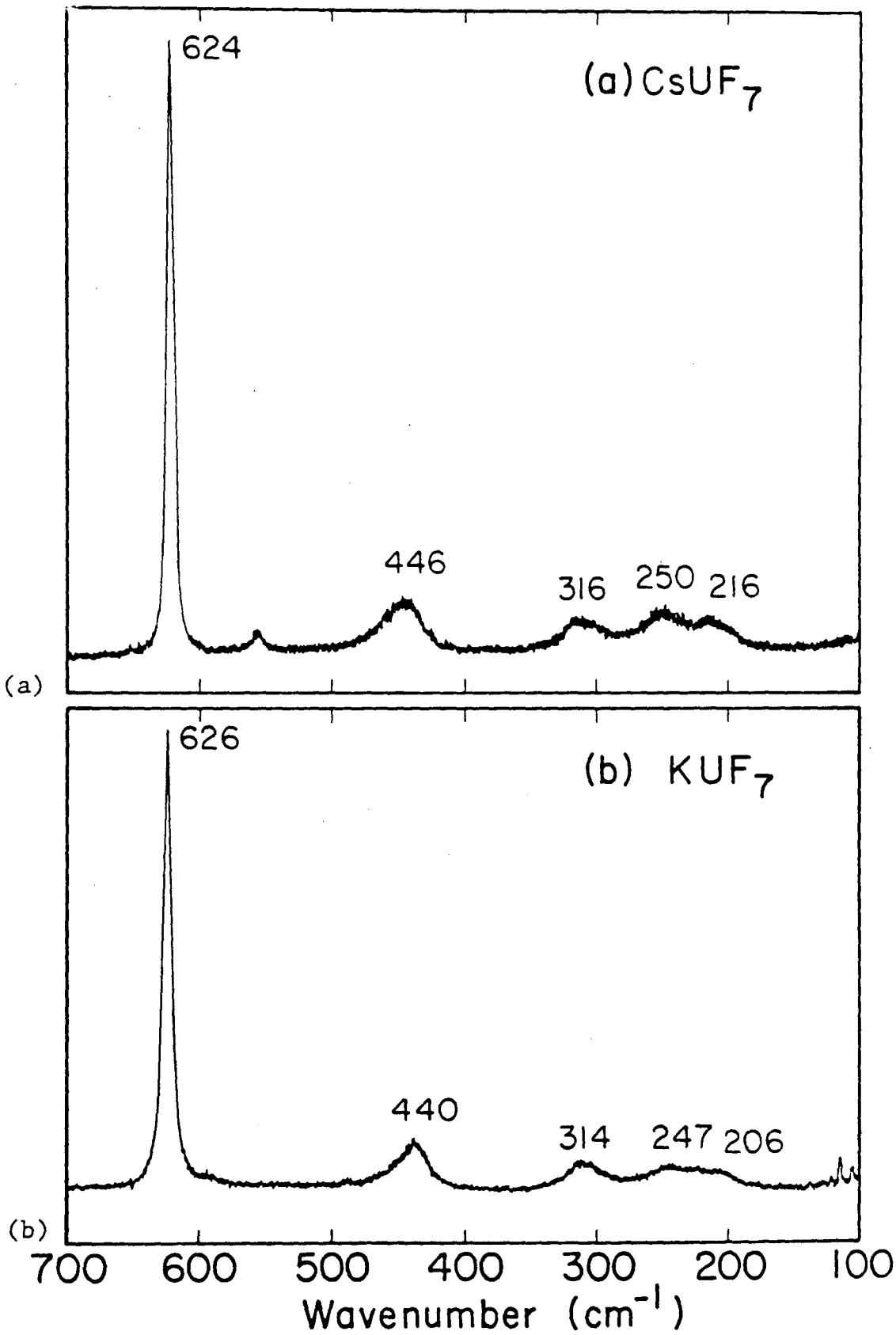
624
(a) CsUF7
446
316
250
216
(a)
626
(b) KUF7
440
314
247
206
(b)
700
600
500
400
300
200
100
Wavenumber (cm-1)

Fig. 4

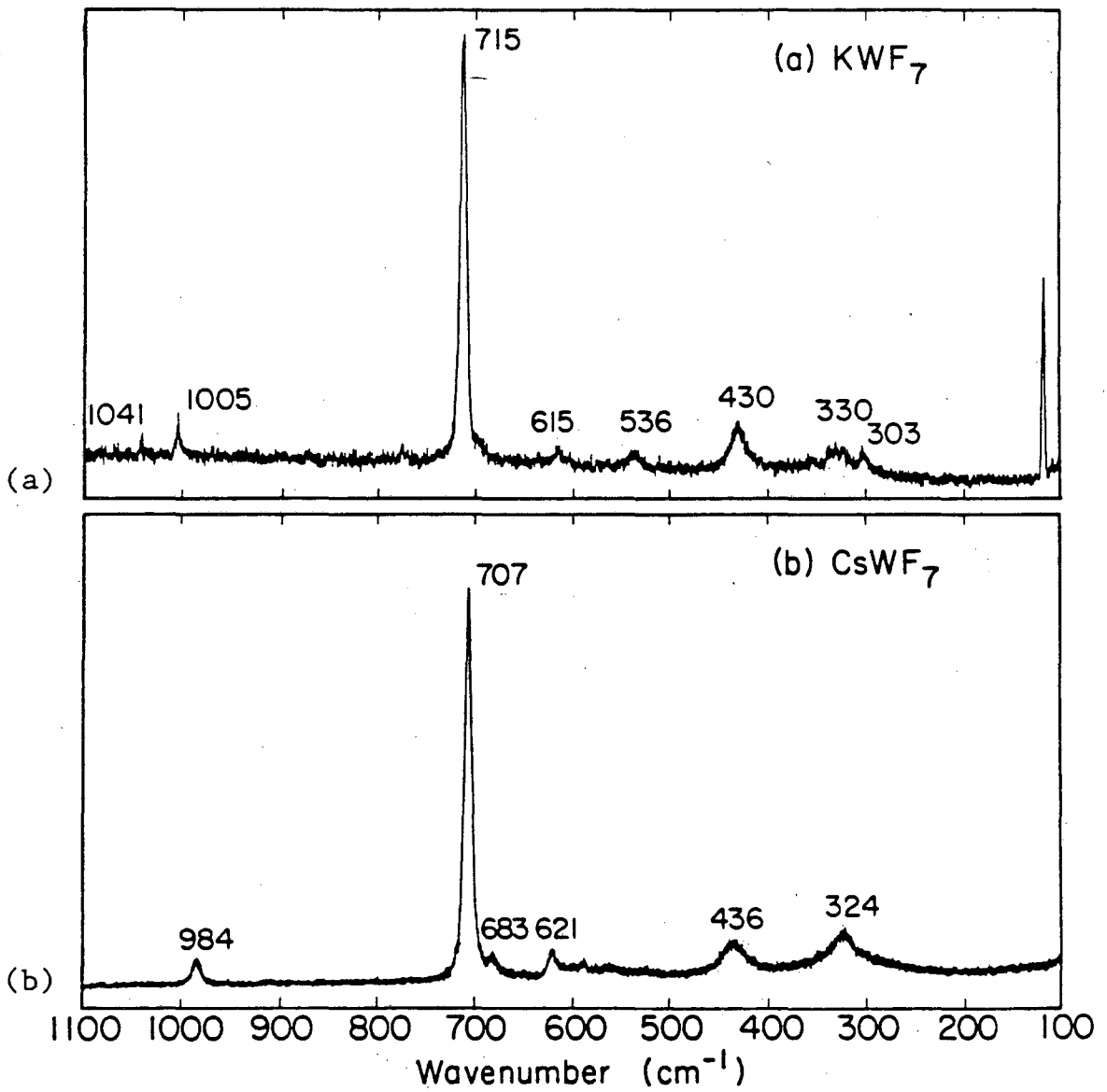
715
(a) KWF7
1041
1005
615
536
430
330
303
(a)
707
(b) CsWF7
984
683
621
436
324
(b)
1100 1000 900 800 700 600 500 400 300 200 100
Wavenumber (cm-1)

Fig. 5

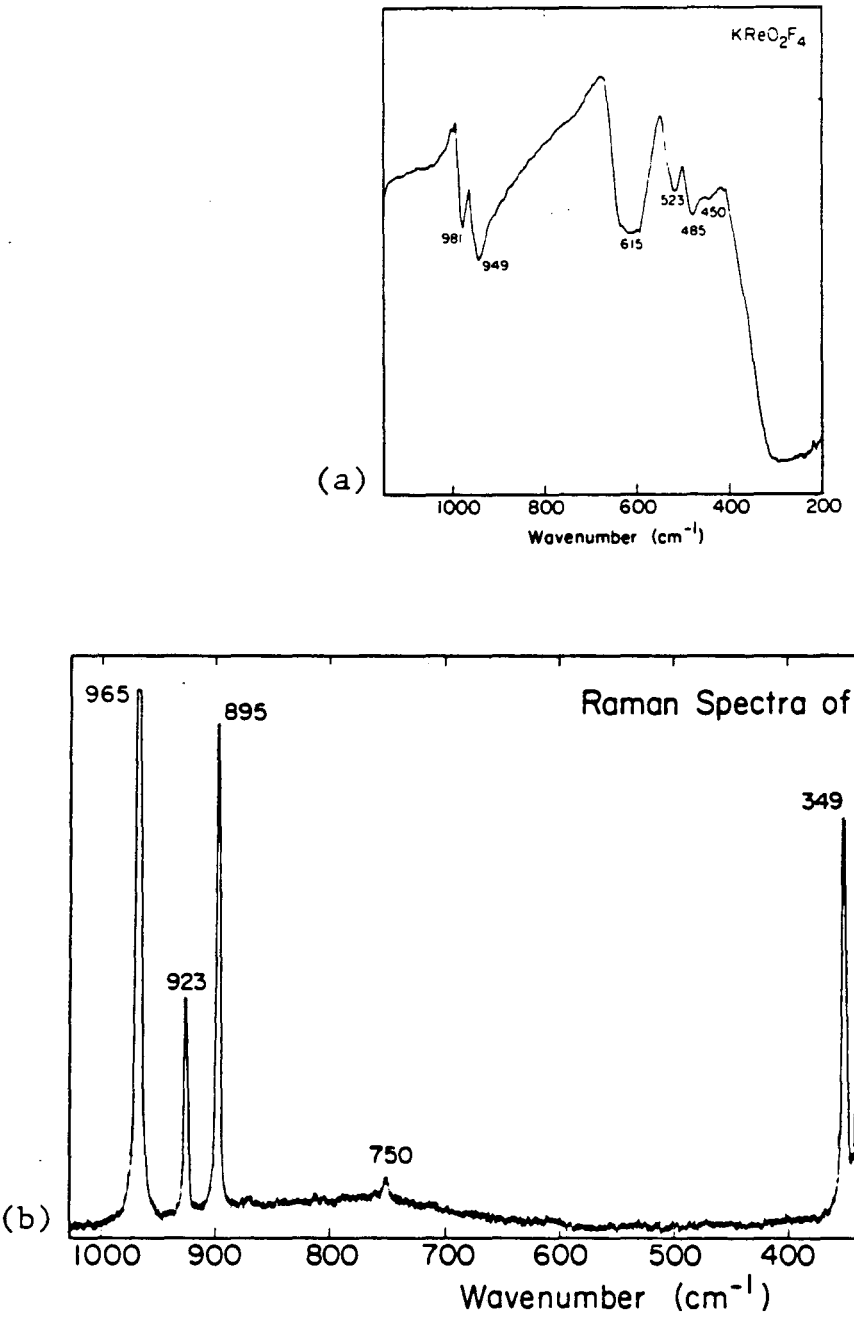
KReO2F4
(a)
981
949
615
523
485
450
1000
800
600
400
200
Wavenumber (cm-1)
Raman Spectra of KReO2F4
(b)
965
895
923
750
335
349
330
108
117
1000
900
800
700
600
500
400
300
200
100
Wavenumber (cm-1)

Fig. 6

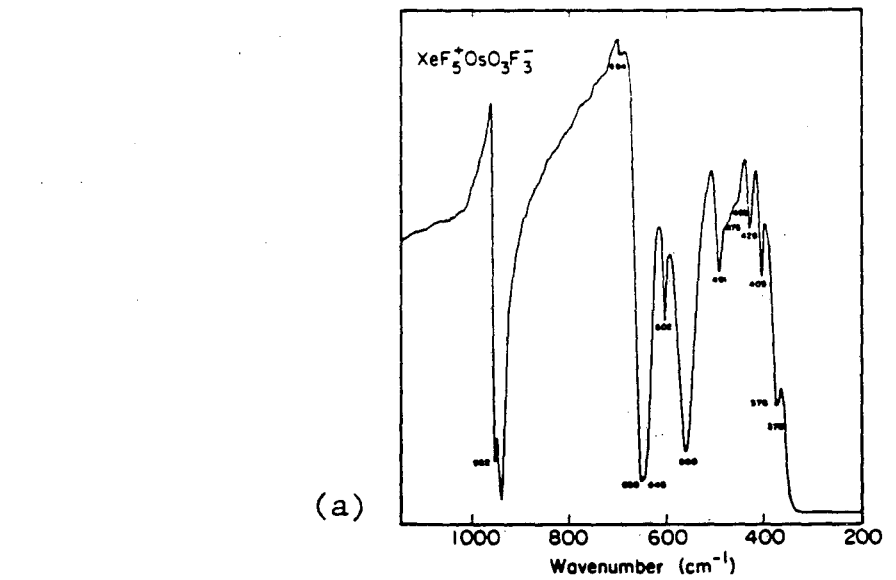
(a)
$XeF_5^+OsO_3F_3^-$
1000
800
600
400
200
Wavenumber (cm^{-1})

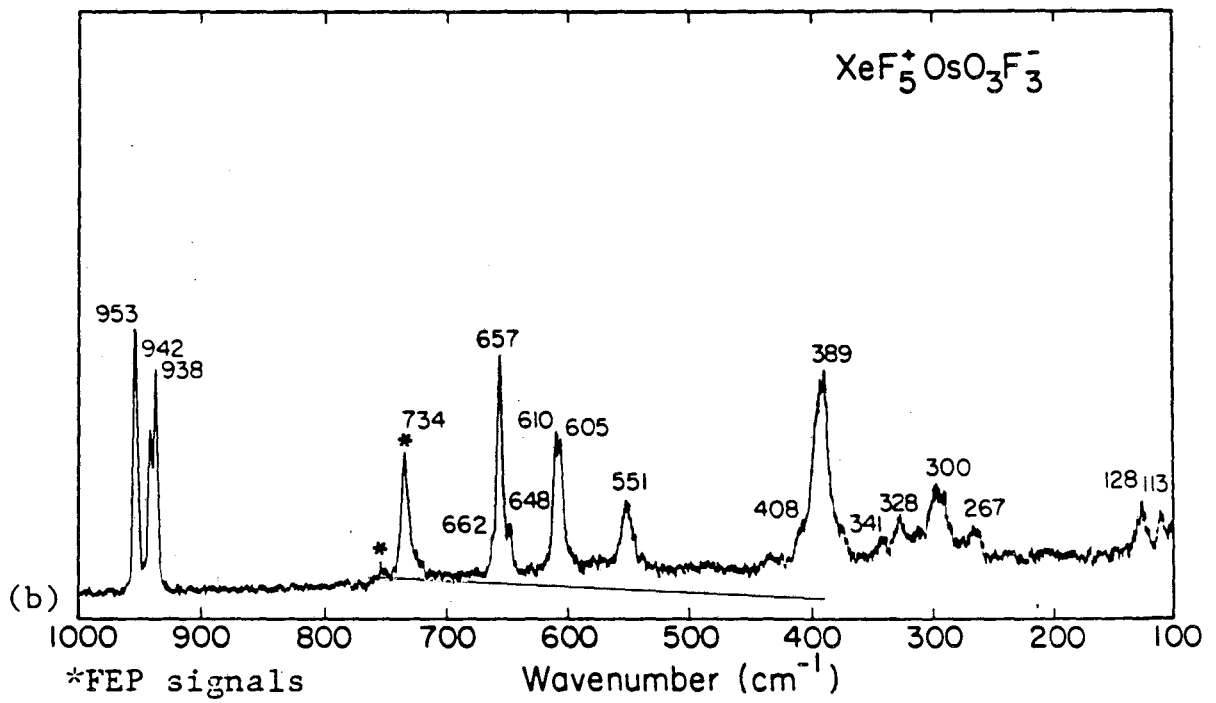
(b)
$XeF_5^+OsO_3F_3^-$
953
942
938
734
657
662
610
605
648
551
408
389
341
328
300
267
128
113
1000
900
800
700
600
500
400
300
200
100
*FEP signals
Wavenumber (cm^{-1})

Fig. 7

CHAPTER 3

INTERACTION OF HF WITH XeF_2, KrF_2 AND KrF_2 SALTS OF AuF_5

I. Introduction

Because of its high polarity and its chemical inertness, HF has been the best solvent available for the fluorides of the noble gases, xenon and krypton, and their derivatives. KrF_2 has very high solubility[1] in HF (16.4 moles/1000 g HF at 0°C) and XeF_2 is fairly soluble (6.38 mole/1000g HF at -2°C) too. BrF_5 is a good solvent for KrF_2 and its derivatives but is subject to oxidation[2,3] by KrF^+ and $Kr_2F_3^+$ species to BrF_6^+. Although ClF_5 is more stable, at low temperature, towards KrF^+ and $Kr_2F_3^+$ (see chapter 6 for the discussion of the attempts to prepare ClF_6^+), the solubilities of these salts in ClF_5 are very low.

Although the Raman spectroscopic studies of the solids $KrF^+M_2F_{11}^-$, $KrF^+MF_6^-$ and $Kr_2F_3^+MF_6^-$ have been reported,[3-5] only nmr studies had been made on the solutions of these species. The $Kr_2F_3^+$ entity has been reported to have a symmetrical V-shaped structure in BrF_5 solution[4] which is different from the asymmetric V-shaped structure in the crystalline salt $Kr_2F_3^+SbF_6^-$ as derived from Ramon spectroscopic data.[4] In this chapter, Raman spectra of the salts of KrF_2 with AuF_5 in HF solution are reported and compared with the solid compounds. We have found that the V-shaped $Kr_2F_3^+$ species is asymmetric in HF solution.

Strong interaction of XeF_2 and KrF_2 with HF are reported here. Three different types of fluorine atom environment are established for the F atom in XeF_2 dissolved in HF, whereas only one is found in the case of KrF_2. KrF_2 in HF solution is similar to KrF_2 in the crystalline solid.

Raman spectroscopy in the region from 2500 cm^{-1} to ~4000 cm^{-1} is also employed to measure the degree of polymerization of liquid HF. Both XeF_2 and KrF_2 are very effective in breaking up $(HF)_n$ chain polymers. The mechanism of this "de-polymerization" is discussed.

II. Experimental

A. Preparation. Sapphire reaction tubes of 1/4" O.D. were used in this study. A nylon swagelok nut fitted with the teflon ferrules was used to connect the sapphire tube to the Monel Whitey value (M-1KS4).

KrF_2 was synthesized by photolyzing a mixture of Kr and liquid F_2 at liquid nitrogen temperature using a high pressure mercury lamp (1000 watts). Experience showed that a sapphire reaction vessel gives much better yileds of KrF_2 than when teflon FEP reaction tubes were used. Because of the very high thermal expansion coefficient of the sapphire, a heating device had to be used to keep the "neck" of the sapphire reaction tube close to the swagelok connector at a temperature of 0°C or warmer. When the temperature of the neck of the sapphire tube was allowed to cool to -50°C a leak would result due to the contraction of the sapphire tube.

Salts of KrF_2 and AuF_5 were prepared as previously reported,[3,6] the KrF_2 rich salts of $Kr_2F_3^+AuF_6^-$ and $Kr_2F_3^+AuF_6^-(KrF_2)_n$ were prepared by permitting a large excess of KrF_2 to interact with Au powder in HF solution at ~-50°C. The $KrF^+AuF_6^-$ salt was obtained by warming the HF solution of $Kr_2F_3^+AuF_6^-$ or $Kr_2F_3^+$ to room temperature. When the $Kr_2F_3^+$ salts decomposed in the solution, the greater part of the $KrF^+AuF_6^-$ would precipitate out of the HF solution because of its lower solubility.

B. Raman spectra. The Raman spectra of the salts of KrF_2 and AuF_5 were obtained by using the red line at 6471Å of the krypton laser. For the study of the HF solutions, since the sapphire tubes exhibited strong fluorescence in the H-F stretching region with the red excitation, it was, in this case, necessary to employ either the blue (4880Å) or, preferably, the purple (4579Å) laser lines, particularly for scan from 2500 cm^{-1} to ~4000 cm^{-1}.

The Raman spectra of the solids were obtained from the solid in contact with the HF solution from which they had been precipitated by cooling that solution. The Raman spectra of the solutions were recorded at various temperatures, ranging from -50°C to room temperature. Care was exercised, when taking the Raman spectra, to ensure the extensive decomposition of the very unstable KrF_2 rich compounds did not occur. When bubbles of Kr and F_2 gases were seen, the laser light was blocked and adequate cooling was ensured. These solutions decompose rapidly above 0°C.

III. Results and discussion

A. KrF_2 solid and solution. Krypton difluoride is very soluble in pure hydrogen fluoride. It has $D_{\infty h}$ symmetry thus only the symmetrical stretching ν_1 mode is active in the Raman.[7,8] Its Raman spectra, in both the solid phase and in HF solution, are given in Fig. 1.

As expected we see mainly one narrow band at 462 cm^{-1} in the solid and at 465 cm^{-1} in solution. In the case of the solid, some additional features appear at low frequency (88, 69 and 40 cm^{-1}) which should be the external vibrations of the crystals. At 461.8 cm^{-1}, we see also the $2\nu_2$ vibration enhanced by Fermi-Resonance with ν_1.

The Raman spectra of the HF solutions give no evidence of dissociation: nothing can be attributed to the KrF^+ or $Kr_2F_3^+$ vibrations. The broad band at 550 cm^{-1} characterizes only the libration of the solvent molecule.[9] In HF, KrF_2 retains its molecular structure, but some interaction occurs with the solvent because the value of ν_1 in solution (465 cm^{-1}) is higher than in gas phase (449 cm^{-1}) where the molecules are isolated.[8]

Scheiner and his coworkers[10] have evaluated the charge on the fluorine atoms in KrF_2 and derive Q = 0.45 from their ^{19}F nmr data. This value is almost identical with the vaue of the charge on fluorine atom in the hydrogen fluoride molecule. Thus, it is believed that the KrF_2 interacts with HF molecules by insertion in the multimers of this solvent. At 20°C, pure HF contains essentially hexamer chains[11] so at low concentration KrF_2 must interact by hydrogen bonding as follows:

$$(FH)_6 \ldots F - Kr - F \ldots (HF)_6$$

When the concentration of KrF_2 increases the molecular ratio HF/KrF_2 decreases and KrF_2 interacts with smaller multimers of HF. This suggests impact upon the stretching vibration of HF. For a multimer, the frequency difference $\Delta\nu$ between maximum of I_{vv} and I_{vH} depends upon the number n of molecules in the multimer, when n decreases, $\Delta\nu$ decreases.[12]

In Table I, the value for $\Delta\nu$ at various KrF_2 concentration are reported, and its variation agrees well with the prediction. This indicates KrF_2 is probably inserted into multimer chains of HF. This hy-

drogen bonding insertion of KrF_2 in the HF multimer structure accounts nicely for the high solubility of KrF_2 in HF.

B. XeF_2 solid and solution in HF. XeF_2 also had $D_{\infty h}$ symmetry and only one vibration, ν_1, is therefore expected in the Raman. Although the spectrum of the solid agrees well with this expectation (see Fig. 2a), the spectra of the solutions in HF (see Fig. 2b,c) are not so readily interpreted.

At all concentration of XeF_2 in HF, there is a broad Raman band which results from the superposition of three bands, at ~540, ~510 and ~472 cm^{-1}. The characteristic vibration[13] of $Xe\text{-}F^+$ ion at 620 cm^{-1} does not appear, hence the F^- exchange with HF seems to be unlikely. Therefore the broad band observed in the ^{19}F nmr of these solutions cannot be attributed to such exchange.[14] The temperature effect on the Raman spectra (see Fig. 3) shows a decrease of the central peak intensity with lowering temperature but the bands at 540 and 472 cm^{-1} are always present with the same relative intensities. The central peak (510 cm^{-1}) is associated with a vibration derived from species A, and the satellite peaks (540 cm^{-1} and 472 cm^{-1}) derived from vibrations of species B. The reversible temperature effect indicates that the two species are in equilibrium.

$$\text{solvent molecules} + A \rightleftharpoons B + \text{solvent molecules}$$

The species A must be the symmetrical form of XeF_2 because its frequency agrees well with the ν_1 value observed in the solid XeF_2 (Fig. 2a). The nature of the species B is indicated from a comparison

of its frequencies with those of XeF_2 species in[15] the compounds $XeF_2(XeF_5^+AsF_6^-)_2$ and $XeF_2(XeF_5^+AsF_6^-)$. For the former compound, the crystallographic structure shows that XeF_2 is symmetrical because it has a symmetrical environment of XeF_5^+ cations. The XeF_2 in this salt has only one Raman band at 496 cm^{-1}. In the second salt, XeF_2 has a disymmetrical enviornment of XeF_5^+, which produces a disymmetrical molecule of XeF_2. In this case the XeF_2 is characterized by two bands at 559 cm^{-1} and 433 cm^{-1}. We note that XeF_2 is very sensitive to the symmetry of its environment. By comparison with the salts, it appears probable that XeF_2, in HF solution, can assume disymmetric shape in species B. This disymmetric XeF_2 gives rise to the Raman bands at 540 and 472 cm^{-1}.

There must be rapid exchange between form A and B of XeF_2, in the HF, to account for the broad bands observed[14] in the ^{19}F nmr. The interaction of XeF_2 and HF is very sensitive to temperature, and the XeF_2 concentration at saturation decreases quickly with the temperature. The effect is also clearly evident in the Raman spectra of solutions in the HF stretching region (see Fig. 4). The band is broader than in pure HF, being extended both on the low frequency and high frequency side. The disymmetric XeF_2 is on the way to becoming an ion pair $FXe^+\cdots F^-$. The more anionic component of this species will therefore hydrogen bond to HF more strongly than the F ligand of symmetrical XeF_2. Such a strong interaction tend to produce smaller HF containing speies (e.g. FHF^-, $FHF\cdots HF^-$ etc.) than the multimers associated with pure HF, or even symmetric XeF_2 and HF system.

C. $\underline{KrF^+AuF_6^-}$. The Raman spectrum of this solid is given in Fig. 5a. More vibrations are observed than expected for a diatomic cation and an isolated octahedral anion:

$Kr-F^+$ ---> $\nu_1(Kr-F^+)$

ν_1 symmetrical stretching, A_{1g}

$AuF_6^-(O_h)$ ---> ν_2 symmetrical stretching, Eg

ν_5 symmetrical deformation, T_{2g}

As in the case of other salts[4] of $KrF^+MF_6^-$, a strong anion-cation interaction must exist. This interaction produces a distorsion of the octahedral anion by the formation of a fluorine bridge. Following Sladky et al.,[13] it is appropriate to suppose a structure:

$$F-Kr^+-----F-AuF_5^-$$

The symmetry group of AuF_6^- is at best C_{4v} and can be as low as C_s. Table II represents the correlation between O_h, C_{4v} and C_s symmetry. In C_{4v} and C_s symmetry, all vibrations are active in the Raman. The observation supports this representation and their interpretation has been aided by previous studies[4] involving $XeF^+SbF_6^-$, $XeF^+AsF_6^-$, $KrF^+AsF_6^-$ and $KrF^+SbF_6^-$.

The frequency of ν_1 is insensitive to the change in symmetry and it is situated at 599 cm^{-1}, not much shifted from ν_1 in O_h species as observed by Leary[16] et al. at 595 cm^{-1}. In the isolated[16] AuF_6^-, ν_2 has a very low intensity at 520 cm^{-1}. In $KrF^+AuF_6^-$ it has two compo-

nents as is appropriate for C_{4v} symmetry, these components are therefore assigned to ν_2 (529 cm^{-1}) and ν_5 (542 cm^{-1}) in C_{4v} symmetry.

The ν_3 band in O_h symmetry is only active in the infrared. It splits, under C_{4v}, into two bands ν_4 and ν_8, both are active also in the Raman. The ν_8 vibration is most antisymmetrical stretching of the group AuF_5, and cannot be very far from the value of ν_3 in O_h AuF_6^-. Thus, we attribute this vibration to peak at 650 cm^{-1} (but there is a weak peak at 670 cm^{-1} also observed). The ν_4 vibration represents the stretching vibration of the fluorine bridge F---Au, we locate this mode at 470 cm^{-1}.

For O_h symmetry, ν_4 is active only in infrared but under C_{4v}, there are two components, ν_3 and ν_{11}, each active in the Raman and infrared. The ν_3 is the symmetrical deformation of the group AuF_4 and ν_{11} the deformation of the bridge F---AuF_5. By comparison with the value of ν_3 in O_h symmetry, we select ν_3 (C_{4v}) at 278 cm^{-1} and ν_{11} at 266 cm^{-1}.

From the O_h-C_{4v} correlation (see Table II), ν_5 (O_h) must split into two vibration ν_7 and ν_9, but in this range of frequency the spectrum is more complicated and we observed three peaks at 234, 225 and 220 cm^{-1}. We shall come back later on this splitting.

The ν_6 band can only be calculated[17] because it is inactive in Raman and in infrared spectroscopy. But this value is usually not far from $\nu_5(O_h)/\sqrt{2}$. In this case, the evaluation gives ν_6 = 159 cm^{-1} and thus we attribute the ν_6 and ν_{10} vibration, in C_{4v} symmetry, to the band located at 162 cm^{-1}.

The attribution of the KrF^+ cation is easier. We locate the $\nu(Kr-F^+)$ at 601 cm^{-1} which is in the frequency range found experimentally[4] and theoretically.[18] Expectations for the vibration of the bridge $\nu(Kr...F)$ agree well with the value of the band at 343 cm^{-1}, and is comparable with some fluorine bridges of xenon compounds.[13] Finally, we can attribute the band at 134 cm^{-1} with confidence to the deformation of the bridge $\nu_\delta(F-Kr\cdots F)$. These assignments are given in Table III.

The C_{4v} symmetry accounts for the Raman spectrum of $KrF^+AuF_6^-$ quite well, but in the structures[19,20] of the solid $XeF^+AuF_6^-$ and $XeF^+ReF_6^-$, the fluorine bridges are not linear and the symmetry of the formula unit is only C_s. The splittings that we observe on ν_5 (three bands) indicates this symmetry. Moreover, the observed spectrum shows two bands in the region of ν_8 (670 and 650 cm^{-1}) when only one band is anticipated in C_{4v} symmetry. Threrefore, the compound $KrF^+AuF_6^-$ is better represented by C_s symmetry, with a bent fluorine bridge:

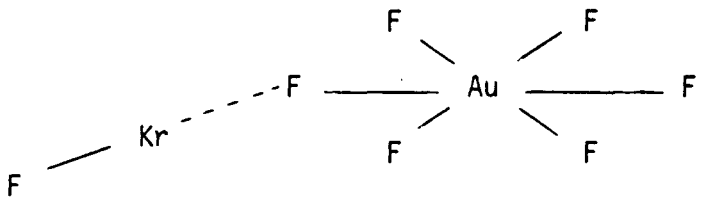

Solution of the $KrF^+AuF_6^-$ salt in HF (in which it is slightly soluble) gives a Raman spectrum (Fig. 6a) which is very differnt from that of the solid (Fig. 5a). In the solution spectrum there are only two strong bands. The most intense one at ~600 cm^{-1} corresponds to the superposition of $\nu(Kr-F^+)$ and $\nu_1(AuF_6^-)$. The second one at 220 cm^{-1} corresponds to ν_5 of AuF_6^-. The weak band at 150 cm^{-1} is attributable to the

stretching vibration of the hydrogen bond in HF.[9] The ν_2 (O_h, AuF_6^-) vibration or its lower symmetry relatives (ν_2 and ν_5 in C_{4v}) is not observed but the appearance of a weak peak at 645 cm^{-1} indicates a remnant of ν_3 (AuF_6^-), indicative of symmetry lower than O_h. The departure from O_h symmetry is, however, unlikely to be great. The KrF^+ cation is probably bonded to F of a solvent molecule, which is then bonded to an $(HF)_n$ multimer.

D. $\underline{Kr_2F_3^+}\underline{AuF_6^-}$. This salt is very unstable and all the spectra were taken below -20°C. Few salts of $Kr_2F_3^+$ have been reported in the literature. The solid $Kr_2F_3^+MF_6^-$ have been studied,[4,21] but the Raman spectra of the solutions in HF had not been examined. The Raman spectrum of solid $Kr_2F_3^+AuF_6^-$, given in Fig. 5b, shows a quasi-octahedral symmetry because no splitting in the O_h assignments of the vibrational modes is discerned. For example, it is not possible to observe a doublet in the ν_5 peak even under high resolution. But the anion should be slightly deformed because the ν_3 vibration at 650 cm^{-1} is not completely inactive. The ν_2 vibration is observed at 530 cm^{-1} under signal of high gain. It is safe to conclude that the interaction between the ions in this salt are less important than in the salt of $KrF^+AuF_6^-$. The highly polarizing KrF^+ cation interacts strongly with electron-rich centers and that is why the AuF_6^- in $KrF^+AuF_6^-$ is appreciably distorted. In the $Kr_2F_3^+$ case, the KrF^+ interacts mainly with KrF_2 hence the AuF_6^- anion approaches O_h symmetry. This implies that the F ligands of KrF_2 are more electron rich than the F ligands in AuF_6^-.

The Raman spectrum (see Fig. 5b and Table III) represents the characteristics bands of $Kr_2F_3^+$ as interpreted by Gillespie and his coworker[4] on the basis of a disymmetrical cation:

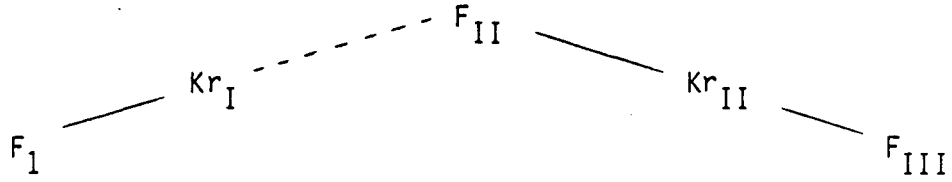

This disymmetrical cation can be regarded, as a first approximation, as a complex of a KrF^+ ion and KrF_2 molecule. This is different from $Xe_2F_3^+$ where one negative fluorine is solvated by two XeF^+ ions.[22] The $Kr_2F_3^+$ cation stretching vibrations are assigned as in Table III. The spectrum shows one band at 182 cm^{-1}, not far from the value of the deformation modes (232 cm^{-1}) for pure KrF_2. Thus, this band is attributed to the deformation of the angle $F_{II}Kr_{II}F_{III}$.

In the HF solution the bands of $Kr_2F_3^+$ are slightly broader than in the solid (Fig. 6b) and the vibrations at 566, 329 and 182 cm^{-1} can clearly be seen. This shows $Kr_2F_3^+$ persist in the HF solution and retains the same symmetry as in solid. Thus, this is in contrast with that Gillespie and his coworkers[4] concluded from ^{19}F nmr studies of $Kr_2F_3^+$ in BrF_5 solution that the cation had C_{2v} symmetry. That is possible for that solvent but it is also possible that rapid ^{19}F exchange could have masked an underlying C_{2v} symmetry. It is probable that the slightly broader bands observed in the solution Raman (compare with the solid Raman) derive from a multiple of species including the extreme

forms shown below:

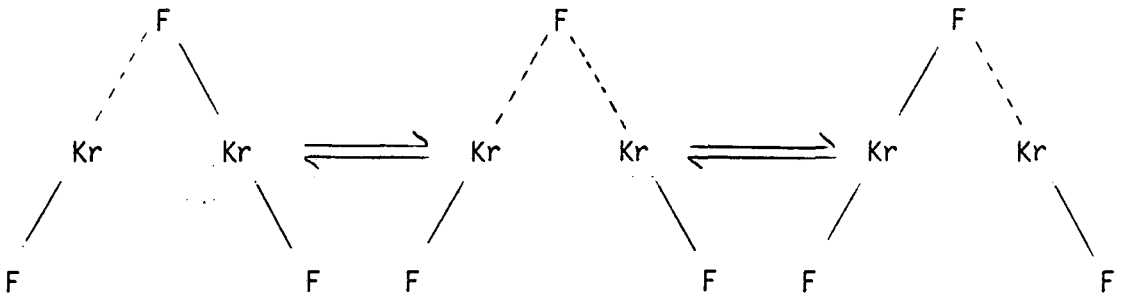

The positioning of solvent molecules may well determine the extent of the disymmetry.

E. $\underline{Kr_2F_3^+AuF_6^-(KrF_2)_n}$. In the presence of an excess KrF_2 in the preparation of $Kr_2F_3^+AuF_6^-$ another salt precipitates which contains some molecules of KrF_2. Gillespie and his coworker[4] found similar behavior for salts of $Kr_2F_3^+AsF_6^-$ and $Kr_2F_3^+SbF_6^-$. They formulate these compounds as $Kr_2F_3^+MF_6^-(KrF_2)_n$.The Raman spectrum of solid $Kr_2F_3^+AuF_6^-(KrF_2)_n$ (Fig. 5c) agrees well with this formulation. The spectrum reveal simultaneously the vibration of AuF_6^- (598 and ~225 cm^{-1}), KrF_2 (465 cm^{-1}) and $Kr_2F_3^+$ (562, 555, 471, 305 and 187 cm^{-1}). Evidently the interactions between KrF_2 and the ions must be weak because the frequencies of $Kr_2F_3^+$ and KrF_2 are not greatly affected. The presence of a neighboring peak at 471 cm^{-1} to the ν_1 (KrF_2) at 465 cm^{-1} indicates that there is some coupling between KrF_2 species. Unfortunately the absence of detailed structural information limits comment on such subtlties.

Raman spectrum of the HF solution of $Kr_2F_3^+AuF_6^-$ $(KrF_2)_n$ (Fig. 6c) is similar to that of $Kr_2F_3^+AuF_6^-$ (Fig. 6b) although the strongest peak is now due to KrF_2 (467 cm^{-1}). AuF_6^- vibrations are seen at 600 cm^{-1} (ν_1) and 216 cm^{-1} (ν_5), the reminant ν_3 at 648 cm^{-1} again indicates slight distortion of AuF_6^- from O_h symmetry. The bands attributable to $Kr_2F_3^+$ are seen at 564, 328 and 180 cm^{-1} indicates again that it retains the same symmetry as in the case of $Kr_2F_3^+AuF_6^-$.

REFERENCES

1. N. Bartlett and F. O. Sladky, "The Chemistry of krypton, xenon and radon", in "comprehensive Inorganic Chemistry", Pergamon Press Oxford and New York.
2. R. J. Gillespie and G. J. Schrobilgen, Inorg. Chem., 13, 1230 (1974).
3. V. B. Sokolov, N. V. Prusakov, A. W. Ryzhkov, Yu. Y. Drobysheveskii and S. S. Khovoshev, Akad. Nauk. SSSR, 229, 884 (1976).
4. R. J. Gillespie and G. J. Schrobilgen, Inorg. Chem., 15, 22 (1976).
5. B. Frelec and J. H. Holloway, Inorg. Chem., 15 1263 (1976).
6. J. H. Holloway and G. J. Schrobilgen, J. Chem. Soc. Chem. Comm., 623 (1975).
7. J. J. Turner and G. C. Pimentel, Science 140, 974 (1963).
8. H. H. Classen, G. L. Goodman, J. G. Malm, and F. Schreiner, J. Chem. Phys., 42, 1229 (1965).
9. I. Scheft, A. J. Perkins, J. Inorg. Nucl. Chem., 38 665 (1976).
10. F. Schreiner, J. G. Malm and J. C. Hindman, J. Amer. Chem. Soc., 87 25 (1965).
11. B. Desbat, Ph.D. Thesis, Universite de Bordeaux, France, 1980.
12. R. Zbinden, "Infrared spectroscopy of high polymers", Ed. Academic Press, London, 1964, p. 134.
13. F. O. Sladky, P. A. Bulliner and N. Bartlett, J. Chem. Soc., A 2179 (1973).

14. J. C. Hindman and A. Srirmickas, in "Noble Gas Compounds", H. H. Hyman ed. University of Chicago Press, Chicago and London, 1963, p. 251.

15. B. W. McQuillan, Ph.D. Thesis, University of California, Berkeley, 1981.

16. K. Leary and N. Bartlett, J. Chem. Soc. Chem. Comm., 903 (1972) and Inorg. Chem., 13 775 (1974).

17. K. Nakamoto, "Infrared and Raman Spectra of Inorganic and Coordination Compounds", 1978, third edition, Ed. J. Wiley and Sons, New York, p. 156.

18. B. Lui and H. F. Schaefer, J. Chem. Phys., 55 2369 (1971).

19. H. Zalkin, D. L. Ward, R. N. Biagioni, D. H. Templeton and N. Bartlett, Inorg. Chem., 17 1318 (1978).

20. N. Bartlett, M. Gennis, D. D. Gibbler, R. B. Morrell and A. Zalkin, Inorg. Chem., 12 1717 (1973).

21. B. Frlec and J. H. Holloway, J. Chem. Soc. Chem. Comm., 89 (1974).

22. F. O. Sladky, P. A. Bulliner, N. Bartlett, B. G. DeBoer and A. Zalkin, J. Chem. Soc. Chem. Comm., 1048 (1968).

Table Contents

Table I
ν(H-F) of KrF_2/HF Solutions

	$\nu(I_{VV})$	$\nu(I_{VH})$	$\Delta\nu = \nu_{VH} - \nu_{VV}$
Pure HF	3269	3460	195 cm^{-1}
Solution KrF_2/HF diluted	3315	3490	175 cm^{-1}
Solution KrF_2/HF Saturated	3425	3525	100 cm

Table II

A correlation diagram and Raman fundamentals assignments for AuF_6^- anions in $Cs^+AuF_6^-$(s), $KrF^+AuF_6^-$(s) and $Kr_2F_3^+AuF_6^-$(s)

O_h		C_{4v}			C_s	
$Cs^+AuF_6^-$ (ref. 10)		$Kr_2F_3^+AuF_6^-$			$KrF^+AuF_6^-$	
$\nu_1(A_{1g})$	595 (cm^{-1})	$\nu_1(A_1)$	599	ν(MFax)	$\nu(A')$	599
$\nu_2(E_g)$	530	$\nu_2(A_1)$	530*	$\nu_{sym}(MF_4)$	$\nu(A')$	529
		$\nu_5(B_1)$	-	$\nu_{sym}(MF_4)$ out of plane	$\nu(A')$	542
$\nu_3(T_{1u})$	-	$\nu_4(A_1)$	-	ν(M---F)	$\nu(A')$	470
		$\nu_8(E)$	650	$\nu_{asy}(MF_4)$	$\nu(A')$	650
					$\nu(A'')$	670
$\nu_4(T_{1u})$	-	$\nu_3(A_1)$	-	$\delta_{sym}(MF_4)$ out of plane	$\nu(A')$	278
		$\nu_{11}(E)$	-	δ (F...MF_4)	$\nu(A')$	266
$\nu_5(T_{2g})$	224	$\nu_7(B_2)$	220	$\delta_{sym}(MF_4)$ in the plane	$\nu(A'')$	234
		$\nu_9(E)$		$\delta(F_{ax}-MF_4)$	$\nu(A')$	225
					$\nu(A'')$	220
$\nu_6(T_{2u})$		$\nu_6(B_1)$		$\delta_{asy}(MF_4)$ out of plane	$\nu(A')$	162
		$\nu_{10}(E)$		$\delta_{asy}(MF_4)$ in the plane	$\nu(A'')$	162

*observed in high-gain signal only.

Table III
Vibrational assignments for cations in $Kr_2F_3^+AuF_6^-$ and $KrF^+AuF_6^-$.

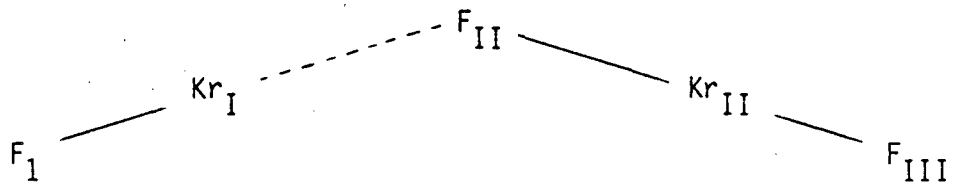

$Kr_2F_3^+$

Assignments	in AuF_6^-	in SbF_6^- (ref. 4)
$\nu(Kr_I-F_I)$	598*	603-594
$\nu(Kr_{II}-F_{III})$	560 555	555
$\nu(Kr_{II}-F_{II})$	465	456
$\nu(Kr_I-F_{II})$	302	330
$\delta(F_{II}-Kr_{II}-F_{III})$	182	180

F-Kr------F

ν(Kr-F)	601
V(kr----F)	343
δ(F-Kr--F)	143

*in Cm^{-1}

Figure Captions

Figure 1. Raman spectra of a) KrF_2 solid and b) KrF_2 in HF solution.

Figure 2. Raman spectra of a) XeF_2 solid, b) dilute XeF_2 in HF solution and c) saturated XeF_2 in HF solution.

Figure 3. Raman spectra of XeF_2 in HF solution.
(A), (B), (C): dilute XeF_2 solution at 20°C, -20°C and -40°C,
(D), (E), (F): saturated XeF_2 solution at 20°C, 0°C and -40°C.

Figure 4. Raman spectra of the pure HF and the XeF_2/HF solution, in the ν(H-F) stretching region.

Figure 5. Raman spectra of a) $KrF^+AuF_{6(s)}^-$, b) $Kr_2F_3^+AuF_{6(s)}^-$ and c) $Kr_2F_3^+AuF_6^-(KrF_2)_{n(s)}$, in sapphire tubes

Figure 6. Raman spectra of the HF solution of a) $KrF^+AuF_6^-$, b) $Kr_2F_3^+AuF_6^-$ and c) $Kr_2F_3^+AuF_6^-(KrF_2)_n$, in sapphire tubes.

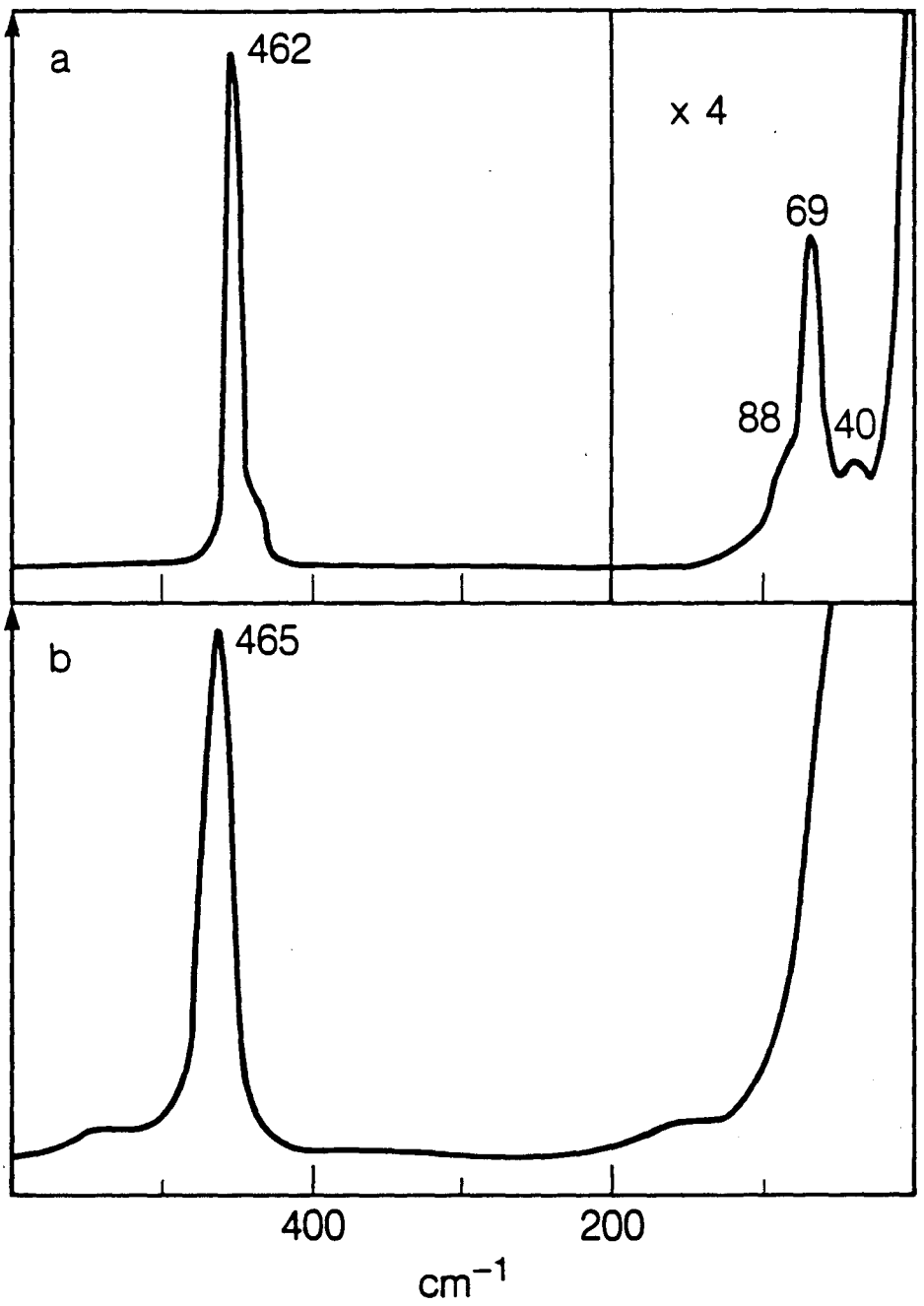

Fig. 1

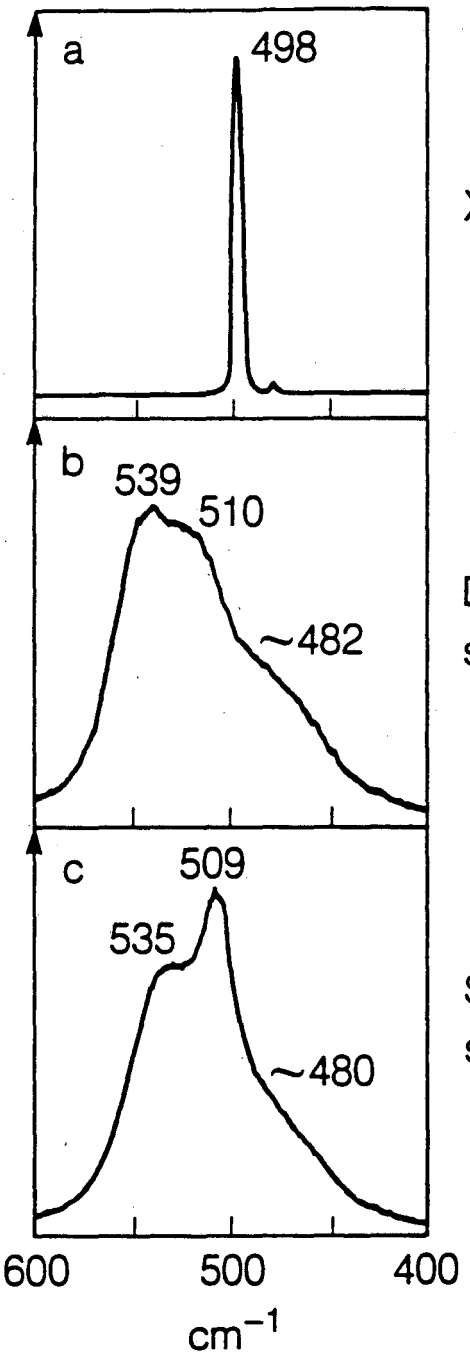

XeF_2 solid

Dilute XeF_2 solution in HF

Saturated XeF_2 solution in HF

XBL 8410-8910

Fig. 2

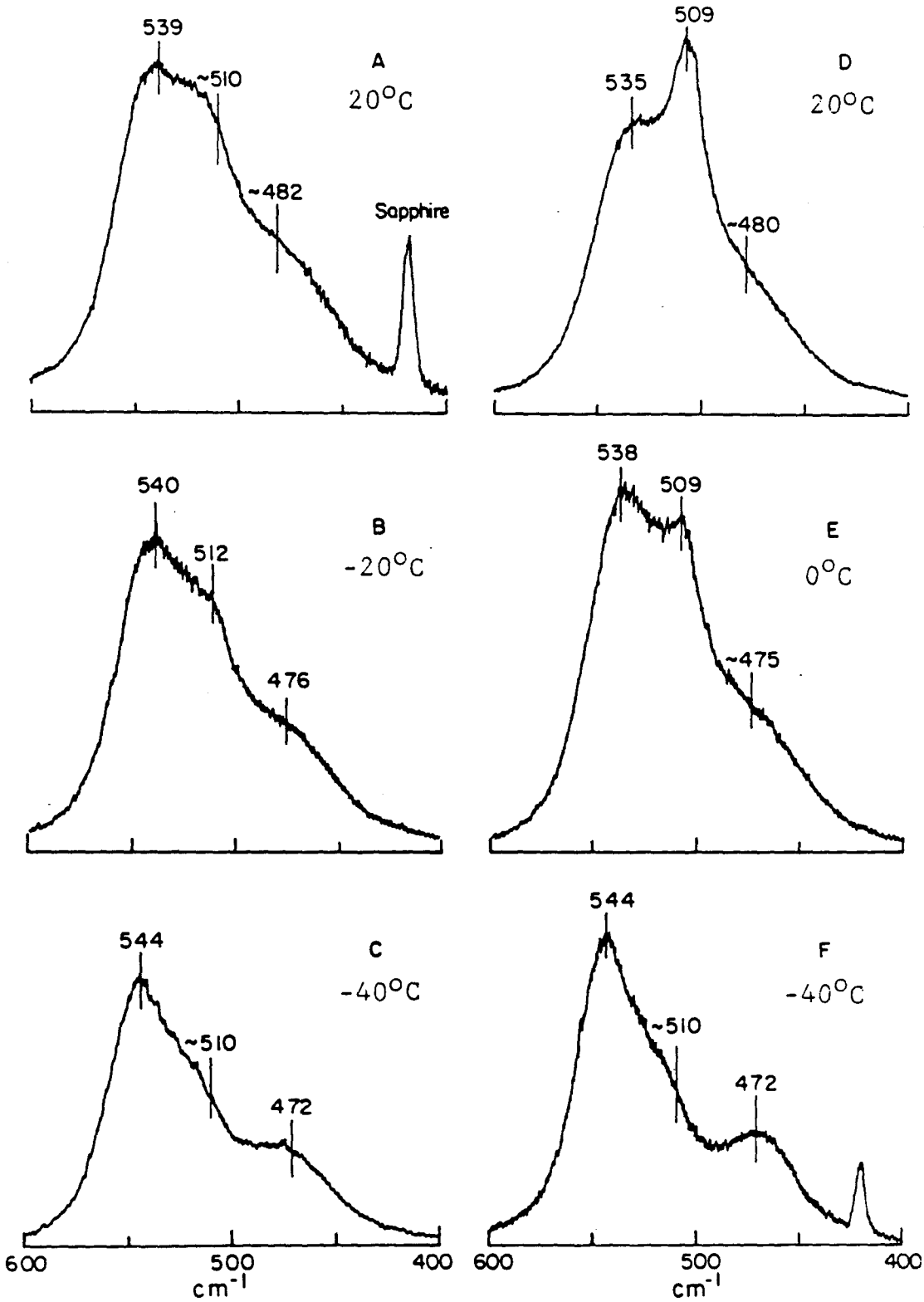

A.B.C.= dilute XeF_2 solutions
D.E.F.= saturated XeF_2 solutions

Fig. 3

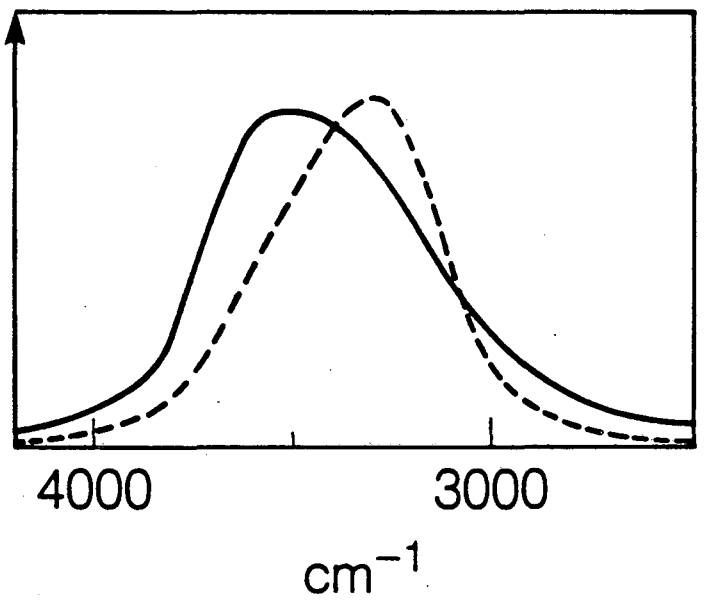

Pure HF (----) and XeF_2 solution in HF (——)

XBL 8410-8909

Fig. 4

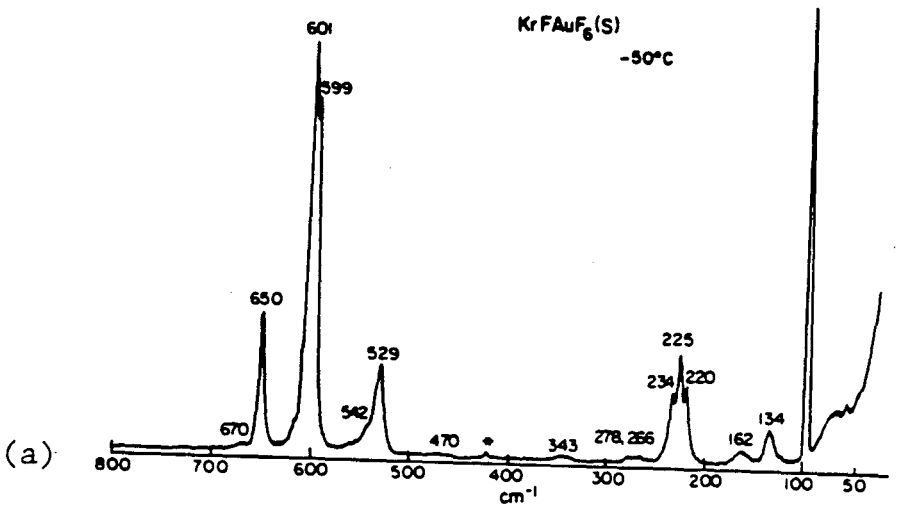

(a)

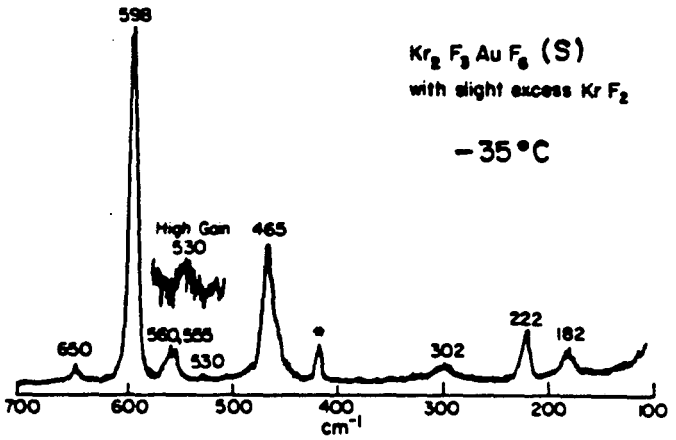

(b)

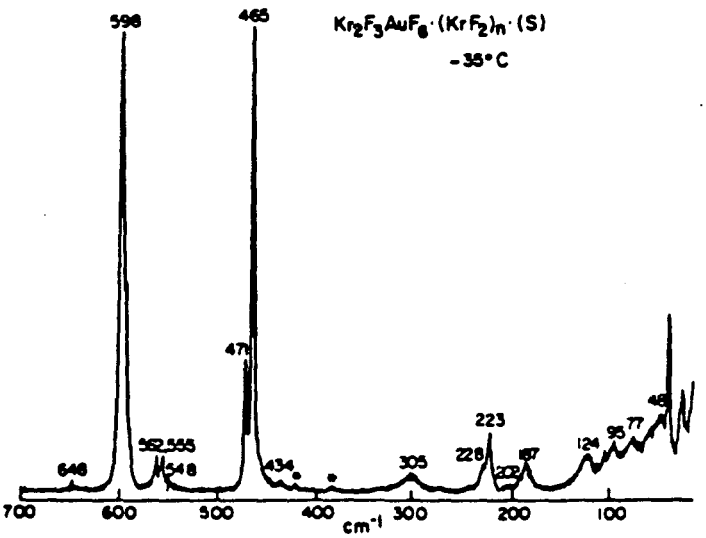

(c)

*sapphire signals

Fig. 5

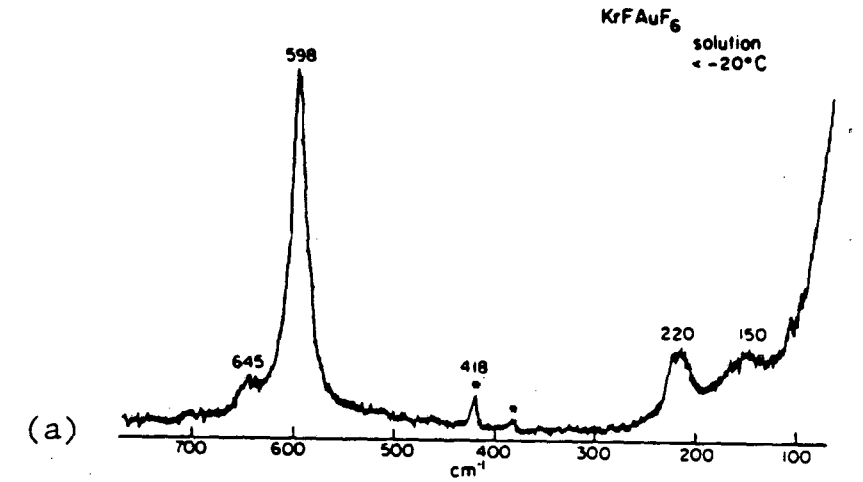

(a)

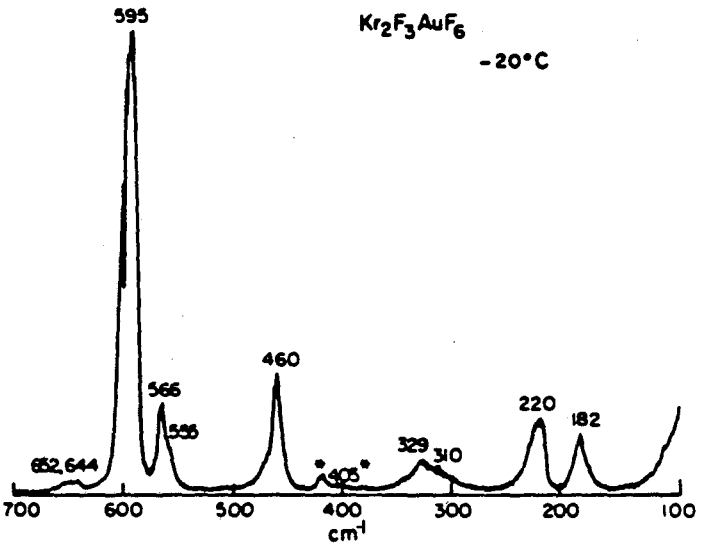

(b)

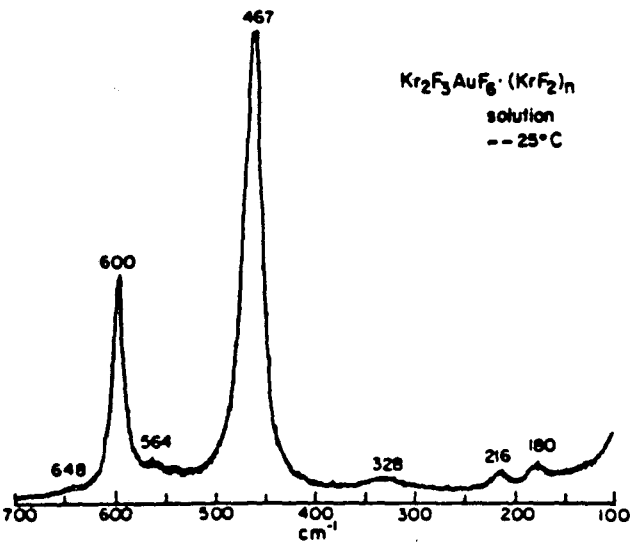

(c)

*sapphire signals

Fig. 6

CHAPTER 4

PREPARATION AND CHARACTERIZATION OF $ReF_6^+SbF_6^-$ AND $ReF_6^+AuF_6^-$

I. Introduction

Various hexafluoro-halogen cation species XF_6^+ (X = iodine,[1-4] bromine[5-7] and chlorine[8,9,10]) have been prepared, of which IF_6^+ is the most stable and most easily prepared. All of the XF_6^+ species have been well characterized by spectroscopic techniques, particularly vibrational and nmr spectroscopy. The crystallographic information is less complete. Unit cells have been given for $IF_6^+AsF_6^-$[2], $IF_6^+SbF_6^-$[3], $BrF_6^+AsF_6^-$[7] and $ClF_6^+AsF_6^-$ [10]. Beaton has described the structure of $IF_6^+AsF_6^-$ but this was based on x-ray powder diffraction data.[11,12] The only known metal relatives are ReF_6^+ salts of SbF_6^- and PtF_6^- reported by Jacob and his coworkers.[13,14] We have investigated these salts and related systems pertinent to our interest in the electron affinities of the third transition series hexafluorides. These investigations have involved a novel synthetic approach to the synthesis of ReF_6^+ salts and have led to the successful preparation of $ReF_6^+AuF_6^-$. The ReF_6^+ salts were also of interest because of their providing a basis for experiments aimed at the synthesis of analogous neptunium(VII) compounds (see Chapter 6).

II. Experimental section

A. Preparation of the low-temperature-structure orthorhombic $ReF_6^+SbF_6^-$ (β-$ReF_6^+SbF_6^-$). The best way to prepare the low temperature structure $ReF_6^+SbF_6^-$ is to oxidize ReF_6 using the KrF_2 salt of SbF_5 in WF_6 at ambient temperature. Excess ReF_6, in WF_6 solution, was transferred into

a reaction tube containing $KrF^+Sb_2F_{11}^-$. The mixture was warmed to ambient temperature. $KrF^+Sb_2F_{11}^-$, floating on top of the solution, reacted slowly with ReF_6 in WF_6, and a milky solid product precipitated. Absence of floating solid and the cessation of gas evolution indicated that the reaction was complete, then the mixture was cooled to -78°C and the non-condensible gases were pumped away at this temperature. WF_6 and excess ReF_6 were removed at 0°C under static vacuum. The finely powdered solid product was dried under vacuum at 0°C for a few minutes. The product gave a complicated x-ray powder pattern (Table I). The Raman spectrum, taken at low temperature, is characterized by a very intense peak at 796 cm^{-1}. The complete spectrum is shown in Fig. 1a and summarized in Table II. The sample remained solid for days at room temperature and for several hours when bathed in 4880 Å laser light. It decomposed within minutes in 5145 Å and 6471 Å radiation. The sample can be stored indefinately at dry ice temperature.

$KrF^+SbF_6^-$ can also be used for this preparation, but the reaction is more violent than when $KrF^+Sb_2F_{11}^-$ is used. Care must be exercised to moderate the reaction (e.g., low temperatures are needed) to prevent the formation of high temperature phase material (see the following section).

B. Preparation of high-temperature-structure-rhombohedral-$ReF_6^+SbF_6^-$ (α-$ReF_6^+SbF_6^-$). Two preparative methods were followed for the synthesis of α-$ReF_6^+SbF_6^-$:

(1) In a typical reaction of ReF_6 with KrF_2 salts of SbF_5 ($KrF^+SbF_6^-$ and $KrF^+Sb_2F_{11}^-$) a large excess of ReF_6 was condensed on top of $KrF^+Sb_2F_{11}^-$ in a FEP reaction tube. As the mixture was warmed up to ambient temperature without using any solvent, ReF_6 melted and reacted violently with $KrF^+Sb_2F_{11}^-$. The mixture was kept at room temperature for an hour to ensure completion of the reaction. The mixture was then cooled to -78°C so that the non-condensible gas (Kr) could be removed. ReF_6 was recovered, (for subsequent use) by distillation under static vacuum at 0°C and finally at room temperature. The solid product was subjected to a dynamic vacuum at 0°C for about one hour.

(2) A mixture of SbF_5 with excess ReF_6, in a fluorine atmosphere, contained in a quartz tube, was photolized using a Xenon lamp at room temperature. The reaction occurred very quickly and a white solid was formed at the bottom of the reaction tube. Excess F_2 was pumped away at -78°C and ReF_6 and ReF_7 were removed by distillation at room temperature. The solid product was subject to a dynamic vacuum at room temperature for a few minutes.

Both samples gave powder patterns resemble that of $Cs^+AuF_6^-$. The pattern was indexed on the basis of a primitive rhombohedral unit cell (see Table III). The Raman spectra, characterized by a very intense 796 cm^{-1} peak, are shown in Figs. 1b and 1c and are summarized in Table II. The sample can be stored indefinately at dry ice tempera-

ture but is not stable at room temperature. It liquefies and dissociates into its components within a few days. Although the dissociation pressure of the material was not measurable with the Helicoid gauge at room temperature (i.e. probably much less than 5 torr), the solid can be slowly pumped away at room temperature under dynamic vacuum. One can even observe the dissociation and vaporization when weighing the sample in the dry box. The volume of the Dri-Lab is very large relative to the sample sizes therefore equilibrium conditions could not be established. It is believed that dissociation is still significant at 0°C.

C. Observation of the structural transition: $\beta\text{-}ReF_6SbF_6 \dashrightarrow \alpha\text{-}ReF_6^+SbF_6^-$. Two studies of the structural transition are described below:

(1) A sample of the low-temperature-structure material $\beta\text{-}ReF_6^+SbF_6^-$, characterized by its Raman spectrum and X-ray powder pattern, was divided into two portions; each was stored in an FEP tube. One sample was kept at dry ice temperature while the other was kept at room temperature. Both samples were occasionally checked by their Raman spectra. The sample kept at room temperature changed completely to the high-temperature-rhombohedral material within a week while the sample kept at dry ice temperature remained as low-temperature-phase material. Keeping the high temperature phase sample at dry ice temperature over an extended period of time did not convert it back to the low-temperature-structural material.

(2) A low-temperature-structure sample, after being characterized by x-ray powder and Raman spectroscopy, was used to follow the structural transition in the 4880 Å laser beam. The sample, in a quartz capillary, was warmed to ambient temperature. Raman spectra, obtained by repeated scanning in the region from <600 cm^{-1} to ~800 cm^{-1}, were used to monitor the transition. The sequence is illustrated in Fig. 2. One can observe the rapid appearance of the peaks at 662 cm^{-1} and 688 cm^{-1}. The intensity of these new peaks increases at the expense of the original peaks at 652 cm^{-1} and 680 cm^{-1}. Two other changes were also observed: The doublet at 731 cm^{-1} and 735 cm^{-1} collapsed as a new peak at 733 cm^{-1} grew, and the weak peak at 600 cm^{-1} gave way to new weak peaks at 608 cm^{-1} and 623 cm^{-1}. The $\underline{\beta}$ to $\underline{\alpha}$ structure transition, with the sample bathed in the 4880 Å laser beam, was much faster than the ambient temperature conversion and was complete within a few hours. Lowering the temperature to about -100°C for several hours did not reverse the process. The X-ray powder pattern showed the solid to be largely of the $\underline{\alpha}$ form (rhombohedral).

D. Mixing of ReF_7 with SbF_5 in HF solution. Excess ReF_7 was mixed with SbF_5 in HF solution in a FEP reaction tube. The mixture was kept at room temperature for 2 days. ReF_7, which is not very soluble in HF, eventually dissolved completely and a light yellow, viscous, solution was obtained. No salt precipitation was observed by lowering the temperature to 0°C. Raman spectroscopy (Fig. 3) of this solution showed only the possibility of a trace of an ReF_6^+ salt, (which shows a strong

ν_1 band at 796 cm^{-1}) but a strong peak at 755 cm^{-1} was seen. The latter cannot be readily accounted for. A check of the ReF_7 starting material showed no impurity of ReF_6 which has a strong ν_1 band at 756 cm^{-1}. It is probable that the 755 cm^{-1} band is indeed due to ReF_6 but it is not clear how the reduction occurred. It was very difficult to remove HF from this solution even under dynamic vacuum at -23°C. This is typical of the behavior of SbF_5 in HF. No solid product was isolated.

E. An attempt to prepare $ReF_6^+AsF_6^-$. Excess ReF_6 in WF_6 solution was used to react with $O_2^+AsF_6^-$. After all of the solid $O_2^+AsF_6^-$ had disappeared, no solid precipitated from the cooled solution at ~0°C. The Raman spectra of this solution and the infrared spectrum of the vapor showed the presence of ReF_6, ReF_7, WF_6 and AsF_5. (The result was consistent with Beaton's[12] study that there was no salt formation when ReF_7 was mixed with AsF_5 in WF_6 solution.)

F. Attempts to prepare $ReF_6^+PtF_6^-$.

(1) Slight excess of PtF_6 was used to react with ReF_6 in a FEP tube at room temperature for two hours. A red solid was left after the volatiles were removed by distillation into another FEP tube. The infrared spectrum of this vapor revealed the presence of PtF_6 and ReF_7 only. The X-ray powder pattern of the solid showed it to be PtF_5. The description of the reaction was similar to that given in Jacob and Fahnle's[13] report. There was no sign of $ReF_6^+PtF_6^-$ formation as Jacob and Fahnle had suggested.

(2) Excess ReF_6 was used to react with PtF_6 in HF solution at room temperature. The dark red color of PtF_6 quickly disappeared. A brown solid remained after HF was slowly removed at -45°C and the other volatiles were distilled into another tube under static vacuum. The infrared spectrum of the volatiles revealed the presence of ReF_6, ReF_7 and HF only. X-ray powder data of the solid showed it to be PtF_4.

G. An attempt to prepare $OsF_6^+PtF_6^-$. Equal amounts of OsF_6 and PtF_6 were condensed into a FEP tube and the mixture was warmed to ambient temperature. No reaction was observed. The mixture was then kept at ambient temperature in a water bath and was irradiated using a mercury lamp for about one hour. The deep red color of PtF_6 vapor completely disappeared. A red solid was collected after F_2 was pumped away at -78°C and OsF_6 had been removed at 0°C under static vacuum. The X-ray powder pattern of the solid was that of PtF_5.

H. Attempts to prepare $ReF_6^+IrF_6^-$. This experiment was closely monitored by Raman spectroscopy.

(1) Reaction of IrF_6 with ReF_6. Nearly stoichiometric amounts of IrF_6 and ReF_6 were condensed into a sapphire tube containing excess WF_6 as a solvent. As the mixture was warmed to ambient temperature, the yellow IrF_6 and ReF_6 mixture melted and reacted very quickly to give a very deep greenish-purple color in the solution. This color gradually faded away and a bright yellow crystalline solid precipitated and finally, after several hours, became brownish. The Raman spectroscopic data (Fig. 4a) show that the final WF_6 solution contained molecular

ReF_6, ReF_7, IrF_6 and IrF_5. The crystalline solid was shown by Raman spectroscopy (Fig. 4b) to be identical with IrF_5 as prepared separately.[15]

When anhydrous HF was introduced into the reaction tube, most of the IrF_5 solid was dissolved and two layers of liquid were observed. At the bottom of the tube was the WF_6 layer which was light brown. Raman spectrum showed the presence of ReF_6, ReF_7 and small amounts of IrF_6. ReF_6 was always present, even when more IrF_6 was introduced into the reaction tube to convert ReF_6 to ReF_7. The HF layer, on top of the WF_6 solution, was also brown. Its Raman spectrum showed the presence of ReF_6, ReF_7, WF_6 and IrF_5. The ν_1 peak of IrF_6 at 702 cm^{-1} may be buried under the peak of IrF_5 in solution because the strongest peak of IrF_5 was shifted from its position of 719 cm^{-1}, in the solid, to a very broad and strong peak centered at 695 cm^{-1} in HF solution.

Most of the HF could be pumped away at -78°C but the last trace of HF was difficult to remove at this temperature and the resultant brown solution showed the presence of ReF_6, ReF_7, WF_6, IrF_6 and dissolved IrF_5, which now had a broad peak at 713 cm^{-1} (Fig. 4c).

IrF_6 also reacted with ReF_6 without the use of a solvent. A deep greenish-purple solid was observed at low temperature when the mixture of IrF_6 and ReF_6 was cooled with liquid nitrogen, this color quickly disappeared when the temperature was raised and a yellow colored vapor was observed in the reaction tube. A non-volatile yellow solid was formed. Throughout the reaction, the deeply colored solid can be reproduced simply by cooling the mixture to liquid nitrogen temperature. The Raman spectrum of the mixture revealed the presence of ReF_6, IrF_6,

ReF_7 and IrF_5. The yellow solid, when isolated from the volatiles, was identified as pure IrF_5 by its X-ray powder pattern and its Raman spectrum.

(2) Interaction of ReF_7 and IrF_5. To establish the reversibility of the reaction, i.e., $ReF_6 + IrF_6 \rightleftharpoons ReF_7 + IrF_5$, excess WF_6 and ReF_7 were condensed into a sapphire tube containing solid IrF_5. A brown color slowly developed in the WF_6 solution, but the reaction was much slower than with an IrF_6 and ReF_6 mixture. The Raman spectroscopy of the WF_6 solution indicates the presence of ReF_6, ReF_7, IrF_6 and IrF_5. The relative intensities of the two peaks attributable to ν_1 of ReF_6 (756 cm^{-1}) and ν_1 of IrF_6 (702 cm^{-1}) remained the same throughout the reaction and were observed to grow slowly with respect to the ν_1 of the WF_6 solvent (771 cm^{-1}). The most intense line (736 cm^{-1}) of the ReF_7 spectrum (ν_1) slowly decreased. After being kept at room temperature for nearly one week, the solution was finally warmed up to 50°C for a day and then cooled to ambient temperature. Since the Raman spectra did not change significantly with this last treatment, the reaction appeared to have reached equilibrium. The Raman spectrum of this equilibrium solution is shown in Fig. 5a.

(3) Observation of ReF_6^+ species in the ReF_6/IrF_6 system. There are indications, from the Raman spectroscopic study, of the possible existence of ReF_6^+ species in the WF_6 solution, which at room temperature contained ReF_6, ReF_7, IrF_6 and IrF_5 in equilibrium:

$$ReF_6 + IrF_6 \rightleftharpoons ReF_7 + \frac{1}{4}(IrF_5)_4$$

Conditions necessary for the observation of a Raman line attributable to ReF_6^+ were as follows:

(1) A sharp strong peak, not attributable to any of the molecular species mentioned above, was observed at 793 cm^{-1} when blue light excitation (4880 Å) was used (Fig. 5b).

(2) When the blue light irradiated only the solution, the 793 cm^{-1} line was not found (see Fig. 5a). The peak was observed only when the light irradiated the interface of the solution and the IrF_5 solid.

(3) The rest of the Raman spectrum did not change when the 793 cm^{-1} peaks was observed, i.e., there was no additional peak and there was no change of intensity of any other peak. There was no evidence of IrF_6^-, the counterpart of ReF_6^+ species, existing in the solution.

I. Attempts to prepare $ReF_6^+AuF_6^-$

(1) Oxidation of ReF_6 with $Kr_2F_3^+AuF_6^-$ in HF solution. Excess ReF_6 was used to react with $Kr_2F_3^+AuF_6^-$ in HF solution. The solution was slowly warmed up from -78°C to 0°C in an ice water bath. The reaction occurred vigorously at this temperature with much gas evolution. The build up of pressure from evolved gases was occasionally released to the vacuum-line manifold. The solution was eventually warmed up to room temperature to ensure the completion of the reaction. A yellow solid precipitated in the reaction tube. F_2, Kr and HF were pumped away at -78°C, the reaction tube was warmed up to ambient temperature and the other volatiles were recovered by distillation into another FEP tube. Infrared spectra of the volatiles showed the presence of

ReF_7. The Raman spectrum and the X-ray powder pattern of the yellow solid showed it to be AuF_3 only.

(2) Direct mixing of ReF_7 with AuF_5. AuF_5 was obtained by decomposing $KrF^+AuF_6^-$ under dynamic vacuum at room temperature. Excess ReF_7 was condensed on top of it and the mixture was kept in a water bath at $\geq 60^\circ C$ to melt and reflux the ReF_7. There was no sign of salt formation after the ReF_7 was removed.

In another reaction of ReF_7 with AuF_5, HF was used as a solvent. The mixture was kept at room temperature for one hour. There was no sign of salt formation after the volatiles were removed.

J. Preparation of $ReF_6^+AuF_6^-$. Excess ReF_7 was condensed onto a HF solution of $Kr_2F_3^+AuF_6^-$. The mixture was warmed up slowly to $0^\circ C$ and finally to room temperature for a minute to mix the reactants. It was then quickly cooled to liquid nitrogen temperature. HF was removed slowly under dynamic vacuum at $-78^\circ C$ overnight. The solid mixture was then quickly warmed to $\geq 60^\circ C$ in a hot water bath to melt the ReF_7 and to decompose $Kr_2F_3^+AuF_6^-$ or $KrF^+AuF_6^-$. At this point an interaction occurred with violent gas evolution. A light red solid was observed in the yellow ReF_7 liquid. Cessation of gas evolution indicated that the reaction was complete. The mixture was cooled to $-78^\circ C$ and Kr and F_2 were pumped off. Excess ReF_7 was recovered by distillation at $0^\circ C$. A reddish-orange solid remained. The product was stored at low temperature ($-78^\circ C$). The solid was extremely difficult to handle even in the dry atmosphere of the Dri-Lab. It "melted" when crushed for X-ray and Raman sample preparation. A fine powder was preparable by shaking the solid in the reaction tube at $-78^\circ C$. These powders gave the samples

for the Raman spectrum shown in Fig. 6a and the X-ray powder pattern given in Table IV.

K. Interaction of $ReF_6^+AuF_6^-$ with IF_7. Excess IF_7 was used to react with $ReF_6^+AuF_6^-$ at room temperature for 3 days. After removal of the volatiles, the Raman spectrum and the X-ray powder pattern of the yellow solid product showed it to be $IF_6^+AuF_6^-$. It contained a small amount of AuF_3 impurity. All of the $ReF_6^+AuF_6^-$ was consumed, i.e., the following displacement was complete:

$$IF_7 + ReF_6^+AuF_6^- \longrightarrow ReF_7 + IF_6^+AuF_6^-.$$

In another reaction, excess IF_7 was used to react with a mixture of $ReF_6^+AuF_6^-$ and AuF_5 (characterized by Raman spectroscopy) prepared in another reaction. The mixture was kept at room temperature for one day. The yellow solid was collected after the volatiles were removed. The Raman spectrum and the X-ray powder pattern indicated it to be $IF_6^+AuF_6^-$, again with small amounts of AuF_3 impurity. No AuF_5 remained, suggesting:

$$IF_7 + AuF_5 \longrightarrow IF_6^+AuF_6^-.$$

III. Discussion

A. Preparative aspects of $ReF_6^+MF_6^-$ salts

Jacob and Fahnle have described[13,14] the preparation of $ReF_6^+SbF_6^-$ from a gaseous mixture of ReF_7 and SbF_5 in a F_2 atmosphere in a nickel reactor at 250°C. In the present work it has also been made by reflux-

ing an SbF_5/ReF_7 mixture in a FEP tube at $\geq 60°C$. It is also obtained by oxidizing ReF_6 with photoexcited F_2 in the presence of SbF_5. The cleanest preparation, however, is via interaction of ReF_6 with KrF^+ salts of SbF_6^- and $Sb_2F_{11}^-$. The $Kr_2F_3^+SbF_6^-$ and $KrF^+SbF_6^-$ oxidants are more powerful than $KrF^+Sb_2F_{11}^-$ and usually have given the rhombohedral form of $ReF_6^+SbF_6^-$ directly. Interaction of ReF_6 with $KrF^+Sb_2F_{11}^-$ in WF_6, as solvent and moderator, usually gives a solid having a more complex X-ray powder pattern and a more complex Raman spectrum.

It is of interest that HF is not a practical solvent for ReF_6^+ salt formation. Thus the Raman spectrum of an SbF_5/ReF_7 solution in HF (Fig. 3) gives no convincing evidence of ReF_6^+ species, whereas there is clear evidence for the presence of molecular ReF_7 (strong band at 736 cm^{-1}). The strong and broad peaks at 667 cm^{-1} and 688 cm^{-1} are attributable to the Sb-F stretching in the HF solution. The strong and sharp peak at 755 cm^{-1} is not readily accounted for, although the frequency is nearly the same as that of ν_1 of ReF_6, (756 cm^{-1}). The vibrational spectrum of the starting ReF_7 show no evidence of that impurity. It is not clear how reduction of ReF_7 could have occured. The band (at 755 cm^{-1}) might be that of an ReF_7 solvate.

Beaton's failure[12] to prepare a salt $ReF_6^+AsF_6^-$ via interaction of ReF_7 with AsF_5 (in WF_6 solution) was confirmed in the present work. There were two attempts to make $ReF_6^+AsF_6^-$, one involved direct mixing of ReF_7 with AsF_5 in WF_6 and the other oxidation of ReF_6 with $O_2^+AsF_6^-$ in WF_6. Each failed. The results are consistent with the easy dissoc-

iation of $ReF_6^+SbF_6^-$ observed at room temperature (see below) since AsF_5 is known to be a poorer F^- acceptor than SbF_5.

There was some doubt about the existence of $ReF_6^+PtF_6^-$ at room temperature as claimed by Jacob and his coworker.[13] While our observations of the reaction are generally in agreement with theirs, our results showed no sign of the $ReF_6^+PtF_6^-$ salt formation at room temperature, although it is reasonable to suppose that the salt is a reaction intermediate. When excess ReF_6 was used, PtF_4 was formed as shown by its characterized X-ray power pattern.[16] Here we observe ReF_6 as a reducing agent capable of generating Pt(IV) from Pt(VI):

$$PtF_6 + 2ReF_6 \longrightarrow PtF_{4(c)} + 2ReF_7.$$

When excess PtF_6 was used the red solid was PtF_5, again, characterized by its x-ray powder photograph[17]:

$$PtF_6 + ReF_6 \longrightarrow PtF_{5(c)} + ReF_7.$$

To account for the above interactions it is plausible to suppose that the first step in the interactions of ReF_6 and PtF_6 is electron transfer:

$$ReF_6 + PtF_6 \longrightarrow [ReF_6^+PtF_6^-].$$

At room temperature we can suppose that the weak basicity of ReF_7 combined with a fluoride ion acceptor capability of PtF_5, which is insuf-

ficient to counter that weak basicity, leads to the transfer of F^- from anion to cation:

$$[ReF_6^+PtF_6^-] \longrightarrow ReF_7 + PtF_5(\text{monomer})$$

The behavior of $ReF_6^+SbF_6^-$ and $ReF_6^+AuF_6^-$ (see below) suggests that there is a considerable kinetic barrier for the latter type of process. Therefore, by carrying out the ReF_6 with PtF_6 interaction at low temperatures, it may be possible to obtain evidence for the $ReF_6^+PtF_6^-$ intermediate. Jacob prepared[14] his claimed $ReF_6^+PtF_6^-$ in reactions at low temperature, but his characterization is not convincing. The formation of $PtF_{4(c)}$ in the reaction with excess ReF_6 can be attributed to the reduction of PtF_5 monomer by ReF_6:

$$ReF_6 + PtF_5 \longrightarrow ReF_7 + PtF_{4(c)}.$$

but it is possible that a salt $(ReF_6^+)_2PtF_6^{2-}$ could also exist:[18]

$$ReF_6^+PtF_6^- + ReF_6 \longrightarrow (ReF_6^+)_2PtF_6^{2-}$$

and that the latter would, like $ReF_6^+PtF_6^-$, undergo F^- transfer:

$$(ReF_6^+)_2PtF_6^{2-} \longrightarrow 2ReF_7 + PtF_4.$$

The interaction ReF_6 with IrF_6 is the best documented study in this series. PtF_6 is a much more powerful oxidizer than IrF_6. The electron affinity of IrF_6 is apparently just high enough to strip the electron from ReF_6 to form ReF_6^+, but the F^- accepting ability of IrF_5 monomer (which should be comparable to that of PtF_5 monomer) is not great enough to stabilize the $ReF_6^+IrF_6^-$ salt at ordinary temperatures. Thus the salt dissociates into ReF_7 and IrF_5 and the latter polymerizes to $(IrF_5)_4$:

$$ReF_6 + IrF_6 \rightleftharpoons [ReF_6^+IrF_6^-] \rightleftharpoons ReF_7 + \tfrac{1}{4}(IrF_5)_4$$

The extraordinary feature of the reaction is the near equality of the redox couples ReF_7/ReF_6 and IrF_6/Ir_4F_{20}. Thus ΔG° must be close to zero for the equilibrium:

$$ReF_6 + IrF_6 \rightleftharpoons ReF_7 + \tfrac{1}{4}(Ir_4F_{20}).$$

The brown color in the solution is not attributable to any known molecular species in the reaction and the deep green-purple color observed at low temperature indicates that there is a charge-transfer process. Similar charge transfer colors are observed[19] in the interaction of the Xe with IrF_6 at low temperature (where a purple color was observed). This suggests the existence of $ReF_6^+IrF_6^-$ at least as a transient species. The sharp peak observed at 793 cm^{-1}, in the Raman spectra of the ReF_6/IrF_6 or ReF_7/IrF_5 reaction product, is close to the 796 cm^{-1} band of ReF_6^+ as observed in $ReF_6^+SbF_6^-$ and $ReF_6^+AuF_6^-$ (see below).

Observation of this peak only with 4880 Å blue radiation indicates a resonance Raman effect with the ReF_6^+ present only in low abundance. The absence of the peak from the solution spectrum is easily understood since ReF_6^+ salts are unlikely to be soluble in such a poor ionizing solvent as WF_6.

It is clear that an increase of temperature in the system:

$$ReF_6 + IrF_6 \rightleftharpoons [ReF_6^+IrF_6^-] \rightleftharpoons ReF_7 + IrF_5(\text{monomer})$$

would favor dissociation of the $ReF_6^+IrF_6^-$ salt into component molecules (ReF_7 and IrF_5 or ReF_6 and IrF_6). This is simply a consequence of the lower enthropy of $ReF_6^+IrF_{6(c)}^-$ relative to the separate molecular species. The deeply colored $ReF_6^+IrF_6^-$ solid was observed when the temperature was low.

The ReF_6/IrF_6 system offers an opportunity to evaluate the thermodynamic features such as the ionization energy of ReF_6, the F^- affinity of ReF_6^+, the electron affinity of IrF_6 and the other related thermodynamic properties. These thermodynamic aspects will be discussed later.

The observations that (1) ReF_7 does not form stable salts with AsF_5, PtF_5 and IrF_5 under the reaction conditions described, (2) that the presence of HF hinders the salt formation of $ReF_6^+SbF_6^-$ and (3) that $ReF_6^+SbF_6^-$ easily dissociates into its molecular components, all indicate that ReF_7 is a relatively poor F^- donor. It takes the best F^- acceptor, SbF_5 and AuF_5, to stablize ReF_6^+ salts. As in the preparation of SbF_6^- salts of ReF_6^+, the exploitation of the powerful electron oxidizers $Kr_2F_3^+$ and KrF^+ provided an excellent path to $ReF_6^+SbF_6^-$ synthesis.

Oxidation of ReF_6 by $Kr_2F_3^+AuF_6^-$ led to the formation of AuF_3 and ReF_7. This is consistent with the expectation that AuF_5 (which is a stronger oxidizer than PtF_5) should be capable of fluorinating ReF_6 to to ReF_7. Refluxing ReF_7 in the presence of AuF_5 does not lead to the formation of $ReF_6^+AuF_6^-$ salt, this is probably because $ReF_6^+AuF_6^-$ is of marginal stability (see below) and this synthesis also requires the breaking of bonds in polymeric AuF_5. Although AuF_5 has slight solubility in HF, reaction of ReF_7 with AuF_5 in HF did not produce $ReF_6^+AuF_6^-$. The band observed at 755 cm^{-1} in the analogous SbF_5 reaction was not seen in this case but ReF_7 bands were. HF appears to be a stronger base than ReF_7. It competes effectively with ReF_7 as a F^- donor toward AuF_5:

$$ReF_6^+AuF_6^- + (x + 1)HF \longrightarrow (HF)_xH^+AuF_6^- + ReF_7$$

$ReF_6^+AuF_6^-$ is prepared in high yield when ReF_7 is allowed to react with $Kr_2F_3^+AuF_6^-$ or $KrF^+AuF_6^-$. It is important to have a thorough mixing of the two reactants. Since polymeric AuF_5 is less likely to accept F^- from ReF_7 than monomeric AuF_5, it is important to avoid $(AuF_5)_x$ formation. The necessary initial mixing was achieved by cooling an HF solution of $Kr_2F_3^+AuF_6^-$ and excess ReF_7 to -196°C. The HF was then slowly removed under dynamic vacuum at -78°C, then the remaining mixture was quickly warmed up to $\geq$60°C to melt ReF_7 and decompose $Kr_2F_3^+AuF_6^-$. Experience showed that direct mixing of ReF_7 with $Kr_2F_2^+AuF_6^-$ or $KrF^+AuF_6^-$ without using HF always led to some formation of $(AuF_5)_x$ which was easily detected by its Raman spectrum (see Fig. 6c) and by its characteristic reddish color.

B. Raman spectroscopy studies of $ReF_6^+ MF_6^-$ (M = Sb and Au)

It was found that when ReF_6^+ salts were prepared from SbF_5 itself or from $Kr_2F_3^+SbF_6^-$ or $KrF^+SbF_6^-$ the dominant solid product was a rhombohedral material (primitive unit cell, a = 6.01Å, α = 95.92°, V = 213.4Å^3, see Table III) which gives a Raman spectrum indicative of ReF_6^+, SbF_6^-, ReF_7 and SbF_5 monomer (see Fig. 1b and 7b). There can be no doubt of this solid being essentially a rhombohedral variant of the CsCl type arrangement (see below).

When $KrF^+Sb_2F_{11}^-$ was used as the oxidant for ReF_6 in the WF_6 solvent, the X-ray powder photographs showed a complex pattern which has been indexed (tentatively) on the basis of an orthorhombic cell (see Table I). Although it could be argued that this product is $ReF_6^+Sb_2F_{11}^-$, the Raman spectra give no evidence for the existence of $Sb_2F_{11}^-$. Moreover the stoichiometry $KrF^+Sb_2F_{11}^-$ provides for the oxidation of two moles of ReF_6 for each $KrF^+Sb_2F_{11}^-$:

$$2ReF_6 + KrF^+Sb_2F_{11}^- \longrightarrow 2ReF_6^+SbF_6^- + Kr$$

Indeed as with the product described above, the Raman spectra (see Fig. 1a and 7a) indicate a formulation represented by the species ReF_6^+, SbF_6^-, ReF_7 and SbF_5 monomer. Tentatively therefore the material prepared (with rather moderate reaction) involving $KrF^+Sb_2F_{11}^-$ and ReF_6 in WF_6 will be regarded as a low temperature form of $ReF_6^+SbF_6^-$ containing neutral ReF_7 and SbF_5 monomer. This low temperature solid will be referred to as β - $ReF_6^+SbF_6^-$ and the rhombohedral material as α - $ReF_6^+SbF_6^-$.

As will be described below, the Raman spectra of both $\underline{\alpha}$ and $\underline{\beta}$ $ReF_6^+SbF_6^-$ indicate ReF_6^+ and SbF_6^- species intermingled with ReF_7 and SbF_5 monomer. The existence of the last (as distinct from $Sb_2F_{11}^-$ or other polymeric $(SbF_5)_xF^-$ species) suggests that species SbF_5 or SbF_6^- is surrounded by eight ReF_y species (ReF_6^+ or ReF_7), otherwise an SbF_5 close to an SbF_6^- would surely form $Sb_2F_{11}^-$.

There is no convincing evidence for the existence of a superlattice, in either the rhombohedral or the orthorhombic cells, therefore it cannot be asserted that the neutral species are symmetrically distributed within the lattice although that may well be the case. The superlattice will be a fluorine-only superlattice, and hence will have low X-ray diffraction intensity.

Raman spectra of $\underline{\beta}$ and $\underline{\alpha}$ $ReF_6^+SbF_6^-$ and $ReF_6^+AuF_6^-$ are shown in Fig. 7 and Table II. All three spectra were taken at low temperature (~ -50°C). For a regular octahedral species, (O_h point group symmetry) only three vibrational modes (ν_1 (A_{1g}), ν_2 (E_g), and ν_5 (T_{2g})) are expected in the Raman spectrum. The ν_1 fundamental is usually the most intense one in O_h species, and ν_2 is the weakest. Thus, for $AF_6^+BF_6^-$ compounds with discrete AF_6^+ and BF_6^- ions, six Raman peaks can be expected.

For the low temperature structure, β-$ReF_6^+SbF_6^-$, the moderately strong peak at 652 cm^{-1} can be assigned (see Table V) to ν_1 of SbF_6^-, the weak peak at 600 cm^{-1} and the weak and broad peaks close to 300 cm^{-1} can be attributed to ν_2 and ν_5, respectively. The strongest peak at 796 cm^{-1} is assigned to ν_1 of the ReF_6^+ cation and the moderate, broad peak at 358 cm^{-1} to ν_5 of ReF_6^+. We expect ν_1 (the totally symmetric bond stretching mode) to be at higher frequency in ReF_6^+ than

in ReF_6. The ν_1 for the latter is established [20] to be 756 cm^{-1}. Close but distinct relationships between the ν_2 and ν_5 modes of ReF_6 and ReF_6^+ are also to be expected. These assignments of ν_1 and ν_5 of ReF_6^+ are in agreement with Jacob and Fehnle's observations.[13]

The sharp doublet at 731 and 735 cm^{-1} is not readily accounted for. The intensity is too high (~40 percent of ν_1) for a ν_2 peak of ReF_6^+, especially when a regular octahedral coordination is anticipated. The splitting could be due to a site symmetry effect because the doublet persists as long as does the structure form which is associated with the spectrum (in this case the β form). There is also a medium strong peak at 680 cm^{-1} which is not easily accounted for. This latter peak has approximately the same intensity as ν_1 SbF_6^-. It appears to be associated with an Sb-F stretching mode. The assignments for the doublet at ~733 cm^{-1} and the peak at 680 cm^{-1} are made easier by a comparison of the Raman spectra of β-$ReF_6^+SbF_6^-$ with $ReF_6^+AuF_6^-$ (see Table II and Fig.7). The Raman spectrum of $ReF_6^+AuF_6^-$ also possesses an intense peak at 796 cm^{-1} (which is assigned to ν_1 ReF_6^+), a moderate peak at 358 cm^{-1} (which is assigned to ν_5 ReF_6^+) and a moderately intense band at 733 cm^{-1} (see Fig. 6c). In this case however the peak at 680 cm^{-1} is not observed. This immediately suggests that the ~733 cm^{-1} doublet in β-$ReF_6^+SbF_6^-$ is associated with a rhenium species and the 680 cm^{-1} with the antimony species.

The high temperature α-$ReF_6^+SbF_6^-$ gives a similar pattern (see Fig. 1b and 7b) in the Raman spectrum to that of β-$ReF_6^+SbF_6^-$. There are, however, significant changes in frequency for most of the peaks, particularly those associated with antimony species. The doublet at

~733 cm^{-1} associated with an ReF_x species is now single. The peak at 662 cm^{-1} is assigned as ν_1 of SbF_6^- (a rather large shift of 10 cm^{-1} from the low-temperature-structure relative). The ν_2 mode is similarly shifted to 608 cm^{-1} while the ν_5 remains as broad peaks at ~300 cm^{-1} (293 cm^{-1} and 300 cm^{-1}). There is not much change for the peaks associated with the ReF_6^+ species; ν_1 is very strong at 796 cm^{-1} and ν_5 is moderate and centered at 358 cm^{-1}. The peak assigned as due to ν(Sb-F) of some SbF_x species in β-$ReF_6^+SbF_6^-$ appears to be again represented but (like ν_1 SbF_6^- itself) shifted to higher frequency at 688 cm^{-1}. Again, this mysterious peak at 688 cm^{-1} has approximately the same intensity as ν_1 SbF_6^-. We note also that the peak at 733 cm^{-1} tentatively assigned to an ReF_y species also has an intensity (relative to that of ν_1 (ReF_6^+)) which is roughly the same in the α and β forms, when allowance is made for the doublet nature of the peak in the latter.

The Raman spectroscopic data for α-$ReF_6^+SbF_6^-$ are in general agreement with Jacob and Fehnle's report[13] for the first preparation of $ReF_6^+SbF_6^-$. Evidently they had the α (i.e. high-temperature-structure, rhombohedral) phase. Their method of synthesis is consistent with this. Unfortunately they do not provide crystallographic information. They mention the peak at 733 cm^{-1} without comment, but do not report the peak at 688 cm^{-1}.

Before we turn to the more precise assignment of the 733 cm^{-1} and 688 cm^{-1} peaks in $ReF_6^+SbF_6^-$, it is appropriate to discuss the possibility that the β-$ReF_6^+SbF_6^-$ might be an $Sb_2F_{11}^-$ salt. There is no doubt that the high temperature phase (α-$ReF_6^+SbF_6^-$) must be an 1:1 complex of ReF_y and SbF_x species. The X-ray powder pattern is indexed

on the basis of a primitive rhombohedral cell. The unit cell volume (213.4 $Å^3$) indicates, on the basis of Zachariassai's criteria of ~18 $Å^3$ per F, that a formula $ReSbF_{12}$ is appropriate for this primitive cell. It is also seen in Table III that there is a pseudo body centering of the cell since when Σh+K+l is even the line intensity is high and when Σh+K+l is odd, the line intensity is low.

The complexity of the X-ray powder pattern of the low temperature phase material (β-$ReF_6^+SbF_6^-$) leaves us without such strong crystallographic guidance. The tentative indexing on the basis of an orthorhombic unit cell, however, yields a cell volume of 862 $Å^3$ which is approximately four times that of the rhombohedral cell (4 x 213.4 $Å^3$ = 853.6 $Å^3$). If the indexing is correct this confirms that the β form is again of an $ReSbF_{12}$ formula unit. Moreover, an $Sb_2F_{11}^-$ entity gives rise to quite different Raman spectra (particularly in peak intensities) from that observed for the low-temperature (β) form. Thus, we see from the data in Table V that the $Sb_2F_{11}^-$ in the O_2^+ salt has a medium peak at 688 cm^{-1}, but we also note peaks at 659 cm^{-1} and 596 cm^{-1}, the last two being very similar to ν_1 and ν_2 of SbF_6^-. The 596 cm^{-1} peak in $O_2^+Sb_2F_{11}^-$, however, is much more intense than is usual for a ν_2 mode (see $IF_6^+SbF_6^-$). The peak at ~600 cm^{-1} in β-$ReF_6^+SbF_6^-$ is much more like a ν_2 (MF_6, E_g) mode. Also, in the Raman spectroscopic study of the phase transition (see Fig. 2, and the experimental part, section C), the transition of the two patterns was smooth and clean and no SbF_5 polymer was observed, such would have been the case if the transition was a follows:

$$ReF_6^+Sb_2F_{11}^- \longrightarrow ReF_6^+SbF_6^- + \frac{1}{x}(SbF_5)_x.$$

Also when a sample of β-$ReF_6^+SbF_6^-$ was kept in a small FEP tube at room temperature until it had transformed completely to α-$ReF_6^+SbF_6^-$, there was no production of $(SbF_5)_x$, which the previous dissociation requires.

The Raman spectrum of $ReF_6^+AuF_6^-$ (Fig. 6a and 7c) has a similar pattern to that of α-$ReF_6^+SbF_6^-$. The peaks associated with Re-F vibration are present at exactly the same frequencies (796 cm^{-1}, 733 cm^{-1} and 356 cm^{-1}) as observed in $ReF_6^+SbF_6^-$. The 733 cm^{-1} peak overlaps with the Teflon FEP (Fig. 6a) signal but can be observed when a sapphire tube or quartz capillary tube is used (Fig. 6c). This strongly suggests that we have the Re(VII) species in the same chemical environment in all three materials. For the peaks associated with AuF_6^- species, the strongest, at 600 cm^{-1}, is assigned (following Bartlett and Leary[4]) to be ν_1 and the medium-weak doublets at 223 cm^{-1} and 213 cm^{-1} are assigned to ν_5 (In $IF_6^+AuF_6^-$, ν_1 AuF_6^- = 595 cm^{-1} and ν_5 AuF_6^- = 220 cm^{-1}). As usual for AuF_6^- salts, ν_2 was absent. The simplicity of the AuF_6^- part of the spectrum hints at a nearly perfect O_h symmetry. These assignments leave only the medium-strong peaks at 658 and 733 cm^{-1} unassigned. The latter appears to be due to the same ReF_y species as occurs in $ReF_6^+SbF_6^-$. The former must be associated with some AuF_x species. Just as there is an unassigned SbF_x species accompanying the unassigned ReF_y species in $ReF_6^+SbF_6^-$, there is an unassigned AuF_x species accompanying the 733 cm^{-1} band-producing ReF_y species in the case of $ReF_6^+AuF_6^-$. The Raman spectra of $ReF_6^+AuF_6^-$ and AuF_5

polymer are shown in Fig. 6. Clearly the species giving rise to the 658 cm^{-1} peak cannot be AuF_5 polymer, nor can it be due to AuF_3.[4]

The assignment of the 733 cm^{-1} peak (associated with ReF_y species) in all three spectra seems clear. ReF_7 has a totally symmetric vibrational peak at 733 cm^{-1} and it is the only strong peak in the spectrum of the pure material.[21] The splitting of the 733 cm^{-1} peak into a doublet of equal intensity at 731 and 735 cm^{-1} in β-$ReF_6^+SbF_6^-$ can be attributed to the crystal symmetry since the X-ray powder data indicate an orthorhombic unit cell. The site symmetry may therefore be only C_s or at best D_{2h}.

Of course if ReF_7 occurs in $ReF_6^+MF_6^-$ salts it is reasonable to expect to find MF_5 also. We have noted that polymeric AuF_5 and polymeric SbF_5 do not occur. But what of the monomers? A high temperature Raman spectroscopic study[22] of SbF_5 at 350°C shows that monomeric SbF_5 has a strong Raman peak at 683 cm^{-1}. This is in excellent agreement with the peaks observed at 688 cm^{-1} (α-$ReF_6^+SbF_6^-$) and at 680 cm^{-1} (β-$ReF_6^+SbF_6^-$) which have been tentatively assigned to be of an SbF_x species. Although vibrational data for the monomeric AuF_5 are not available, one expects that it should have a strong symmetric Au-F stretching frequency at 650 cm^{-1} or higher. The peak at 658 cm^{-1} in $ReF_6^+AuF_6^-$ is consistent with that.

The Raman spectra of $ReF_6^+SbF_6^-$ (both $\underline{\alpha}$ and $\underline{\beta}$ forms) and $ReF_6^+AuF_6^-$ are most reasonably interpretated on the basis of them arising not only from the ReF_6^+ and MF_6^- but also from ReF_7 and MF_5 monomer species. Thus the rhombohedral form of $ReF_6^+SbF_6^-$ cannot be simply an assemblage of ReF_6^+ and SbF_6^- in an approximately CsCl like array, such as the

X-ray powder data indicates. It is necessary to allow for the ReF_7 and SbF_5 monomer species also being present. Unfortunately there are only powder data and there is, presently, no evidence for a superlattice which would signify a larger unit cell. The conclusions we will presently come to require that there should be such a superlattice, although, because it is a fluorine-only superlattice, it will be hard to detect in the powder data (because of the strong Re and Sb X-ray scatterers).

Turning once more to the Raman data on the ReF_6MF_6 compounds ($ReF_6^+ReF_7MF_6^-MF_5$, set out in Fig. 1 and 7) we note that the intensity of the peaks assigned to the symmetric stretching (ν_1) of SbF_6^- and SbF_5 monomer are roughly the same. The ν_1 AuF_6^- and AuF_5 monomer peaks are also comparable. This suggests that the concentration of the anions and their neutral-monomer relatives are also comparable. It is also notable (see Fig. 1b,c) that the relative intensities of the peaks assigned to ν_1 SbF_6^- and ν_1 SbF_5 do no change markedly with temperature over the range 200 to 300K°, and the ν_1 SbF_5 is sharper than ν_1 SbF_6^- and may be sharper at higher temperature (see Fig. 1c). There is also no change whatsoever in the relative intensities of these peaks (see Fig. 2) in the case of the $\underline{\beta}$ form (orthorhombic form). This suggests that the entropy changes associated with the conversion of ReF_6^+ and MF_6^- to ReF_7 and MF_5 (all trapped in the crystal lattice) is small. This suggests that the neutral species are in ordered array. A reasonable supposition is that there are equal numbers of anionic, cationic and neutral species distributed in ordered fashion on interpenetrating ZnS type arrays as shown in Fig. 8. But why should such a structure be preferred?

As we shall shortly discuss (see below) ReF_7 is a rather weak base. The observed instability of $ReF_6^+SbF_6^-$ toward dissociation into components, shows that the F^- transfer to ReF_6^+ occurs spontaneously at room temperature. The salts $\underline{\alpha}$ and $\underline{\beta}$ "$ReF_6^+SbF_6^-$", and "$ReF_6^+AuF_6^-$", appear to have only kinetic stability with respect to ReF_7 and the polymeric pentafluoride at ambient temperatures. The preparations, when carried out at low temperature, however, yield the materials which we favor as being formulated as $ReF_6^+ReF_7MF_6^-MF_5$. Such an ordered arrangement of neutral and charged species as we proposed in Fig. 8 will be more stable to dissociation into neutral components than the salt $ReF_6^+MF_6^-$. This is because each ion has a neutral relative screening it from its like neighbor. Thus the like charge repulsions are much reduced in the $ReF_6^+ReF_7MF_6^-MF_5$ lattice compared with the $ReF_6^+MF_6^-$ lattice. This screening by the neutral species and the overall diminution of the charges in the lattice leads to an expansion of the anion array in the former, relative to the latter. Clearly if we separate the opposite charges more (and the loss of Coulomb attraction is compensated for, to some extent, by the dielectric screening effect) we reduce the likelihood of F^- transfer between anion and cation.

C. On the thermodynamic aspects

The poor fluoro-base character of ReF_7 is illustrated by the displacement of ReF_7 from ReF_6^+ salts in HF:

$$ReF_6^+MF_6^- + (n+1)HF \longrightarrow H(HF)_n^+ + MF_6^- + ReF_7$$

The stability of the $ReF_6^+MF_6^-$ salts (M = As, Sb, Au, Pt and Ir) pro-

vides a basis for quantifying that stability. To do so, Born-Haber cycle of the following form is used:

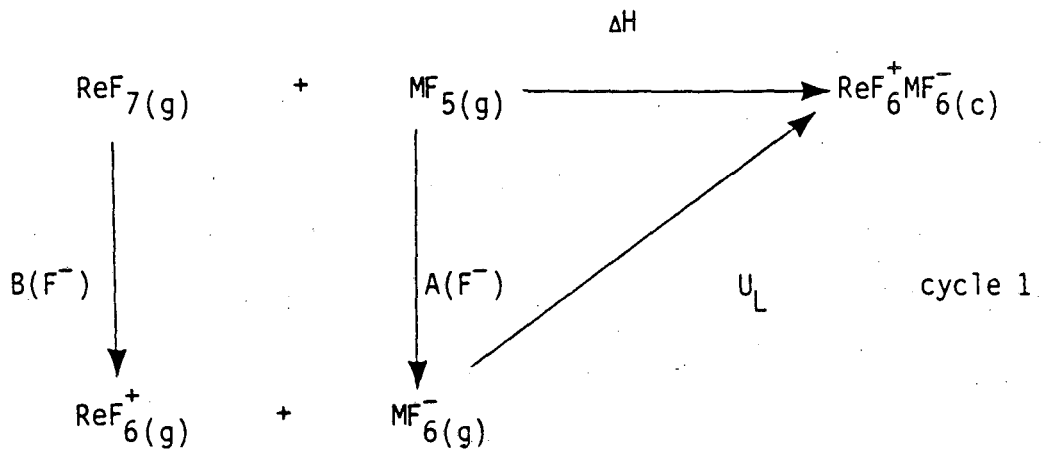

where $\Delta H = B(F^-) - A(F^-) - U_L$

and ΔH: heat of reaction

$B(F^-)$: F^- basicity of ReF_7

$A(F^-)$: F^- affinity of MF_5

U_L: lattice energy of $ReF_6^+MF_6^-$ salts

MF_5: M = As, Sb, Au, Pt and Ir.

Since the data for the heat of reactions are not available, at the present time one can only estimate ΔG ($\Delta G = \Delta H - T\Delta S$) to be positive or negative based upon the experimental observation of the stability of the $ReF_6^+MF_6^-$ salts with respect to their molecular components, e.g. ΔG would be negative in cycle 1 for $ReF_6^+MF_6^-$ to be stable. An estimate of the change of entropy in the reaction is required.

One can assume that the lattice energy for all $AF_6^+BF_6^-$ salts would be approximately the same. This is based on the observation[18] that all MF_6 have approximately the same volume (~105 $Å^3$). The ligand fractional charges are probably close in all AF_6^+ and in all BF_6^-. Forming

a cation would mean a small volume reduction which would be balanced by the small volume increase associated with anion formation. As an example, $IF_6^+AsF_6^-$ has a formula unit volume of 214 $Å^3$. The structural data derived from the X-ray powder patterns of the $AF_6^+BF_6^-$ salts, prepared in this work, show the effective packing volume per formula unit are close to 214 $Å^3$. The only available structural parameters for an $AF_6^+BF_6^-$ salts are those of $IF_6^+AsF_6^-$, derived from Beaton's[12] X-ray powder diffraction analysis. The lattice energy of $IF_6^+AsF_6^-$ has been calculated using Berteau's[23] method, as modified by Templeton,[24] where the atomic charges on the elements in the $IF_6^+AsF_6^-$ salt have been calculated according to Jolly's[25] equation. A value of 126 kcal has been obtained.[26] This value is more reliable than the value of 119 kcal from Gibler's[11] evaluation based on Kapustinskii's[27] second equation and that of 120 kcal derived from a plot[26] of lattice energy versus the inverse of the cubic root of the effective molecular packing volume. These latter approximate evaluations do not deal adequately with the London energy, which is a rather large term in the $IF_6^+AsF_6^-$ lattice energy evaluation. It is reasonable to assume that the $ReF_6^+MF_6^-$ (but not the $ReF_6^+ReF_7MF_6^-MF_5$) lattice energy will be close to the 126 kcal $mole^{-1}$ found for $IF_6^+AsF_6^-$ by Mallouk.[26]

The F^- affinity of MF_5 (M = As, Sb, Au, Pt and Ir) are known only roughly. The formation of the $ReF_6^+SbF_6^-$ from the components in the gas phase and its instability with respect to ReF_7 and SbF_5 polymer at 300°K indicate that ΔG ($ReF_{7(g)} + (SbF_5)_n \longrightarrow ReF_6^+SbF_6^-(s)$) cannot be far from zero. The similarity of the stability of the AuF_6^- salt to that of its antimony relatives suggests that AuF_5 and SbF_5 may have comparable F^- affinities. It is clear that neither PtF_6^- nor IrF_6^- is able

to stabilize ReF_6^+ at ambient temperature. In no case has an anion been found which will stablize $ReF_6^+MF_6^-$ even at 200°K. In addition, the failure to form a salt between ReF_7 and AsF_5 means that ReF_7 must be a weaker base than IF_7 since $IF_6^+AsF_6^-$ shows considerable stability with respect to dissociation into its components at ambient temperature.

A reliable evaluation of the F^- affinity of ReF_6^+ is not possible from cycle 1. An estimate can be made, however, using another Born-Haber cycle:

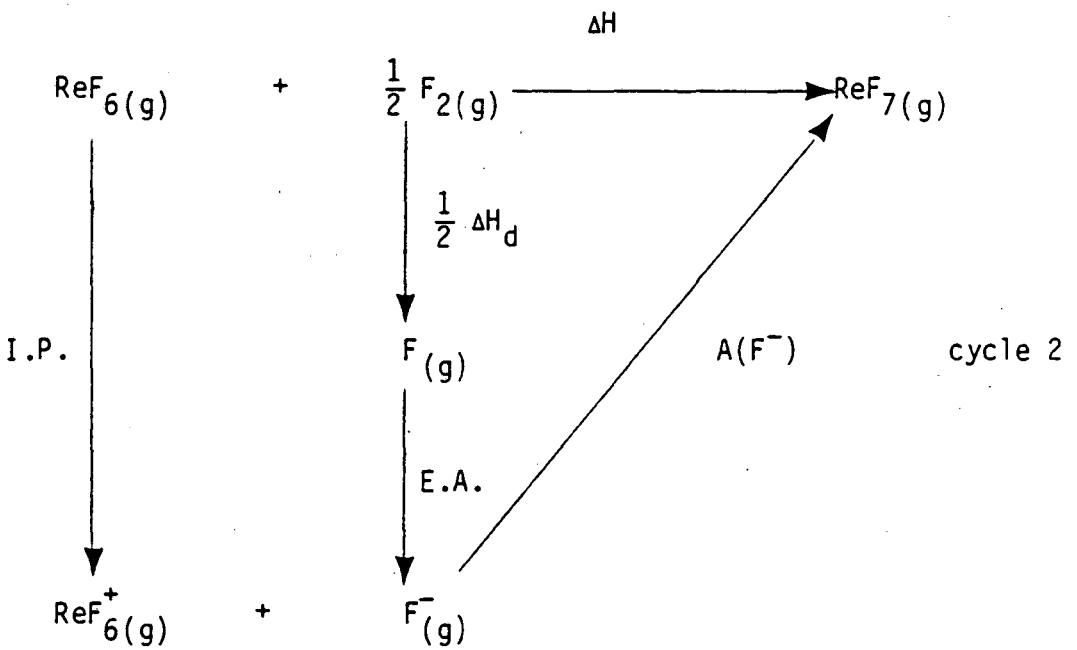

where $\Delta H = I.P. + \frac{1}{2}\Delta H_d - E.A. + A(F^-)$

and ΔH: heat of reaction

I.P.: ionization potential of ReF_6

ΔH_d: dissociation energy of F_2

E.A.: electron affinity of F atom

$A(F^-)$: F^- affinity of ReF_6^+

The heat of formation of ReF_6 and ReF_7 have been given[28,29,30] as 327 kcal and 342 kcal, respectively. The heat of reaction ΔH is therefore known, as are also the dissociation energy of F_2[31] and the electron affinity of F atom.[31] Thus, one has the following relationship between the ionization potential of ReF_6 and the F^- affinity of ReF_6^+:

$$\text{I.P. } (ReF_6) + A(F^-)\ (ReF_6^+) = 47 \text{ kcal}$$

The ionization potential of ReF_6 has been reported by several workers and the values range widely. McDiarmid gives 7.99 e.v.,[32] Ellis finds 10.7 e.v.,[33] Brundle and Jones are quoted[34] as finding 11.15 e.v. and Bloor and Sherrod estimate 11.88 e.v.[34] A photoionization study by Vorna et al.[35] yielded 11.1 ± 0.1 e.v. and this value is quoted in a recent NBS tabulation.[36]

One can evaluate the ionization potential of ReF_6 from its reaction with the powerful oxidizers such as PtF_6 and IrF_6 (as described in the attempts to prepare the $ReF_6^+PtF_6^-$ and $ReF_6^+IrF_6^-$ salts). The Born-Haber cycle is represented below:

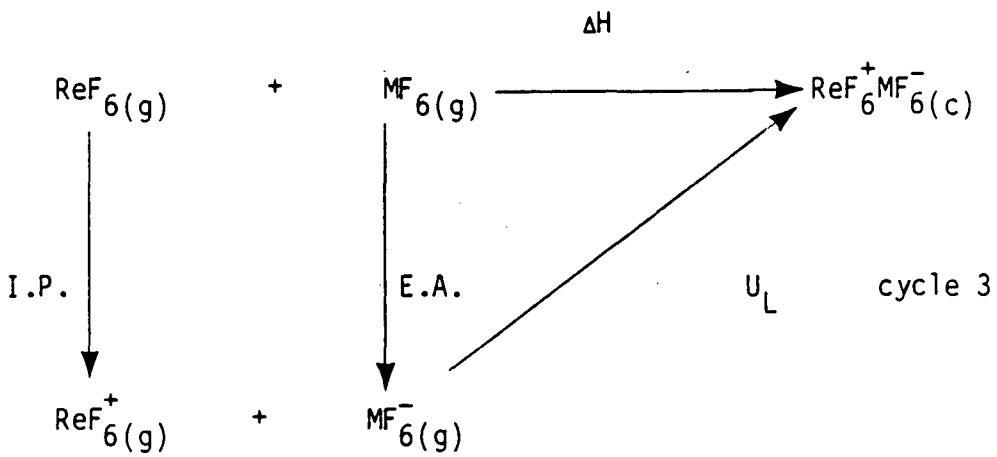

where $\Delta = I.P. - E.A. - U_L$

and ΔH: heat of reaction

I.P.: ionization potential of ReF_6

E.A.: electron affinity of MF_6 (M = Pt,Ir)

U_L: lattice energy of $ReF_6^+MF_6^-$, 126 kcal

The reaction of ReF_6 with IrF_6 can be used to evaluate the thermodynamic energies quantitatively with small uncertainty because one observes the equilibrium between ReF_6/IrF_6 and $ReF_7/\frac{1}{4}(IrF_5)_4$. An $ReF_6^+IrF_6^-$ salt is believed to exist as an intermediate, i.e.:

$$ReF_6 + IrF_6 \rightleftharpoons [ReF_6^+IrF_6^-] \rightleftharpoons ReF_7 + \frac{1}{4}(IrF_5)_4$$

An appropriate Born-Haber cycle is represented below:

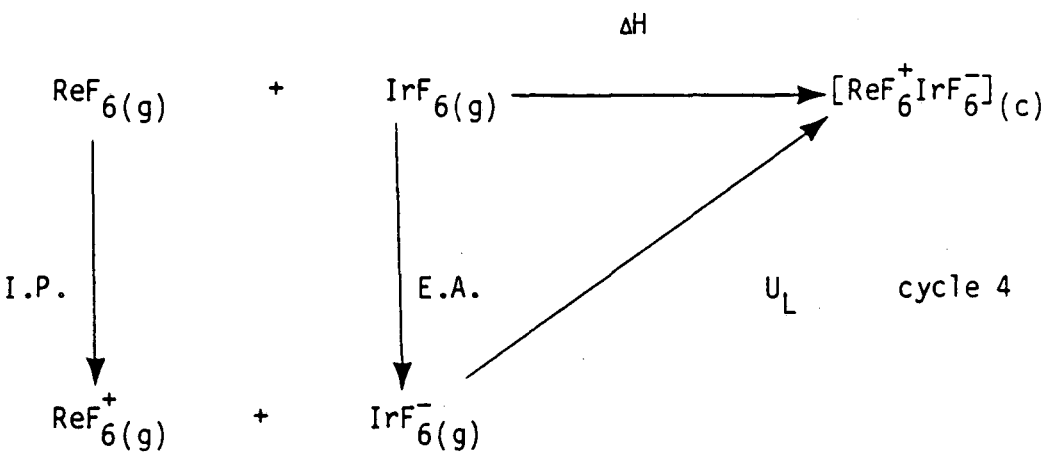

where $\Delta H = I.P. - E.A. - U_L$

and ΔH: heat of reaction

I.P.: ionization potential of ReF_6

E.A.: electron affinity of IrF_6

U_L: lattice energy of $ReF_6^+IrF_6^-$, 126 kcal

Since $ReF_6^+IrF_6^-$ is an intermediate in the equilibrium between ReF_6/IrF_6 and $ReF_7/\frac{1}{4}(IrF_5)_4$ and since ReF_6 and IrF_6 are each in equilibrium with appreciable vapor pressure, ΔG can be estimated to be ~0 kcal for the reaction.

$$ReF_{6(g)} + IrF_{6(g)} \longrightarrow ReF_6^+IrF_6^-(c) \qquad \text{(reaction A)}$$

$$\Delta G = \Delta H - T\Delta S \sim 0 \text{ kcal mole}^{-1}.$$

The estimation of standard entropies for solids is complicated. Latimer[37] has given an empirical basis for finding S°_{298} but his data were inadequate for the present problem. Mallouk[26] has found that the standard entropies S°_{298} of closely packed solids are in approximately linear relationship with their formula unit volumes and that this evaluation is more reliable for complex fluorides than the Debye formula.[38] The relationship is:

$$S^\circ_{298} \text{ (cal mole}^{-1}\text{ k}^{-1}) = 0.44\ V\ (\text{Å}^3)$$

For the salt $ReF_6^+IrF_6^-(c)$, the same volume as $IF_6^+AsF_6^-(c)$ is assumed and S°_{298} is given[31] as 96 cal $mole^{-1}$ k^{-1}. This value is believed to be accurate within ± 10%. Since S°_{298} for $ReF_{6(g)}$ and $IrF_{6(g)}$ are given[31] to be 82 and 85 cal $mole^{-1}$ K^{-1} respectively. $T\Delta S$ can be estimated to be ~-22 kcal $mole^{-1}$. Thus the heat of reaction A is given

$$\Delta H \approx -22 \text{ kcal mole}^{-1}.$$

The lattice energy of $ReF_6^+IrF_6^-(c)$ is estimated to be similar to $IF_6^+AsF_6^-(c)$, thus

$$U = 126 \text{ kcal mole}^{-1}$$

To estimate the ionization potential of ReF_6, one has to know the electron affinity of IrF_6 with some certainty. The best estimate of the electron affinity of IrF_6 is based upon the reaction of Cl_2 with IrF_6. N.K. Jha[39] and L. Graham[15] have each shown that $Cl_{2(g)}$ reacts spontaneously with $IrF_{6(g)}$ to precipitate a 1:1 solid which is probably $Cl_2^+IrF_6^-$ salt. It rapidly rearranges at room temperature to yield the sequence of solids: $Cl_3^+IrF_6^- \longrightarrow Cl_3^+Ir_2F_{11}^- \longrightarrow Cl_3^+Ir_3F_{16}^-$, and finally $(IrF_5)_4$. The spontaneous reaction of Cl_2 and IrF_6 and the ready transformation of $Cl_2^+IrF_6^-$ salt indicates that $\Delta G \approx 0$ for the following reaction:

$$Cl_{2(g)} + IrF_{6(g)} \longrightarrow Cl_2^+IrF_6^-(c) \qquad \text{reaction B}$$

Since the formula unit volume of Cl_2[40] and IrF_6[41] in the solid phases are 57.7 $Å^3$ and 105.4 $Å^3$, the formula unit volume of $Cl_2^+IrF_6^-$ should be close to the volume sum 163 $Å^3$. Thus the entropy and lattice energy can be estimated[26] to be 72 cal $mole^{-1}k^{-1}$ and 128 kcal $mole^{-1}$ respectively. Given[31] $S°_{298}(Cl_2)$ = 53 cal $mole^{-1}$ k^{-1} and $S°_{298}(IrF_6)$ = 55 cal $mole^{-1}$ k^{-1}, $T\Delta S$ for reaction B is -20 kcal. Thus $\Delta H \approx -20$ kcal $mole^{-1}$ is indicated for reaction B.

From the Born-Haber cycle:

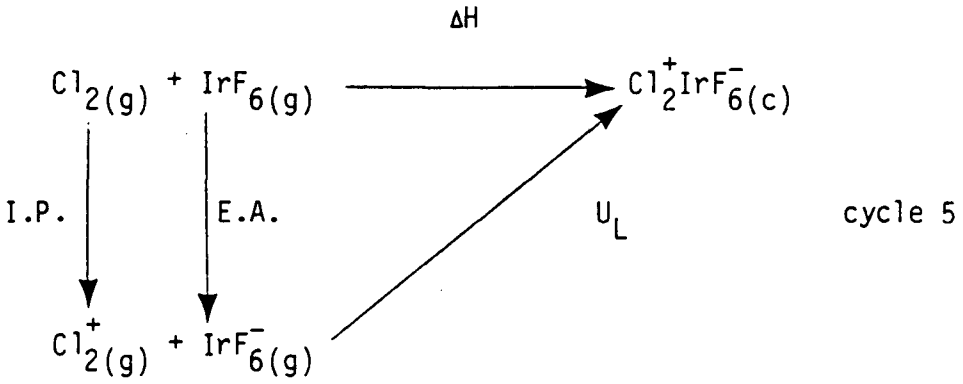

$$\Delta H = I.P. - E.A. - U_L$$

where

ΔH = heat of reaction B; ~ - 20 kcal

I.P. = ionization potential of Cl_2,[42] 265 kcal

E.A. = electron affinity of $IrF_{6(g)}$, to be determined

U = lattice energy of $Cl_2^+IrF_6^-(c)$, 128 kcal[26]

The electron affinity of $IrF_{6(g)}$ is given to be $\geq$ 157 kcal mole^{-1}.

This electron affinity of IrF_6 ($\geq$ 157 kcal mole^{-1}) is lower than the value derived from a spectroscopic study of Xe interacting with IrF_6 from which a value of +180 kcal mole^{-1} was given.[19] The latter value must be too high as the following cycle illustrates:

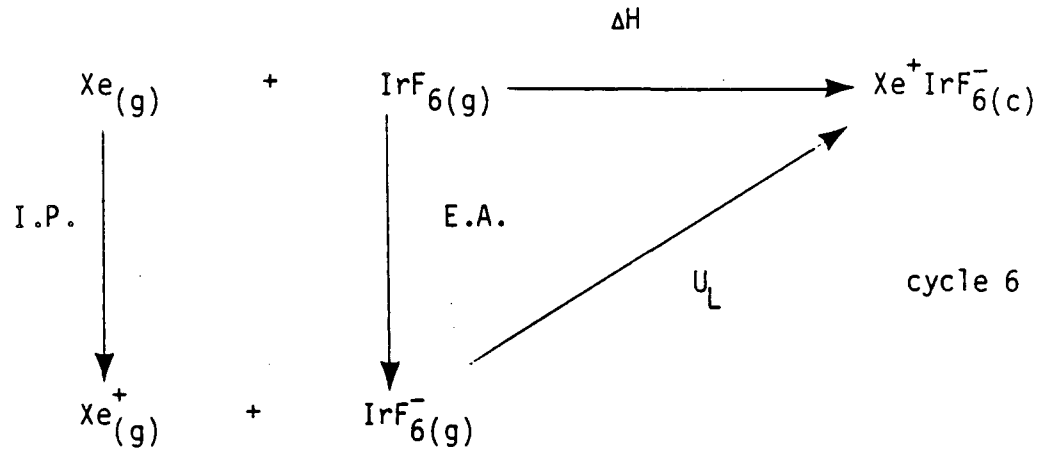

where $\Delta H = I.P. - E.A. - U_L$

and ΔH: heat of reaction

I.P.: ionization potential of Xe, 281 kcal mole^{-1}

E.A.: electron affinity of IrF_6

U_L: lattice energy of $Xe^+IrF_6^-$

The salt $Xe^+IrF_6^-$ would have a lattice energy[26] of ~ + 135 kcal mole^{-1}, hence ΔH would be -34 kcal mole^{-1} if the electron affinity of IrF_6 is 180 kcal mole^{-1}. This ΔH is sufficiently exothermal to balance the entropy change, and $-T\Delta S$ can be no more than ~22 kcal mole^{-1} at 298°K. Thus with an electron affinity as high as 180 kcal mole^{-1} for IrF_6 we conclude that $Xe^+IrF_6^-$ should be stable at ambient temperature and the authors of that value found that it was not. Similar observation could be made on the known[39] instability of $O_2^+IrF_6^-$ with respect to dissociation.

With an electron affinity of ~157 kcal mole^{-1} for IrF_6, ΔH for the cycle 6 can be re-evaluated to be -11 kcal mole^{-1}, which is not exothermal enough to offset the entropy change at room temperature ($-T\Delta S$ ~ 22 kcal mole^{-1}). But $Xe^+IrF_6^-$ ought to be stable at liquid xenon temperature ($-T\Delta S$ ~ 13 kcal mole^{-1}) as observed by Webb and Bernstein.[19]

Using electron affinity of 157 kcal mole^{-1} for IrF_6 in cycle 4, and from the relationship of:

$$\Delta H(\text{reaction A}) = \text{I.P. } (ReF_6) - \text{E.A. } (IrF_6) - U_L(ReF_6^+IrF_6^-)$$

where $\Delta H = -22$ kcal mole^{-1}

$U_L = -126$ kcal mole^{-1}

The ionization potential of ReF_6 is given to be 261 kcal mole^{-1}. This value is close to that quoted in the recent NBS report[36] and that attributed to Brundle and Jones.[34]

Using the relationship established in cycle 2:

$$\text{I.P. } (ReF_6) + A(F^-) \ (ReF_6^+) = 47 \text{ kcal}$$

The F^- affinity of ReF_6^+ is estimated to be -214 kcal mole^{-1}.

Since IF_7 readily displaces ReF_6^+ in $ReF_6^+AuF_6^-$, the F^- affinity of IF_6^+ must be greater than -214 kcal mole^{-1}. A recent study[43] involving the $IF_6^+BF_4^-$ salt has established the F^- affinity of IF_6^+ to be -208 kcal mole^{-1}.

As is so common in chemistry, the marked chemical differences (in fluoro-basicity) between ReF_7 and IF_7 is associated with a relatively small difference in the ionization enthalpy (ΔH $EF_{7(g)} \longrightarrow EF_{6(g)}^+ + F_{(g)}^-$). Indeed the surprise is the closeness of the two values. As may be seen from Table VI, the values are similar to those previously noted for the separation of F^- from the xenon fluorides and SF_4.

The almost constant value of the F^- separation enthalpy for the hypervalent fluorides can be simply accounted for.[44] The enthalpy change can be represented as deriving from the sum of three processes:

(a) the conversion of the resonance hybrid of the two dominant canonical forms of a three-center-four-electron bond $(F\text{-}E)^+F^-$ and $F^-(E\text{-}F)^+$ to one form: an $(F\text{-}E)^+F^-$ ion pair,

(b) The contraction of $(E\text{-}F)^+$ and the enhancement of the energy of that bond $\{(E\text{-}F)^+ \text{long} \rightarrow (E\text{-}F)^+ \text{short}\}$, and

(c) the work necessary to separate $(E\text{-}F)^+$ and F^- to infinity.

The first step is a measure of the more favorable energy associated with the delocalization of an electron over two F ligands rather than its association with one F ligand. For the noble-gas difluorides this resonance energy has been empirically evaluated[44] as contributing approximately 50 kcal $mole^{-1}$ to their stability. Such a resonance stabilization should hold approximately for all of the hypervalent fluorides. The second process exothermically contributes to the F^- separation process by less than 2 kcal $mole^{-1}$. The third process requires the greatest energy. For a separation of ions at 2.0Å the work amounts to 166 kcal $mole^{-1}$. With smaller inter-ion separations the work would, of course, be greater. Thus the sum of the first and third steps is expected to amount to ~ 218 kcal $mole^{-1}$ -- a value close to the observed enthalpies of F^- separation for the hypervalent fluorides and IF_7. Of course in a case where the resonance stabilization does not occur the ion-pair separation work will be the only important term. This probably accounts for the high basicity of ONF, a molecule which appears to be close to an ion pair ON^+F^-.[17,45]

Thus it seems that ReF_7 behaves as a hypervalent molecule. Perhaps in this high oxidation-state compound the 5d orbitals have been greatly contracted by the high ligand field, such that they are behaving more like inner shell orbitals. If so, the bonding of the seven ligands, like the case of IF_7, would be primarily dependent upon the Re 6s and 6p orbitals and the 2p orbitals of the F ligands.

REFERENCES

1. Von F. Seel and O. Detmer, Z. Anorg. Allge. Chem., B301 113 (1959).
2. K. O. Christe and W. Sawodny, Inorg. Chem., 6 1783 (1967).
3. F. A. Hohorst, L. Stein and E. Gebert, Inorg. Chem., 14 2223 (1975).
4. N. Bartlett and K. Leary, Rev. de Chim. Miner., 13 82 (1976).
5. R. J. Gillespie and G. J. Schrobilgen, Inorg. Chem., 13 1230 11974).
6. V. B. Sokolov, V. N. Prusakov, A. V. Ryzhkov, Yu. Y. Droby, V. Shevskii and S. S. Khoroshev, Dokl. Akad. Naus. SSSR, 29 884 (1976).
7. K. O. Christe and R. D. Wilson, Inorg. Chem., 14 694 (1975).
8 F. O. Roberto, Inorg. Nucl. Chem. Letters, 8 737 (1972).
9. K. O. Christe, Inorg. Nucl. Chem. Letters, 8 741 (1972).
10. K. O. Christe, W. W. Wilson and E. C. Curtis, Inorg. Chem., 22 3056 (1983).
11. D. D. Gibler, Ph.D. Thesis, Princeton University, 1973.
12. S. P. Beaton, Ph.D. Thesis, University of British Columbia, Vancouver, Canada, 1963.
13. E. Jacob and M. Fahnle, Angew. Chem. Int. Ed., 15 159 (1976).
14. E. Jacob, 6th European Symposium on Fluorine Chemistry, Mar. 1977.
15. L. Graham, Ph.D. Thesis, University of California, Berkeley, 1978. LBL Report No. 8088.
16. N. Bartlett and D. H. Lohmann, J. Chem. Soc., 619 (1964).
17. B. K. Morrell, A. Zalkin, A. Tressaud and N. Bartlett, Inorg. Chem., 12 2640 (1973).

18. N. Bartlett, Angew. Chem. Int. Ed., 7 433 (1968).

19. J. D. Webb and E. R. Bernstein, J. Amer. Chem. Soc., 100 483 (1978).

20. B. Weinstock and G. L. Goodman, Advances Chem. Physics, 9 169 (1965).

21. H. H. Claassen, E. L. Gasner and H. Selig, J. Chem. Phys., 49 1803 (1968).

22. L. E. Alexander and I. R. Beattie, J. Chem. Phys., 56 5829 (1972).

23. P. F. Berteau, J. Phys. Radium, 13 499 (1952).

24. D. H. Templeton, J. Chem. Phys., 23 1629 (1955).

25. W. Jolly and W. R. Perry, Inorg. Chem., 13 2686 (1974).

26. T. Mallouk, Ph.D. Thesis, University of California, Berkeley, 1982. LBL Report No. 16778.

27. A. F. Kapustinskii, Q. Review. Chem. Soc., 10 283 (1956).

28. J. Burgess, J. Fawcett, N. Morton and R. D. peacock, J. Chem. Soc. (Dalton), 2149 (1977).

29. J. Burgess, C. J. W. Fraser, I. Haigh and R. D. Peacock, J. Chem. Soc. (Dalton), 501 (1973).

30. G. K. Johnson, P. N. Smith and W. N. Hubbard, J. Chem. Thermodynamics, 5 793 (1973).

31. National Bureau of Standard, Technical Notes 270-3 (1968) and 270-4 (1969) and JANAF Tables to 1971 (Dow Chem. Co. Michigan).

32. R. McDiarmid, J. Mol. Spectr., 39 332 (1971).

33. D. E. Ellis, Z. Phys., A283 3 (1977).

34. J. E. Bloor and R. E. Sherrod, J. Amer. Chem. Soc., 102 4333 (1980).

35. V. I. Vorna, A. S. Dubin, L. M. Aukhutskii, S. N. Lopatin and E. G. Ippolitov, Russ. J. Inorg. Chem., 24 135 (1979).

36. NSRDS-NBS Circular 71, U. S. Government Printing Office, Washington D. C. 20402, 1982.

37. W. M. Latimer "Oxidation Potential", 2nd ed., Prentice-Hall Inc. New York, 1952 p. 359.

38. L. E. Moyer and M. G. Mayer, "Statistical Mechanics", 2nd Ed. Wiley, New York and London, 254 (1965).

39. N. H. Jha, Ph.D. Thesis, University of British Columbia, Vancouver, Canada 1965.

40. R. G. Wykoff, Crystal Structures Vol. 1, Interscience Publishers, New York and London 1969.

41. S. Siegel and D. A. Northrop, Inorg. Chem., 5 2187 (1966).

42. A. B. Cornford, D. C. Forst, C. A. McDowell, J. L. Ragle and I. A. Stenhouse, J. Chem. Phys., 54 2651 (1979).

43. N. Bartlett, S. Yeh, K. Koartakis and T. Mallouk, J. Fluorine Chem., 26 97 (1984).

44. M. Wechsberg, P. A. Bulliner, F. O. Sladky, R. Mews and N. Bartlett, Inorg. Chem., 11 3063 (1972).

45. N. Bartlett and P. R. Rao, J. Chem. Soc., Chem. Comm. 252 (1965).

46. J. Berkowitz, W. A. Shupka, P. M. Guyon, J. H. Holloway and R. Spohr, J. Phys. Chem., 75 1461 (1971).

47. T. E. Mallouk, G. L. Rosenthal, G. Muller, R. Brusasco and N. Bartlett, Inorg. Chem., submitted for publication.

48. H. S. Johnston and H. J. Bertin, J. Amer. Chem. Soc., 81 6402 (1959) and J. Mol. Spectroscopy, 3 683 (1959).

Table Contents

Table I.

X-ray powder pattern of β-$ReF_6^+SbF_6^-$

Intensity	$1/d^2$ obs.	$1/d^2$ calc.	hkl
vw	0.0285	0.0288	200
w	0.0346	0.0346	111
vw	0.0413	0.0413	210
m^+	0.0503	0.0498	020
s	0.0556	0.0562	211
s	0.0653	0.0648	300
s	0.0722	0.0722	012
s	0.0787	0.0787	220
vw	0.0851	0.0886	202
w	0.0910	0.0922	311
vvw	0.1148	0.1146	320
m^-	0.1358	0.1371	312
w	0.1403	0.1409	230,103
w^+	0.1654	0.1650	420
vw	0.1715	0.1719	032
vw	0.1829	0.1800	421,430,500
vw	0.1934	0.1935	023
vvw	0.2216	0.2213	141
m	0.2320	0.2298, 0.2367	520,332
m	0.2418	0.2422, 0.2429	431,241
m	0.2551	0.2530, 0.2573	133,114
vvw	0.2657	0.2662	142
w^+	0.2868	0.2866, 0.2871	611,432
w^+	0.3194	0.3190	602
vvw	0.3284	0.3293	441
w	0.3698	0.3688	622
vw	0.3862	0.3862	631
vw	0.3944	0.3941	541
vw	0.4024	0.4026	424,720
vvw	0.4101	0.4126	702
vw	0.4243	0.4258	533

Table I. (continued)

Intensity	$1/d^2$ obs.	$1/d^2$ calc.	hkl
w	0.4736	0.4737	810
w	0.4847	0.4865	703
w	0.4954	0.4919	261
vvw	0.5166	0.5152	162
vw	0.6424	0.6467	363
vw	0.6647	0.6634	535
vw	0.6886	0.6898	155
vw	0.7248	0.7276	700

s = strong m = medium w = weak v = very

Orthorhombic

$\underline{a}$ = 11.77 Å

$\underline{b}$ = 8.96 Å

$\underline{c}$ = 8.18 Å

V = 862.7 $Å^3$

Z = 4

$V_{formula}$ = 215.7 $Å^3$

Table II.

Summary and assignment of Raman spectroscopic data of β-$ReF_6^+SbF_6^-$, α-$ReF_6^+SbF_6^-$ and $ReF_6^+AuF_6^-$

β-$ReF_6^+SbF_6^-$	α-$ReF_6^+SbF_6^-$	$ReF_6^+AuF_6^-$	Assignment
796 (cm^{-1})	796	796	ν_1 (ReF_6^+)
735,731	733	733	ν_1 (ReF_7)
680	688	658	ν_1 (MF_5monomer)*
652	662	600	ν_1 (MF_6^-)
600	623,608	-	ν_2 (MF_6^-)
358	358	356	ν_5 (ReF_6^+)
300(broad)	300,293	223,213	ν_5 (MF_6^-)
			*M = Sb or Au

Table III.

X-ray powder pattern of α-$ReF_6^+SbF_6^-$

Intensity	10^4 $1/d^2$ obs.	10^4 $1/d^2$ calc.	hkl
m^-	266	-	-
vw	284	287	100
vs	509	509	$1\bar{1}0$
vs	641	641	110
w^+	777	795	$\bar{1}11$
w^+	915	-	-
vvw	1078	1059	111
ms	1151	1148	200
vw	1308	1303	$2\bar{1}0$
m	1531	1524	$\bar{2}11$
w	1577	1567	210
w	1626	-	-
m	1661	1656	$2\bar{1}1$
w	1796	-	-
m(b)	2034	2032,2052	211,$2\bar{2}0$
w^+	2135	-	-
vw	2311	2319	$\bar{2}21$
w^+	2399	-	-
w^+	2590	2583	300,$22\bar{1}$
m	2684	2672	$3\bar{1}0$
w	2911	-	-
w	3090	3091	-
w	3126	3111	211

s = strong m = medium w = weak v = very

rhombohedral

$\underline{a}$ = 6.01 Å

α = 95.92°

V = 213.4 Å

Table IV.

X-ray powder pattern of $ReF_6^+ AuF_6^-$

Intensity	$1/d^2$ (obs.)
vw	0.0257
s	0.0459
s	0.0495
vw	0.0601
w	0.0657
s	0.0753
s^-	0.0993
w^+	0.1032
m^-	0.1288
m	0.1530
m	0.1835
m	0.2031
vw	0.2306
vw	0.2501
vvw	0.2568
m^-	0.3143
m	0.3593
m	0.3880
w	0.4074
w	0.4157
vw	0.4423
vw	0.4695
vw	0.5079
m^-	0.5162

s = strong m = medium w = weak v = very

Table V.

Anionic bands in Raman spectroscopy for $O_2^+SbF_6^-$, $XeF_3^+Sb_2F_{11}^-$, $O_2^+SbF_6^-$, $IF_6^+SbF_6^-$, β-$ReF_6^+SbF_6^-$ and α-$ReF_6^+SbF_6^-$ (in cm^{-1}, relative intensities in parentheses).

$O_2^+Sb_2F_{11}^-$ (a)	$XeF_3^+Sb_2F_{11}^-$ (b)	$O_2^+SbF_6^-$ (a)	$IF_6^+SbF_6^-$ (c)	β-$ReF_6^+SbF_6^-$ (d)	α-$ReF_6SbF_6^-$ (d)	$\nu_{MF_6^-}$ (O_h)
	713 (9)					
	701 (11)					
688 (25)						
	681 (23)					
	667 (17)					
659 (100)		656 (100)	661 (47)	652(40)	662(40)	ν_1
596 (20)		592 (5)		600(4)	608(4)	ν_2
		562 (20)	576(6)			
293 (20)	302 (8)	294(5)		300(3,broad)	300(3)	ν_5
	285 (5)	283(10)	278(10)		293(2)	
	267 (7)					
229 (10)	236 (8)					
	220 (shoulder)					

(a) D. E. McKee and N. Bartlett, Inorg. Chem. 12, 2738 (1973).

(b) D. E. McKee, C. J. Adams and N. Bartlett, Inorg. Chem., 12 1722 (1973)

(c) Reference 3.

(d) this work

Table VI.

Enthalpies of fluoride ion separation from ReF_7, IF_7 and other fluorides

Process	ΔH (cal $mole^{-1}$)	reference
$ReF_{7(g)} \longrightarrow Re^{+}_{6(g)} + F^{-}_{(g)}$	214 ± 8	This work
$IF_{7(g)} \longrightarrow IF^{+}_{6(g)} + F^{-}_{(g)}$	208 ± 6	(43)
$XeF_{6(g)} \longrightarrow XeF^{+}_{5(g)} + F^{-}_{(g)}$	209	(46)
$XeF_{4(g)} \longrightarrow XeF^{+}_{3(g)} + F^{-}_{(g)}$	221	(46)
$XeF_{2(g)} \longrightarrow XeF^{+}_{(g)} + F^{-}_{(g)}$	216	(46)
$SF_{4(g)} \longrightarrow SF^{+}_{3(g)} + F^{-}_{(g)}$	211 ± 8	(47)
$ONF_{(g)} \longrightarrow ON^{+}_{(g)} + F^{-}_{(g)}$	188 ± 1	(31,48)

Figure Captions

Figure 1. Raman spectra of

a) β-$ReF_6^+SbF_6^-$, in quartz, at -50°C

b) α-$ReF_6^+SbF_6^-$, in quartz, at -50°C

c) α-$ReF_6^+SbF_6^-$, in quartz, at room temperature.

Figure 2. Raman spectra of β → α phase transition of $ReF_6^+SbF_6^-$, under 4880Å light irradiation at room temperature.

Figure 3. Raman spectra of ReF_7 and SbF_5 in HF solution, in FEP tube.

Figure 4. Raman spectra of

a) products of IrF_6 and ReF_6 interaction in WF_6 solution, in sapphire tube

b) crystalline IrF_5 product from the reaction of IrF_6 and ReF_6 in WF_6 solution, in sapphire tube

c) the resultant product with some HF in the solution, in sapphire tube.

	ReF_6^+	WF_6	ReF_6	ReF_7	IrF_5	IrF_6
ν_1 (cm^{-1})	793	771	756	736	719	702

Figure 5. a) Raman spectrum of the resultant solution from the reaction of ReF_7 and IrF_5 in WF_6 solution, in sapphire tube, 4880 Å light irradiates only the solution.

b) Raman spectrum of the ReF_6^+ species in the ReF_6/ReF_7 $IrF_6/IrF_5/WF_6$ system, in sapphire tube, 4880 Å irradiates the interface of solid and solution.

	ReF_6^+	WF_6	ReF_6	ReF_7	IrF_5	IrF_6
ν_1 (cm^{-1})	793	771	756	736	719	702

Figure 6. Raman spectra of

a) $ReF_6^+AuF_6^-$, in FEP tube

b) AuF_5, in sapphire tube

c) $ReF_6^+AuF_6^-$ and AuF_5, in sapphire tube, some $ReOF_4^+AuF_6^-$ impurity (see Chapter 5) was also observed.

Figure 7. Raman spectra of

a) β-$ReF_6^+AuF_6^-$, in quartz, at -50°C

b) α-$ReF_6^+SbF_6^-$, in quartz, at -50°C

c) $ReF_6^+AuF_6^-$, in FEP tube, at -50°C.

Figure 8. Proposed structure of $ReF_6^+ReF_7MF_6^-MF_5$

a) side view

b) top view.

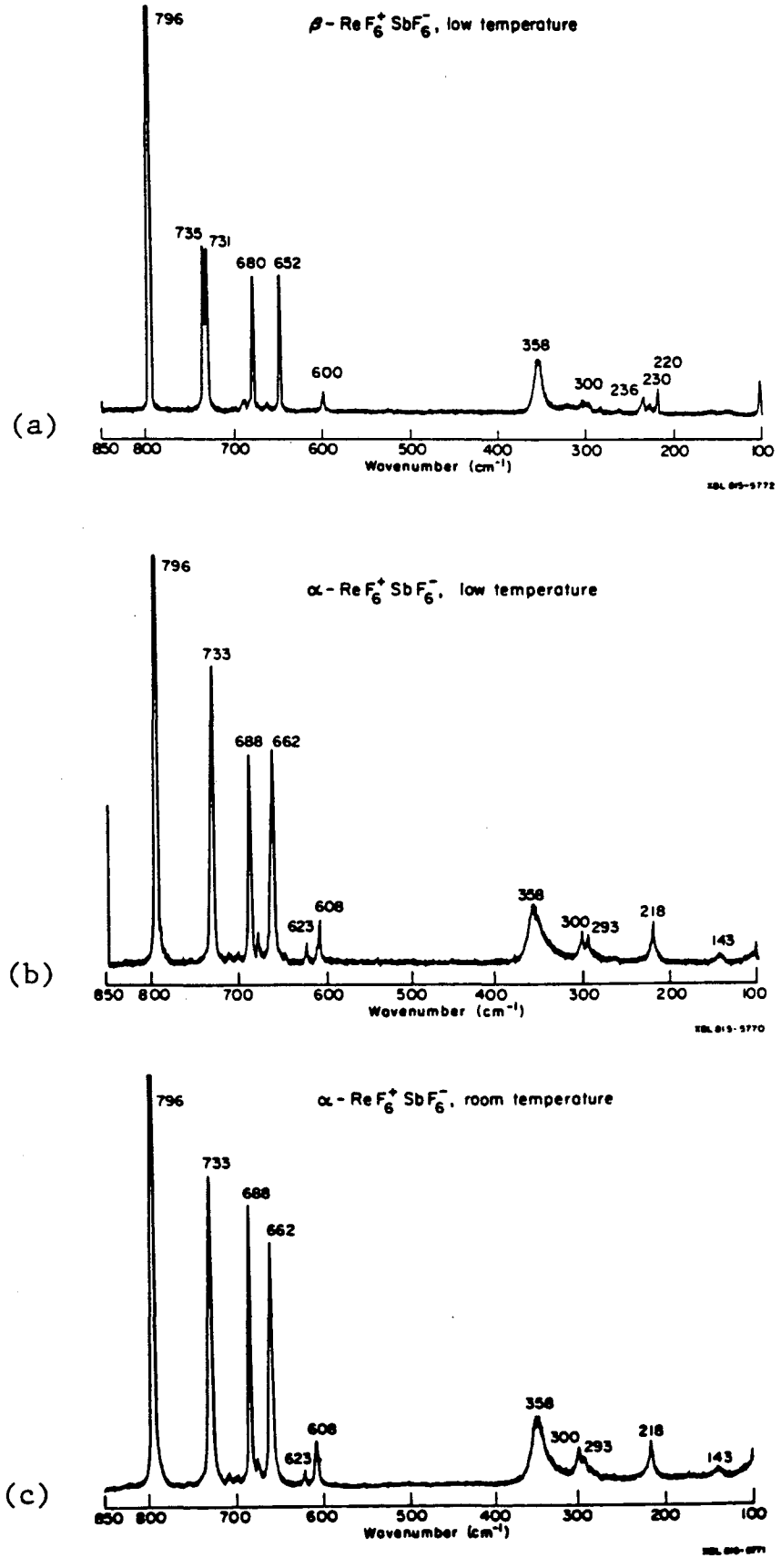
(a)
β - $ReF_6^+ SbF_6^-$, low temperature
796
735
731
680
652
600
358
300
236
220
230
850 800 700 600 500 400 300 200 100
Wavenumber (cm^{-1})
(b)
α - $ReF_6^+ SbF_6^-$, low temperature
796
733
688
662
623
608
358
300
293
218
143
850 800 700 600 500 400 300 200 100
Wavenumber (cm^{-1})
(c)
α - $ReF_6^+ SbF_6^-$, room temperature
796
733
688
662
623
608
358
300
293
218
143
850 800 700 600 500 400 300 200 100
Wavenumber (cm^{-1})

Fig. 1

Phase change studies of $ReF_6^+ SbF_6^-$

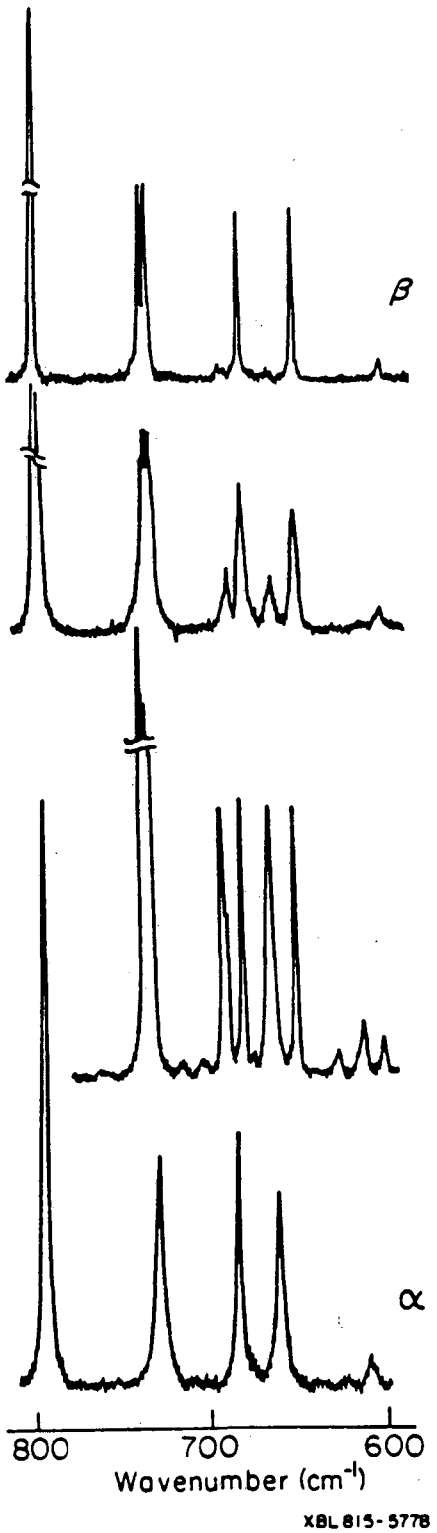

Fig. 2

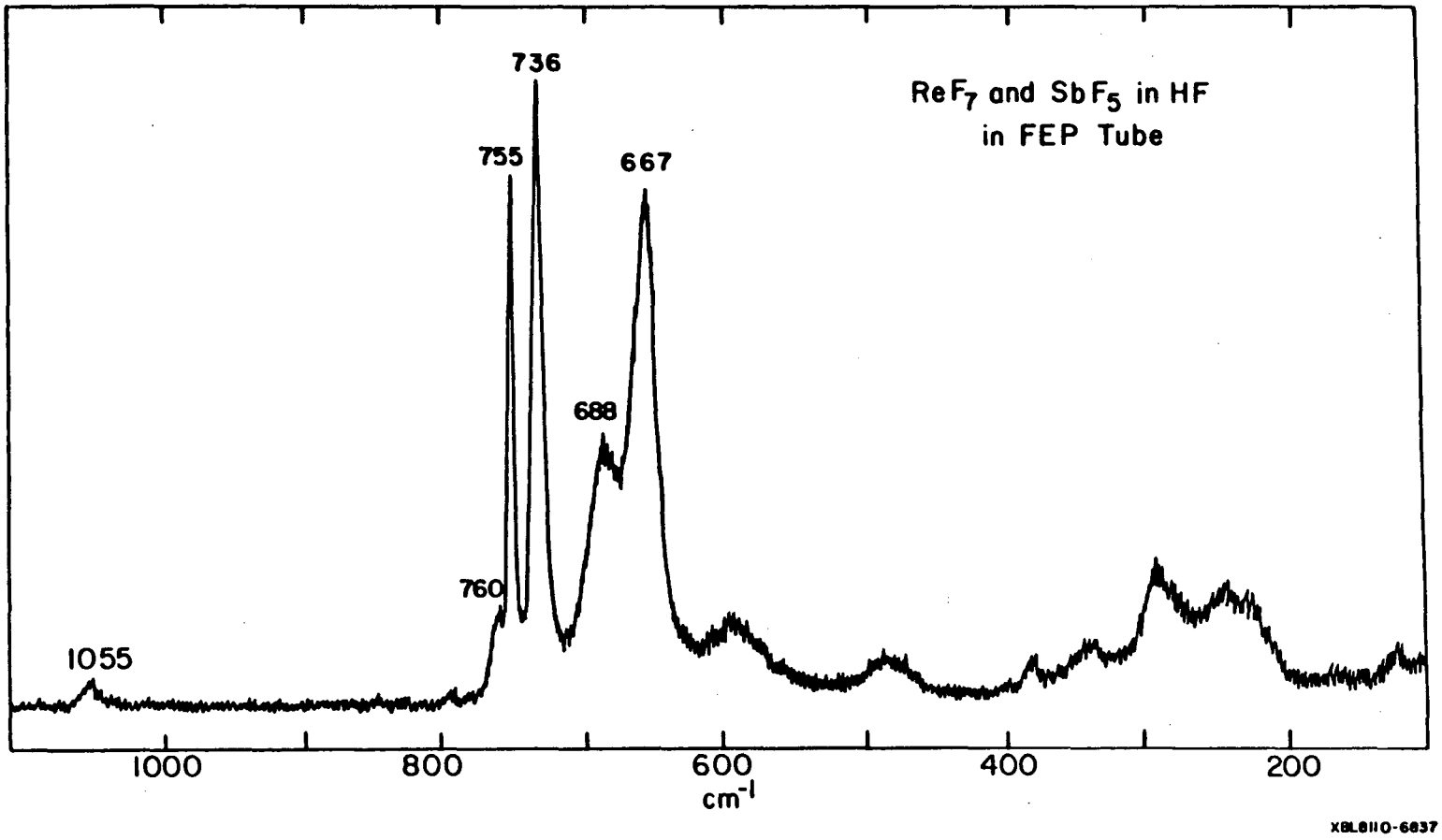
736
755
667
688
760
1055
ReF7 and SbF5 in HF
in FEP Tube
1000
800
600
400
200
cm-1
XBL8110-6837

Fig. 3

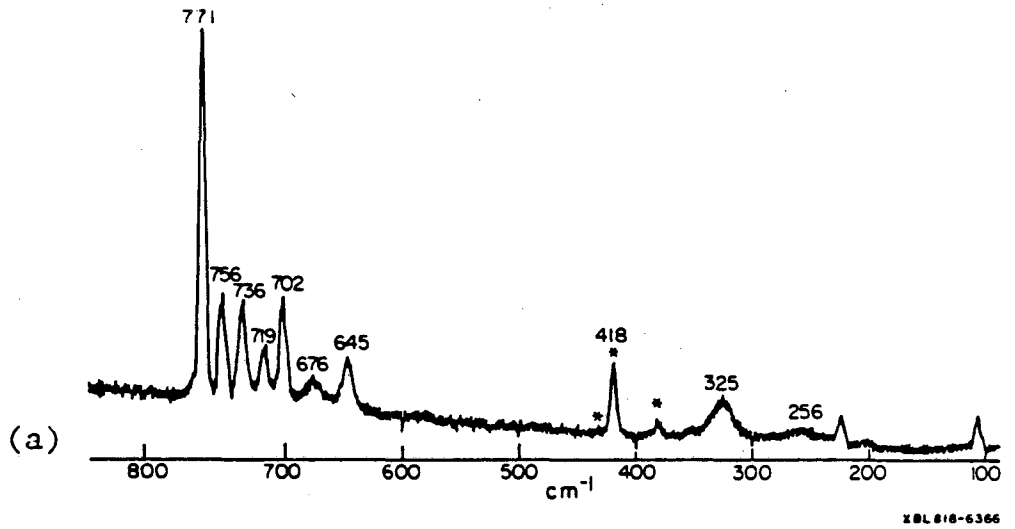

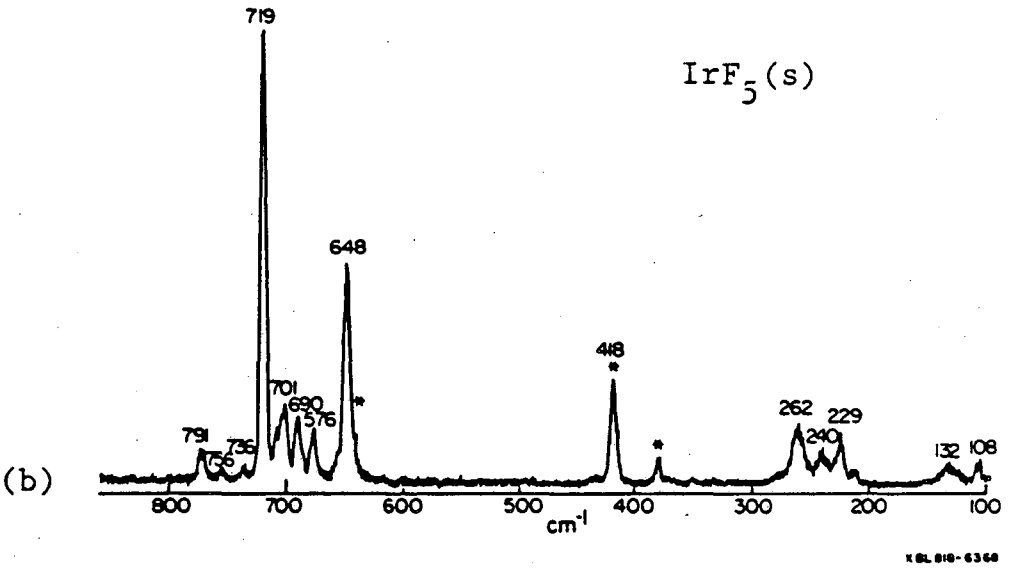

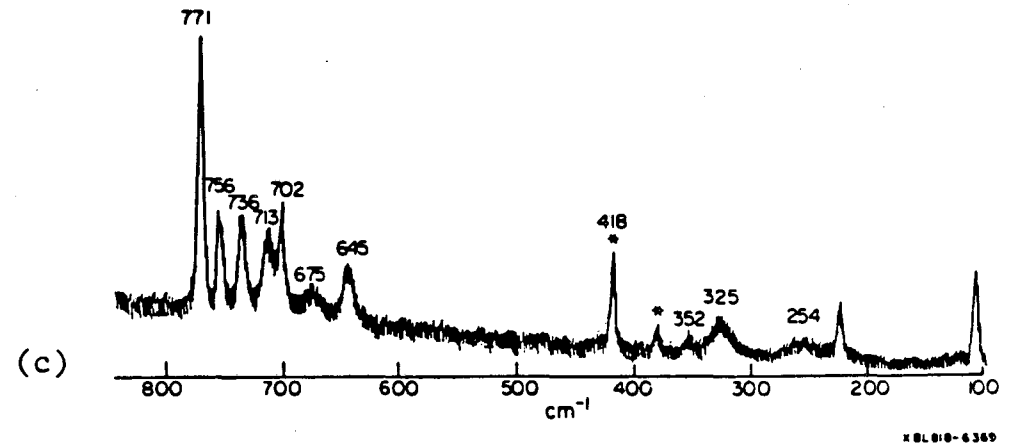

*sapphire signals

Fig. 4

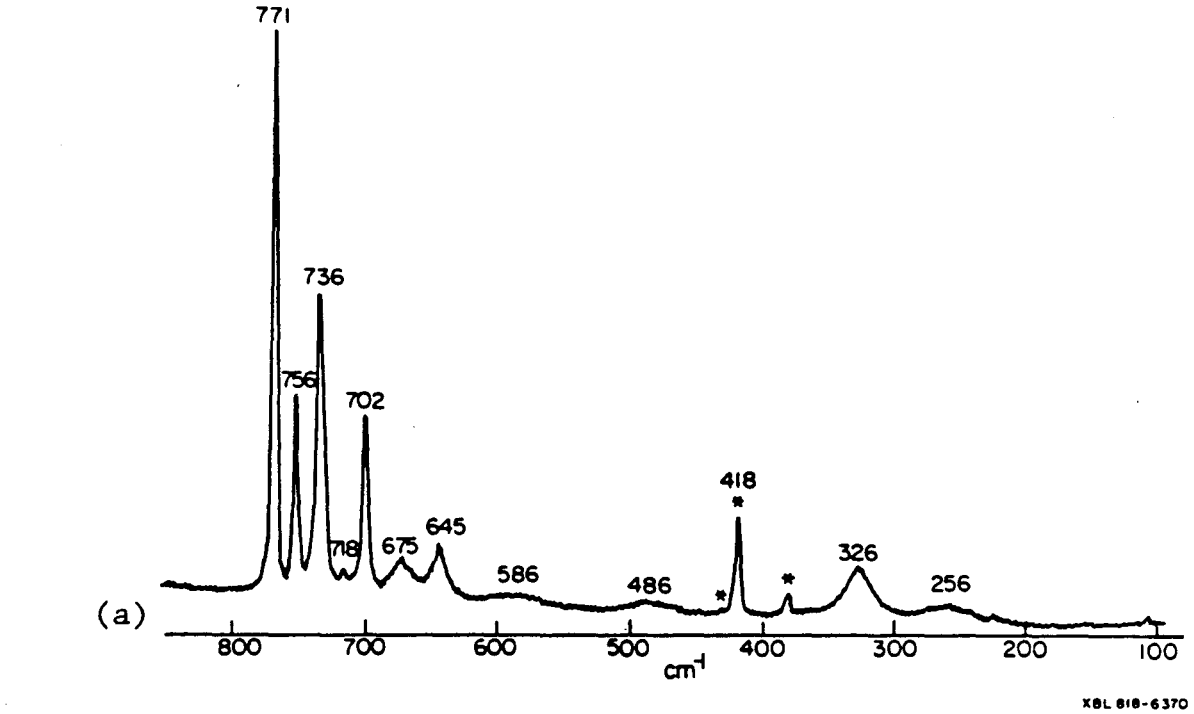

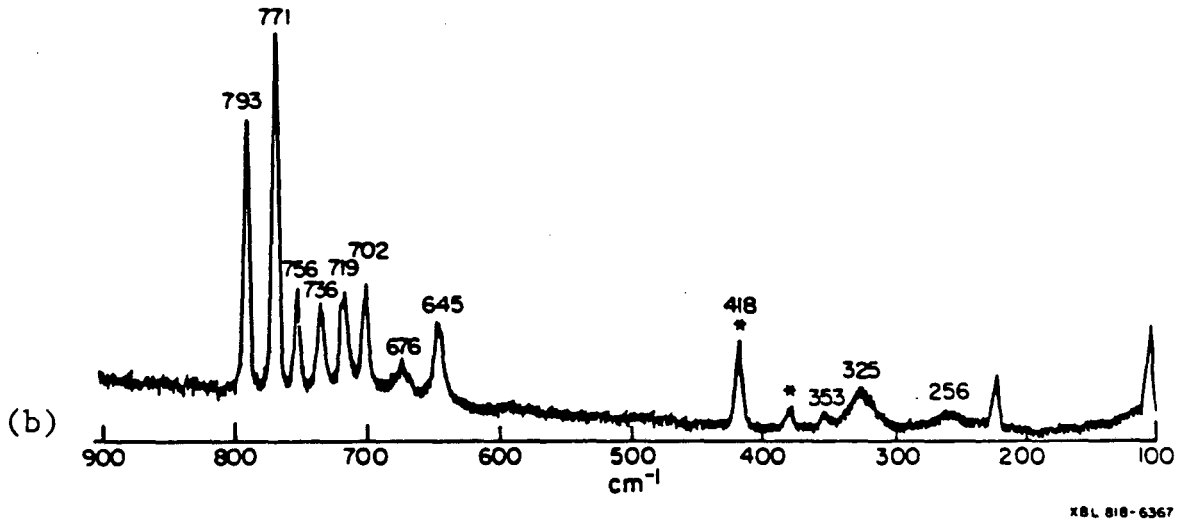

*sapphire signals

Fig. 5

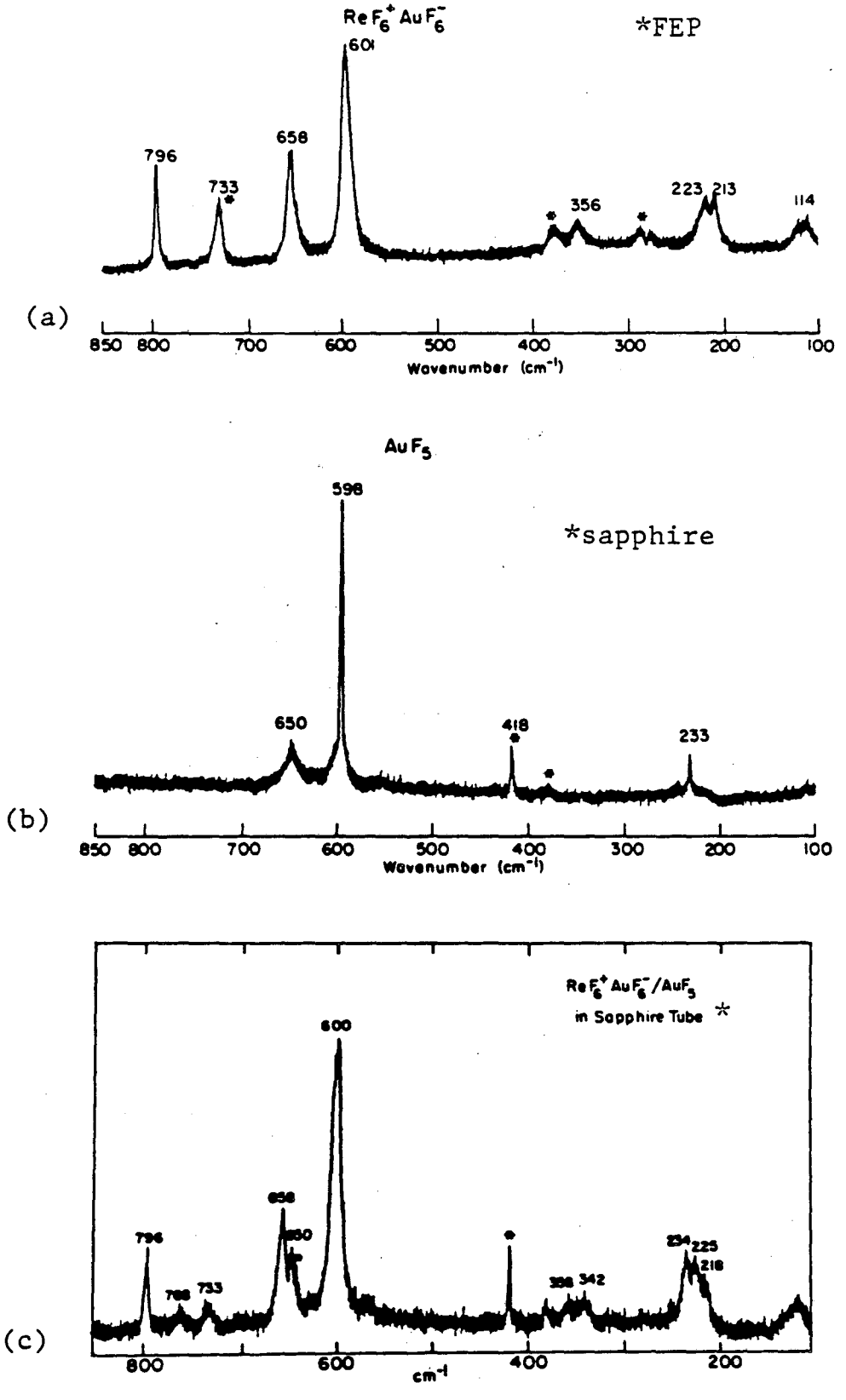
ReF6+ AuF6−
*FEP
601
658
796
733
356
223
213
114
(a)
850 800 700 600 500 400 300 200 100
Wavenumber (cm−1)
AuF5
598
*sapphire
650
418
233
(b)
850 800 700 600 500 400 300 200 100
Wavenumber (cm−1)
ReF6+ AuF6−/AuF5
in Sapphire Tube *
600
658
796
733
234
225
218
342
(c)
800
600
400
200
cm−1

Fig. 6

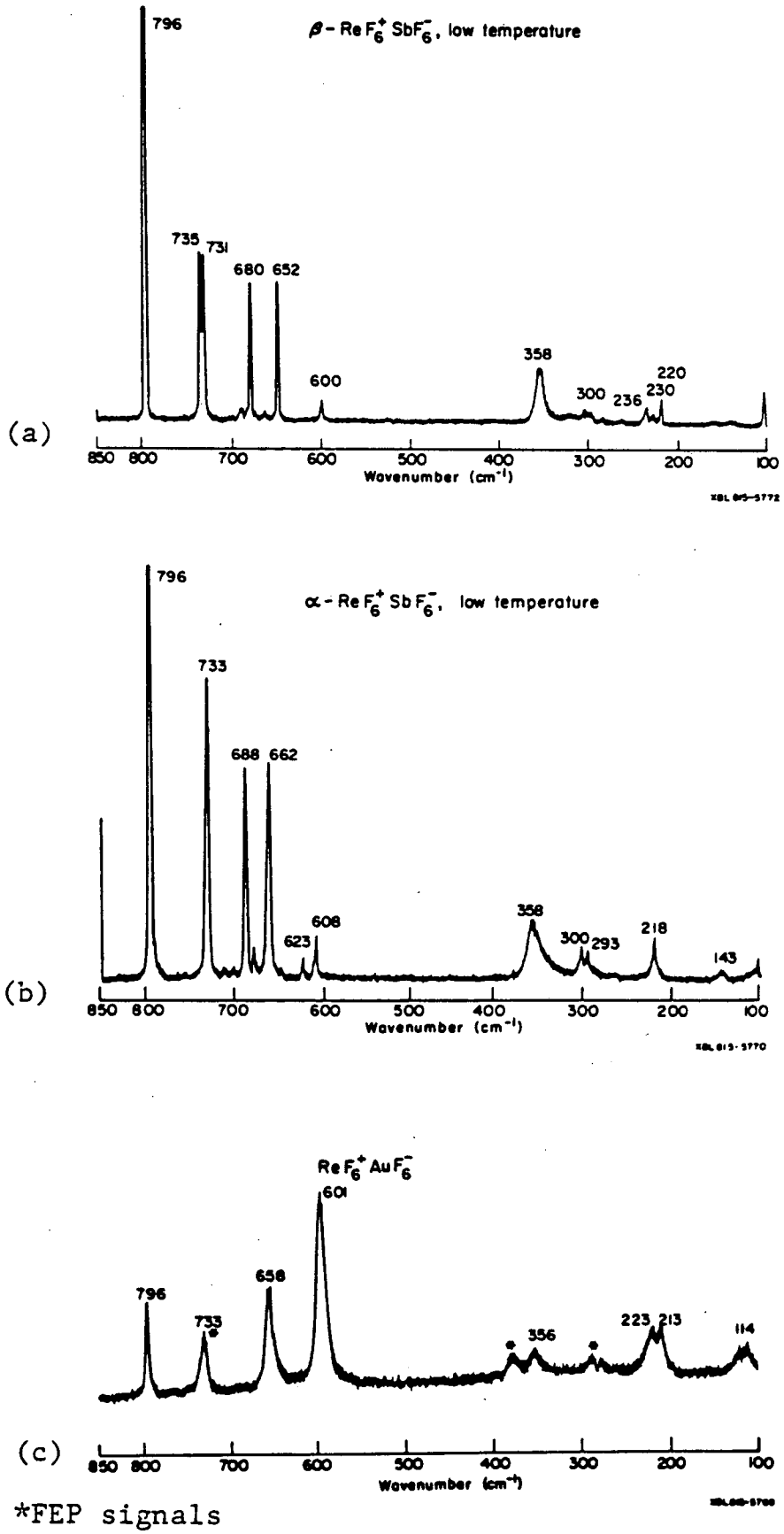

*FEP signals

Fig. 7

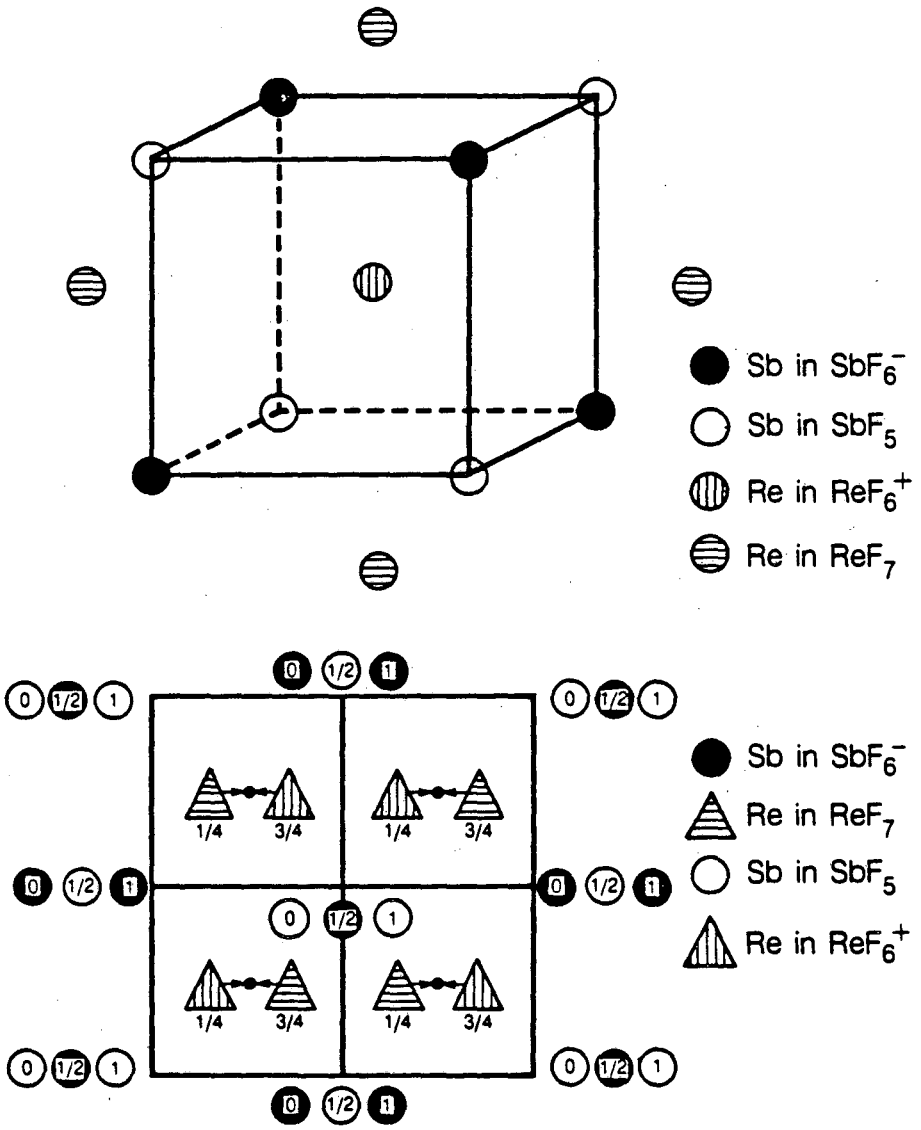
Sb in SbF_6^-
Sb in SbF_5
Re in ReF_6^+
Re in ReF_7
0
1/2
1
1/4
3/4
XBL 8410-8912

Fig. 8

CHAPTER 5

PREPARATION OF $ReOF_4^+MF_6^-$ COMPOUNDS, M = Sb, Au AND As

1. Introduction

$ReOF_4^+$ salts of SbF_6^- were first observed when $ReF_6^+SbF_6^-$ was accidentaly hydrolyzed by exposing it to moist air in the vacuum system. $ReOF_4^+SbF_6^-$ demonstrates greater thermal stability than $ReF_6^+SbF_6^-$. Moreover, $ReOF_4^+$ salts have also proved to be preparable with AuF_6^- and AsF_6^- anions, although the last one dissociates easily into its components. $ReOF_5$ therefore appears to be a better fluoride ion donor than ReF_7. This is contrast with the main group element analogues IOF_5 and IF_7.

II. Experimental

A. Preparation of $ReOF_4^+SbF_6^-$. In an attempt to grow single crystals by sublimation of $ReF_6^+SbF_6^-$, the high-temperature-structure α-$ReF_6^+SbF_6^-$ was loaded into a Monel can which had two nickel plates welded to the dismountable lid. Excess ReF_7, containing $ReOF_5$ impurity (as shown by its gas infrared spectrum), was introduced into the can. The mixture was heated to 100°C overnight in an oil bath while the lid was water cooled. The volatiles were removed by distillation at 0°C and the solid product was collected in the dry box. Its vibrational spectra are given in Fig. 1b (Raman) and 2 (infrared) and are summarized in Table I. They indicate that the solid should be formulated as $ReOF_4^+SbF_6^-$. Its X-ray powder pattern is shown in Table II and is indexed on the basis of an orthorhombic unit cell. The indexing indicates a C centered cell but the data are insufficent for precise space group assignment.

The same type of displacement reaction was observed when the α-$ReF_6^+SbF_6^-$ was reacted with a mixture of ReF_7 and small amounts of $ReOF_5$ in a FEP reaction tube at 80°C. A mixture of α-$ReF_6^+SbF_6^-$ and $ReOF_4^+SbF_6^-$ was observed (the identification being easily made on the basis of their Raman spectra). Exploiting of the thermal instability of $ReF_6^+SbF_6^-$, the $ReOF_4^+$ salt was obtained by heating the mixture at ~40°C under dynamic vacuum for several hours. Raman spectra of the solid indicated that only $ReOF_4^+SbF_6^-$ remained. $ReOF_4^+SbF_6^-$ also dissociated when the temperature was raised to 80°C.

In another preparation, a sample of ReF_7, with some impurity of $ReOF_5$, was introduced into a Teflon TEP reaction tube containing some SbF_5. The mixture was kept in a hot water bath at $\geq$60°C for several hours. ReF_7 was recovered by distillation at 0°C. The recovered ReF_7 sample was free of $ReOF_5$ as checked by its vibrational spectra. The white solid left was a mixture of α-$ReF_6^+SbF_6^-$ and $ReOF_4^+SbF_6^-$. Each was identified by its Raman spectrum.

B. Preparation of $ReOF_4^+AuF_6^-$. When an excess of impure ReF_7, containing $ReOF_5$, was used in interaction with $KrF^+AuF_6^-$ in an attempt to prepare $ReF_6^+AuF_6^-$ as described in Chapter 4, only $ReOF_4^+AuF_6^-$ was obtained. Its Raman spectrum is shown in Fig. 1c. The golden yellow solid is stable at room temperature and can be stored at -15°C indefinitely. Although the Raman spectra did not show any change, the freshly prepared sample gives a more complex X-ray powder pattern than a sample stored for a lengthy period at -15°C. Both patterns are given in Table III.

C. Preparation of $ReOF_4^+AsF_6^-$. In an attempt to purify ReF_7 from $ReOF_5$, a mixture of ReF_7 and $ReOF_5$ was treated at room temperature with a large excess of AsF_5 in a Teflon FEP reaction tube. AsF_5 was removed at -78°C under dynamic vacuum. The other volatiles, at 0°C, were distilled under static vacuum into a FEP reaction tube. The infrared spectra of these volatiles indicated the presence of ReF_7, $ReOF_5$ and AsF_5. The white solid left in the FEP reaction tube had some vapor pressure over the solid at room temperature, and the infrared spectrum of this vapor revealed the prsence of $ReOF_5$ and AsF_5 only. The solid vaporized quickly at room temperature when it was exposed to the large volume in the dry-box. The white solid gave the Raman spectrum shown in Fig. 1a and is attributable to $ReOF_4^+AsF_6^-$.

III. Discussion

The difference in fluoride-ion donating ability between ReF_7 and $ReOF_5$ is in sharp contrast with their iodine analogues. IF_7 has been demonstrated to be a better F^- donor than ReF_7 (see Chapter 4); it readily displaces ReF_7 from $ReF_6^+AuF_6^-$ salt to form $IF_6^+AuF_6^-$ and forms a thermally stable $IF_6^+AsF_6^-$ salt with AsF_5. IF_7 also reacts readily with polymeric AuF_5 to form $IF_6^+AuF_6^-$. On the other hand, IOF_5 is a rather poor base.[1] It forms a weak adduct with AsF_5 in SO_2F_2 solution at temperatures below -110°C. IOF_5 also interacts weakly with SbF_5 at -100°C to give a 1:1 adduct which dissociates to give a 1:2 adduct of $IOF_5 \cdot (SbF_5)_2$ as the temperature is raised. Raman and nmr spectroscopy show that the interaction between IOF_5 and the acid is weak and the linkage is via the oxygen atom. In contrast to IOF_5, the interactions between $ReOF_5$ with MF_5 (M = As, Sb and Au) are much stronger

and appear to be via fluorine bridges or F^- donation. Thus, the Re = O stretching frequency increases from 990 cm^{-1} in the molecular $ReOF_5$ to $\geq$1050 cm^{-1} in the $ReOF_5 \cdot MF_5$ complexes. This is in contrast to the I=O stretching[1] in the IOF_5 adducts where appreciable decrease in ν (I=O) is always observed (e.g., ν(I=O) in $IOF_5 \cdot SbF_5$ is at 864 cm^{-1} and IOF_5 molecule at 920 cm^{-1}).

Raman spectra of $ReOF_5 \cdot MF_5$ (M = As, Sb and Au) give similar patterns (see Fig. 1) for the bands associated with the Re species, indicating a similar chemical environment around the Re atom in each case. Since the vibrational characteristics of AsF_6^-, SbF_6^- and AuF_6^- species are known under various departures from O_h symmetry it is best to attend to the assignments of anion bands at the outset. The Raman bands of the anionic MF_6^- species are easily identified and are summarized in Table I. For the AsF_6^- species,[2] the bands at 686 and 583 cm^{-1} are attributable to ν_1 and ν_2 respectively (ν_5 is obscurred by a FEP band at 377 cm^{-1}). For the SbF_6^- species,[3] ν_1, ν_2 and ν_5 are easily identified at 655, 603 and 213 and 230 cm^{-1} respectively. The band at 688 cm^{-1} may be due to the ν_3 (Sb-F) band forbidden in O_h symmetry being allowed by symmetry lowering. Similar observation pertain to the $ReOF_4^+AuF_6^-$ salt. Here the forbidden ν_3 band in O_h symmetry for AuF_6^- is again seen and at the frequency appropriate for ν_3 AuF_6^- at 654 cm^{-1}. The typical[4] Raman frequencies for AuF_6^- are also observed: ν_1 at 600 cm^{-1} and ν_5 at 225 and 216 cm^{-1}. Thus, in all cases there appears to be an approximation to an octahedral MF_6^- species. A cationic $ReOF_4^+$ species is therefore to be expected. As has already been stated the ν (Re=O) stretching vibrations are consistent with a cationic formation. The

vibrational data is insufficient (e.g, polarization information was not obtainable) to provide a definitive treatment. The symmetry of the cation could be either C_{2v} (based on a D_{3h} geometry with Re = O in the equatorial plane) or C_{4v}. The simplicity of the Re-F stretching band pattern hint however that the geometry is not of lower symmetry then C_{2v}. The proposed cationic species $ReOF_4^+$ is identified with the vibrational modes listed in Table I.

In the case of $ReOF_4^+MF_6^-$ salts, neutral monomeric MF_5 species are believed to be absent. If the bands attributed to ν_3-like mode are due to manomer, the concentration must be very much less then in the $ReF_6^+ReF_7SbF_6^-SbF_5$ materials. Moreover the ν (Re = 0) at 990 cm^{-1}, characteristics of molecular $ReOF_5$, is entirely absent from the spectra all three salts (see Fig. 1).

IV. Conclusions

The findings in this work indicate that $ReOF_5$ is a superior fluoride ion donor to its close geometric relative[5,6] IOF_5. This is all the more interesting because of the superior fluoride ion donating capability of IF_7 over ReF_7. One can, of course, simply attribute these difference to the more ready availability of d orbitals at Re than at I. Thus, the bonding of the seven fluorine ligands to Re may be anticipated to be stronger than to I. In this fashion, it is possible to account for the poorer basicity of ReF_7. The similar basicities of ReF_7 and IF_7, however, cautions us that the extent of d orbital participation may not be large in ReF_7. The greater stability of the $ReOF_4^+$ relative to the IOF_7^+ ion must then be attributed to the availability of d orbitals at the Re atom for π bonding to the oxygen ligand. In the case of

IOF_4^+, it can easily be argued that the d orbitals are too large for effective overlap. But it would be misleading to view the bonding in these species to be markedly different since the vibrational analysis and the ^{19}F nmr[5] spectra indicate that EOF_5 and EF_7 molecules are remarkably similar. As we have seen large differences in basicity are derived from small energy differences.

REFERENCES

1. M. Brownstein, R. J. Gillespie and J. P. Krasznai, Can. J. Chem., 56 2253 (1978)
2. A. Zalkin, D. L. Ward, R. N. Biagioni, D. H. Templeton and N. Bartett, Inorg. Chem., 17 1318 (1978)
3. D. E. McKee and N. Bartlett, Inorg. Chem., 12 2738 (1973)
4. K. Leary, A. Zalkin and N. Bartlett, Inorg. Chem., 13 775 (1974)
5. N. Bartlett, S. Beaton, L. W. Reeves and E. J. Wells, Can. J. Chem., 42 2531 (1964)
6. N. Bartlett and N. K. Jha, J. Chem. Soc. (A), 536 (1968)

Table Contents

Table I

Vibrational modes of $ReOF_4^+MF_6^-$ salts (M = As, Sb, Au).

$ReOF_4^+$ cation, (in cm^{-1})

Assignment	$ReOF_4^+AsF_6^-$	$ReOF_4^+SbF_6^-$	$ReOF_4^+AuF_6^-$
Raman			
ν(Re = O)	1056 (50)*	1054 (50)	1053 (5)
ν_a(Re-F)	766 (60)	759 (100)	762 (10)
ν_b(Re-F)	696 (20)	696 (10)	696 (3)
ν_c(ReF)	340 (40)	340 (40)	340 (20)
IR			
ν(Re = O)		1052 (w)	
ν_a(Re -F)		740 (m)	
ν_b(Re-F)		695 (w)	
ν_d(Re-F)		650 (s)	
ν_e(Re-F)		480 (m)	

* relative intensity in parenthesis, w = weak m = medium s = strong

MF_6^- anions, (in cm^{-1})

Assignment	$ReOF_4^+AsF_6^-$ (a)	$ReOF_4^+SbF_6^-$ (b)	$ReOF_4^+AuF_6^-$ (c)
ν_1	686 (20)	655 (40)	600 (100)
ν_2	580 (15)	603 (10)	--
ν_3	---	688 (25)	654 (30)
ν_5	371 (30)	239 (5)	225 (15)
		213 (10)	216 (5)

* forbidden in O_h symmetry, being allowed in symmetry lowering of MF_6^-.

(a) ref. 2, (b) ref. 3, (c) ref. 4

Table II

X-ray powder patern of $ReOF_4^+SbF_6^-$

Intensity	$\frac{1}{d^2}$ obs.	$\frac{1}{d^2}$ calc.	hkl
vw	.0292	.0293	200
s	.0391	.0393	111
s	.0529	.0528	201
s	.0574	.0574	021
m^+	.0631	.0633	220
m	.0747	.0745	310
m^-	.0839	.0837	130
w	.0936	.0940	002
vw	.1072	.1072	131
vvw	.1229	.1233	202
w^+	.1406	.1410	401
w^-	.1517	.1514	420
w	.1574	.1573	222
w	.1659	.1659	331
w	.1772	.1777	132
vvw	.2162	.2155	510
vvw	.2279	.2273	113
m^+	.2435	.2429	151
vw	.2596	.2599	530
w	.2647	.2644	600
vw	.2776	.2782	350
vw	.3053	.3055	060

Table II (continued)

w	.3218	.3218	620
w	.3527	.3539	532,333
w	.3580	.3583	261,602
w	.3715	.3722	352
vvw	.4001	.4002	640
vw	.4192	.4192	551
vvw	.4304	.4310	153

orthorhomic

$\underline{a} = 11.67\text{Å}$

$\underline{b} = 10.86\text{Å}$

$\underline{c} = 6.52\text{Å}$

$V = 825.6\text{Å}^3$

$z = 4$

$V_{formula} = 206.4\text{Å}^3$

Table III

X-ray powder patter for $ReOF_4^+AuF_6^-$

Intensity	$\frac{1}{d^2}$ (freshly prepared)	Intensity	$\frac{1}{d^2}$ (stored for 1 year)
vvw	.0157		-
vvw	.0207		-
vvw	.0264		-
vvw	.0308		-
m	.0366		-
s	.0396	s	.0404
m	.0482		-
vs	.0547	s	.0559
vs	.0571	s	.0578
vvw	.0614		-
m	.0645	m	.0656
m^-	.0689		-
vw	.0726		-
m	.0783	m	.0797
m	.0828	m	.0840
m^-	.0944	m	.0954
w	.1022	w	.1032
w	.1100	vvw	.1080
w	.1175		-
w^+	.1251		-
m^-	.1342		-
m^-	.1493	m^-	.1503
m^-	.1587	S	.1601
w^+	.1692	m	.1711
vvw	.1734	w	.1754
vw	.1773	m^-	.1786
vw	.1821		-

Table III (continued)

Intensity	$\frac{1}{d^2}$ (freshly prepared)	Intensity	$\frac{1}{d^2}$ (stored for 1 year)
vw	.1888	vvw	.1890
vvw	.2035		-
vw	.2178		-
w^+	.2282	m	.2302
w^+	.2344	vvw	.2356
w^+	.2403	w^+	.2418
w^+	.2442	w^+	.2434
vvw	.2528	vw	.2540
w^+	.2640		-
w^+	.2710	vw	.2740
vw	.2806	m^+	.2825
vw	.2907		-
vvw	.3198	vw	.3023
w^+	.3381	w	.3405
vvw	.3454		-
w^+	.3578	m^-	.3593
vvw	.3660	vvw	.3679
w^+	.3745	w^+	.3769
vw	.3944	vw	.3981
vw	.4170	vw	.4180
vw	.4282		
vw	.4389		
vw	.4586		
vvw	.5012		
vvw	.5122		
vvw	.5254		
vvw	.5344		

s = strong m = medium w = weak v = very

Figure Captions

Figure 1. Raman spectra of (a) $ReOF_4^+AsF_6^-$, (b) $ReOF_4^+SbF_6^-$ and (c) $ReOF_4^+AuF_6^-$.

Figure 2. (a) Infrared and b) Raman spectra of $ReOF_4^+SbF_6^-$.

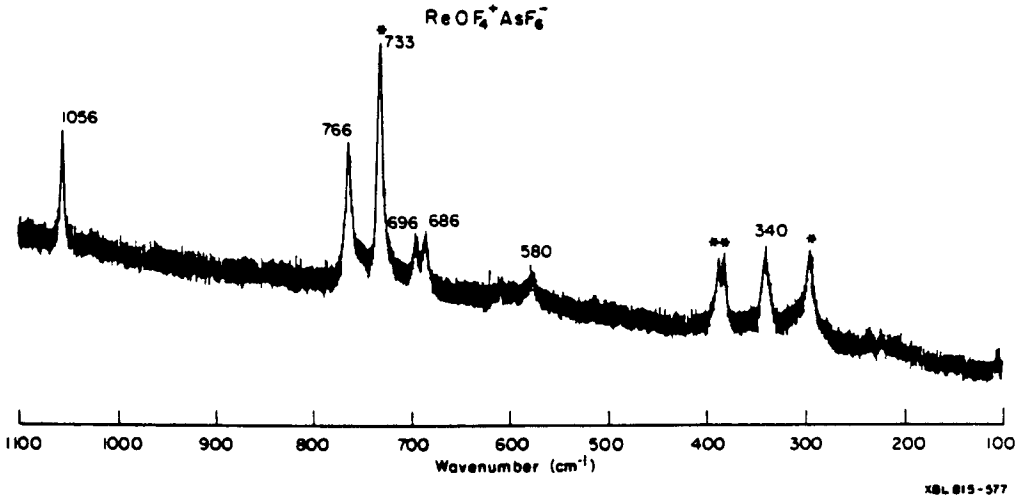

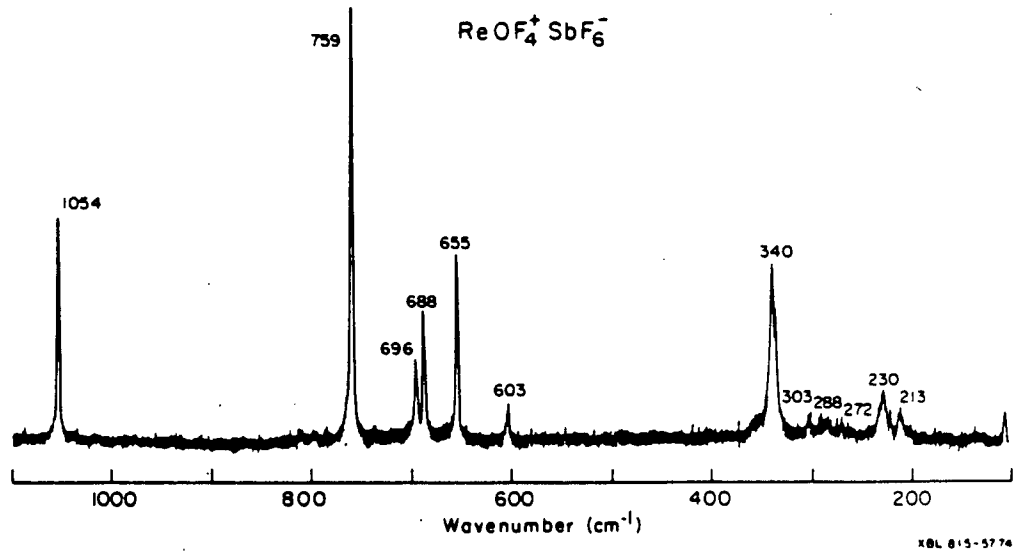

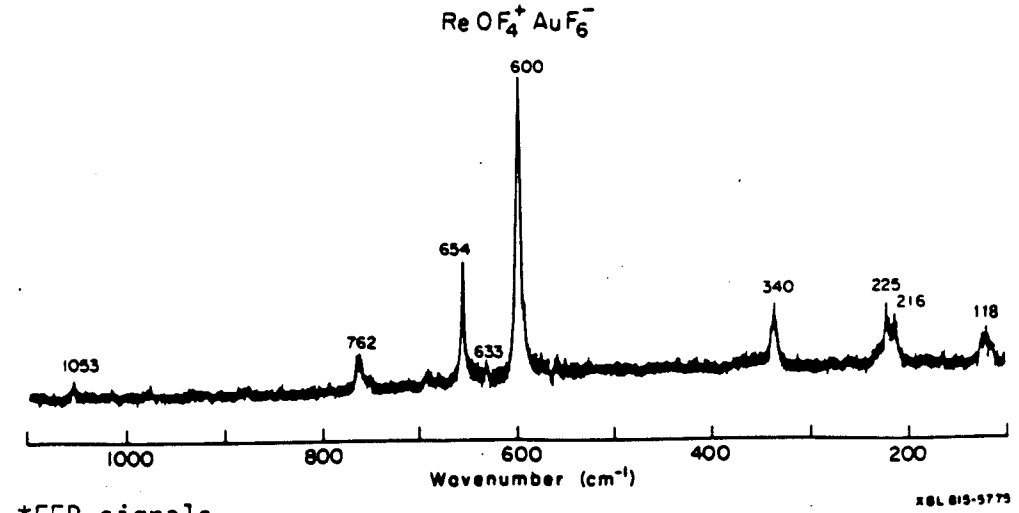

*FEP signals

Fig. 1

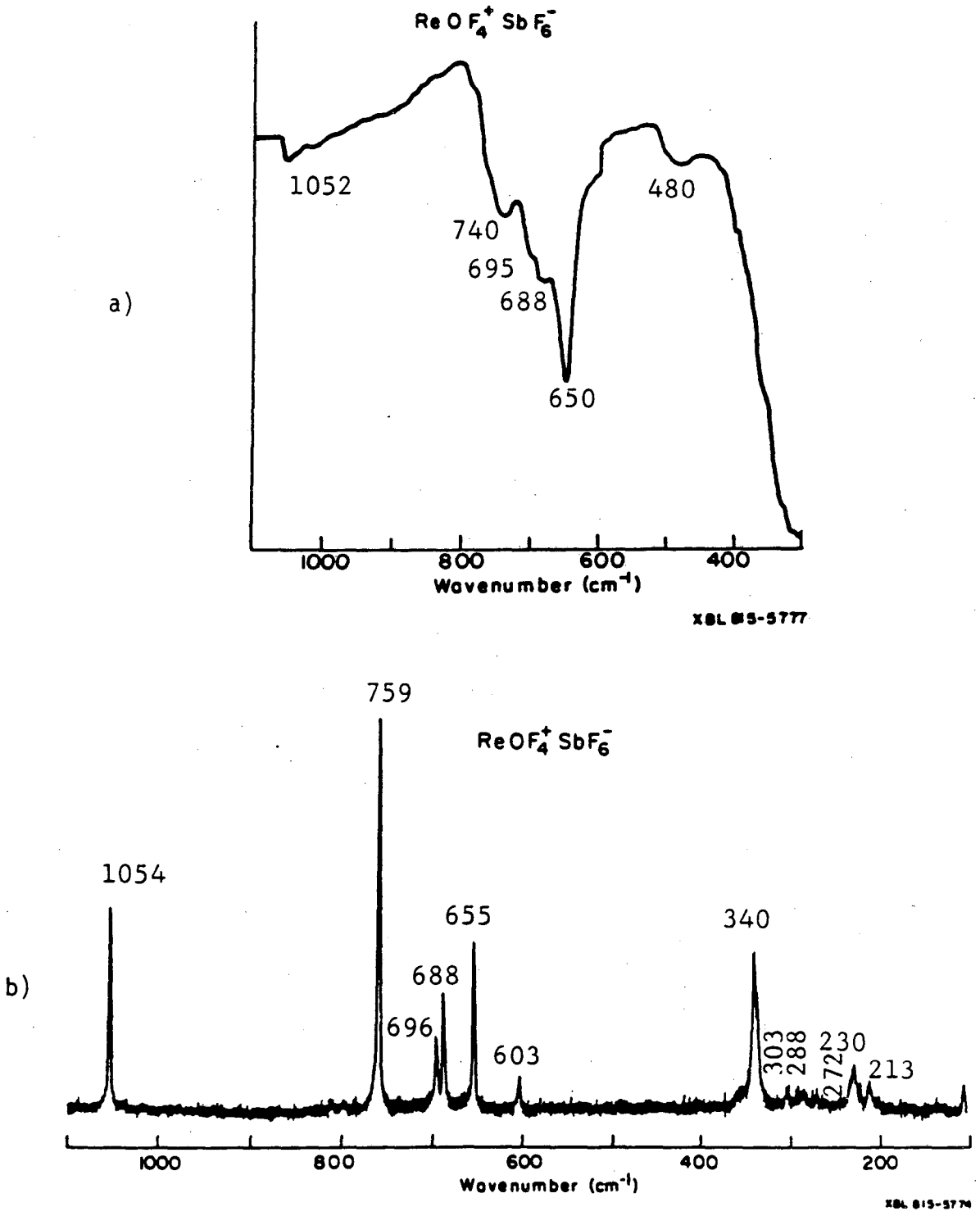
a)
$ReOF_4^+ SbF_6^-$
1052
740
695
688
650
480
1000
800
600
400
Wavenumber (cm^{-1})
XBL 815-5777
b)
759
$ReOF_4^+ SbF_6^-$
1054
655
688
696
603
340
303
288
272
230
213
1000
800
600
400
200
Wavenumber (cm^{-1})

Fig. 2

CHAPTER 6

TOWARDS THE SYNTHESIS OF A NEW ClF_6^+ SALT AND Np(VII) COMPOUND

I. Introduction

Although all seven electrons in the valence shell of neptunium can be involved in chemical bonding, no molecular Np(VII) compound has yet been reported. The only reported Np(VII) compounds are oxide complexes of type of Li_5NpO_6 and Ba_2LiNpO_6[1-4]. The diamagnetism of these compounds indicates their heptavalent oxidation state. Burns and his coworkers[5] have also established Np(VII) in $LiCo(NH_3)_6\ Np_2O_8\ (OH)_2\ 2H_2O$ from their single crystal X-ray diffraction study.

Because of its strong oxidizing ability, molecular KrF_2 had been employed previously in these laboratories[6] in interaction with the neptunium compounds of lower oxidation state. Similar reactions had also been tried by Drobyshevskii et al[7,8], but no Np(VII) compound had been prepared in this way hitherto. Use of excess KrF_2 led only to the formation of NpF_6. It therefore appeared likely that molecular NpF_7 is thermally unstable at ordinary temperature. It did appear to be possible, however, that a neptunium (VII) compound could be obtained in the form of $NpF_6^+MF_6^-$, an analogue of $ReF_6^+MF_6^-$ (M = Sb, Au). The latter salts have been discussed in Chapter 4. The advantage presented by $NpF_6^+MF_6^-$ over NpF_7 derives from the smaller ligand repulsion in the NpF_6^+ species compared with NpF_7.

The powerful oxidizing capabilities of PtF_6 and the $Kr_2F_3^+$ or KrF^+ salts of AuF_6^- have been demonstrated in Chapter 4. These powerful oxidizing agents have been employed here towards the synthesis of NpF_6^+ salts. Parallel studies of bromine (VII) and chlorine (VII) analogues are also reported.

II. Experimental

Safety precautions and special equipment for handling the hazardous radioactive neptunium materials have been described in Chapter 1.

A. Towards the synthesis of new neptunium (VII) compounds

(1) Reaction of NpF_6 with $KrF^+Sb_2F_{11}^-$ in HF solution. In a Teflon reaction vessel, a mixture of nearly stoichiometric amounts of NpF_6 (~ 1.1 mole) and $KrF^+Sb_2F_{11}^-$ (~ 0.56 m mole) were allowed to react in HF solution at -23°C. Gas evolution was observed. THe reaction vessel was allowed to warm up slowly to room temperature to ensure the completion of the reaction. Completion was indicated by the cessation of gas evolution. The characteristic orange-yellow color of NpF_6 was not observed. The solution was colorless. The volatiles were removed under dynamic vacuum with the sample at -78°C. THe vacuum was applied for a few minutes. The solution which remained was clear and colorless. A large portion of the HF solvent was then pumped away in dynamic vacuum for several hours at -45°C and a colorless, mobile, low-vapor pressure liquid remained. (This resembles the $ReF_7/SbF_5/HF$ experience described in Chapter 4). Attempts to isolate solids by removals of HF or by cooling the system were not successful. The hazardous nature of the material and the unsuitable container ruled out Raman spectroscopic work.

(2) Reaction of NpF_6 with PtF_6 in WF_6. Excess PtF_6 was allowed to mix with NpF_6 in WF_6 solution, at room temperature, in a Teflon FEP tube. No sign of reaction was observed. All volatiles (NpF_6, PtF_6 and WF_6) were collected in another FEP tube by distillation under static vacuum at room temperature. No material was left in the original reaction tube.

(3) Reaction of NpF_6 with $KrF^+PtF_6^-$. $KrF^+PtF_6^-$ was prepared by reacting KrF_2 and PtF_6 at room temperature as described[9]. Excess of NpF_6 and WF_6 were then distilled into the FEP tube containing $KrF^+PtF_6^-$. The mixture was allowed to warm up to room temperature. Evaluation of gas was observed for a few minutes. It was assumed that the reaction was complete when gas evolution ceased. With the mixture held at -78°C, volatiles (Kr and F_2) were removed under dynamic vacuum. The NpF_6 and WF_6 were recovered by distillation at room temperature under static vacuum. A red solid remained and was shown by its X-ray powder pattern to be PtF_5. The safety requirements prevented Raman spectroscopic examination of the volatiles collected.

B. Oxidation of BrF_5 with $KrF^+AuF_6^-$

Pure $KrF^+AuF_6^-$ was obtained in a sapphire tube by decomposing $Kr_2F_3^+AuF_6^-$ in HF solution at room temperature. HF was completely removed under dynamic vacuum overnight at -78°C. Pure BrF_5, as checked by its Raman spectrum, was distilled into the sapphire tube and was allowed to react with $KrF^+AuF_6^-$ at room temperature. The Raman spectrum of the resultant solution is illustrated in Figure 1 and indicates the presence of BrF_6^+ and AuF_6^-. The Raman peak at 598 cm^{-1}, which is polarized, is assigned to $\nu_1(AuF_6^-)$, the peaks at 238 and 218 cm^{-1} are attributed to $\nu_5(AuF_6^-)$ which is usually split (see Chapter 3) by site-symmetry effects. Another polarized peak at 658 cm^{-1} is assigned to $\nu_1(BrF_6^+)$, and ν_5 of BrF_6^+ is observed as a weak shoulder at 405 cm^{-1}. ν_2 of BrF_6^+, at 688 cm^{-1}, is buried under the strong peak at 684 cm^{-1} of the BrF_5 solvent. These assignments of the Raman bands are consistent with those reported[10,11] for BrF_6^+ and AuF_6^- ions. The

results are tabulated for BrF_6^+ and AuF_6^- in Table I. The X-ray powder pattern is isomorphous with that of $IF_6^+AuF_6^-$, indicating a cubic unit cell. A preliminary report of $BrF_6^+AuF_6^-$ has been given by Zuchner and Bartlett[12].

C. Towards the synthesis of $ClF_6^+AuF_6^-$ [12]

Pure ClF_5 was obtained by allowing ClF_5 to react with $Kr_2F_3^+AuF_6^-(KrF_2)_n$ in a FEP reaction tube. By this process, ClO_2F impurity in the ClF_5 precipitated as the $ClO_2^+AuF_6^-$ salt and ClF_3 impurity was fluorinated to ClF_5. The purified ClF_5 was then distilled into an adjacent FEP reaction tube containing $Kr_2F_3^+AuF_6^-(KrF_2)_n$. The mixture of ClF_5 and $Kr_2F_3^+AuF_6^-(KrF_2)_n$ was allowed to react. At a temperature below 0°C, decomposition of the KrF_2-rich salt of AuF_5 was observed, with formation of the thermally more stable $KrF^+AuF_6^-$ salt. At ambient temperature, vigorous evolution of gases was observed and the pressure build up in the FEP tube had to be released into the vacuum line occasionally to avoid explosion. The solid product, after the removal of Kr and F_2 and recovery of ClF_5, was shown by its Raman spectrum (see Figure 2) to be $ClF_4^+AuF_6^-$.

III. Discussion

A. BrF_6^+ and ClF_6^+

Of the XF_6^+ (X = I, Br and Cl) salts, the IF_6^+ salts are most easily prepared and most stable (see Chapter 4 and 5). BrF_6^+ salts have been prepared by reacting[9,11] BrF_5 with KrF_2 salts of MF_5 (M = As, Sb and Au). The effectiveness of the BrF_6^+ synthesis by $KrF^+AuF_6^-$ is again demonstrated here. The polarization information, with the Raman spectrum of $BrF_6^+AuF_6^-$ in BrF_5 solution, shows that the peaks at 598

and 658 cm^{-1} are polarized. They are therefore attributed to ν_1 (AuF_6^-) and ν_1 (BrF_6^+) respectively. THe spectrum also indicates that both the AuF_6^- anion and the BrF_6^+ cation are close to the O_h symmetry observed for AuF_6^- in HF solution (see Chapter 3).

The first difficulty encountered in the attempts to prepare a ClF_6^+ salt by the reaction of ClF_5 with $Kr_2F_3^+AuF_6^-$ or $KrF^+AuF_6^-$ is the purity of the starting material ClF_5. It usually contains impurities such as ClF_3 and ClO_2F. ClF_3 reacts more readily with oxidizing agents than ClF_5 and ClO_2F is probably a better fluoro-base than ClF_7. Therefore the ClF_5 to be used in the preparation of ClF_6^+ was first treated with a sample of $Kr_2F_3^+AuF_6^-$ $(KF_2)_n$ to remove these impurities. Unfortunately, the synthesis of $ClF_6^+AuF_6^-$ did not succeed. This was probably due to the low solubility of $Kr_2F_3^+AuF_6^-$ $(KF_2)_n$ salt in ClF_5. Subsequent work by Christe et al[13], involving the related synthesis of $ClF_6^+AsF_6^-$ and $ClF_6^+SbF_6^-$, did succeed and the notable feature of their synthetic procedure is that they permitted the KrF^+ and $Kr_2F_3^+$ reactants to interact with ClF_5 at room temperature over a long period (two days for the reaction of ClF_5 with $KrF^+AsF_6^-$) and finally at 35°C or higher. Christe et al removed the $ClF_4^+MF_6^-$ impurity, formed in substantial quantities along with $ClF_6^+MF_6^-$, by exploiting the high dissociation pressure of the impurity, which was thereby removed by vacuum sublimation. ClF_5 is a poor fluoro-base and the salt has low kinetic stability towards dissociation because the highly unsymmetrical[14] cation distorts the anion by polarization:

$$ClF_4^+AsF_6^- \dashrightarrow ClF_5 + AsF_5$$

It is possible that the stability of $ClF_6^+MF_6^-$ salts could be kinetic at ambient temperature. The high symmetry (O_h) of cation and anion reduces the opportunity for charge localization at any F ligand.

The other reported ClF_6^+ compound is $ClF_6^+PtF_6^-$ prepared by photoreaction[15,16] of ClF_5 or ClO_2F with PtF_6. Since AuF_5 has been found to be a good fluoro-acid, comparable to SbF_5 and better than PtF_5 and AsF_5, in the preparation of ReF_6^+ salts (see Chapter 4), there is no reason why $ClF_6^+AuF_6^-$ can't be prepared. Clearly, following the experience of Christe and his co-worker's[13], it will be necessary, in future preparative work, to maintain a large excess of KrF_2 in the ClF_5 solution of $Kr_2F_3^+AuF_6^-$ and to hold that solution at 25°C or higher for many hours until all KrF_2 is consumed or decomposed. In any case, high yields of $ClF_6^+AuF_6^-$ are not to be expected.

B. Np (VII) compounds

Disappearance of the characteristic orange-yellow color of NpF_6 and the formation of a colorless solution containing neptunium, in the reaction of NpF_6 with $KrF^+Sb_2F_{11}^-$ in HF solution, is very strong evidence for oxidation of the NpF_6. Since Np(VII) has no non-bonding valence electrons, colorless species are anticipated. The decomposition of $KrF^+PtF_6^-$ to form PtF_5 in the presence of NpF_6 could also signify Np(VII) formation. It is necessary to assume the formation of NpF_7, or complexes of it, to account for these observations since $KrF^+PtF_6^-$ is thermally stable under the condition used. Thus the overall reaction may have been:

$$2NpF_6 + KrF^+PtF_6^- \rightarrow Kr + 2NpF_7 + PtF_5$$

Unfortunately, the absence of Raman spectroscopic facilities at the neptunium laboratory prevented adequate characterization of the volatiles. In spite of the failure to confirm Np(VII) compounds, these experiments permit us to draw tentative conclusion relevant to the thermochemistry.

The failure of NpF_6 and PtF_6 to interact ($NpF_6 + PtF_6 \text{ --X--> } NpF_6^+PtF_6^-$) provides an estimate of the minimum value for the ionization potential of NpF_6. In the following Born-Haber cycle:

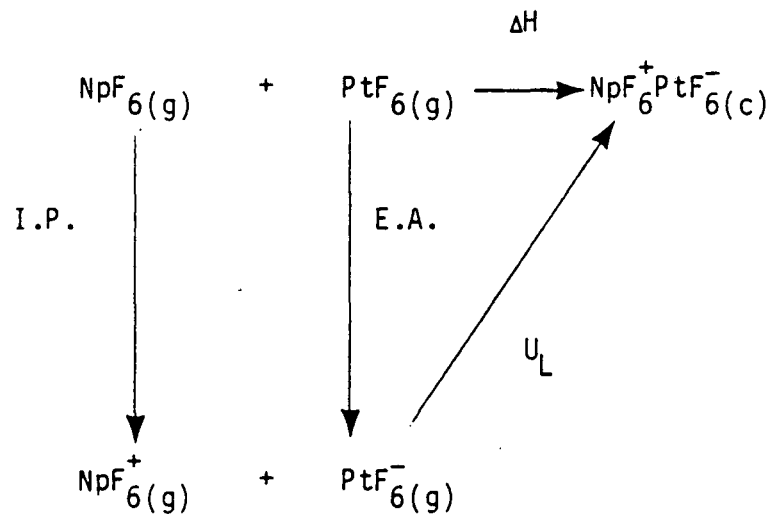

where $\Delta H = I.P. - E.A. - U_L$

and ΔH: heat of reaction

I. P.: ionization potential of NpF_6

E. A.: electron affinity of PtF_6 = 187 Kcal $mole^{-1}$ (17)

U_L: lattice energy of $NpF_6^+PtF_6^-$ = 126 Kcal $mole^{-1}$ (see Chapter 4)

the formation of $NpF_6^+PtF_6^-$ would be spontaneous only if the ΔH is more exothermal than $T\Delta S$ of the reaction. Estimates of the latter

or an analogous system (see Chapter 4) indicate that ΔH would have to be more exthormic than -23 kcal $mole^{-1}$. The failure of the oxidation therefore indicates that:

$$I.P.-E.A. - U_L \geq -23 \text{ kcal mole}^{-1}$$

This sets the lower limit of the ionization potential of NpF_6 at 291 kcal $mole^{-1}$.

Since KrF^+ appears to be able to oxidize NpF_6, as observed in the decolorization of NpF_6 when it interacts with $KrF^+Sb_2F_{11}^-$ and in the decomposition of $KrF^+PtF_6^-$ at the presence of NpF_6, it is possible that the first step of the reaction involves electron transfer with NpF_6^+ existing at least transitiently. However, the anions (PtF_6^- and $Sb_2F_{11}^-$) appear to be unable to stablize the NpF_6^+ ion. Yet the HF solution is colorless, hence it is possible that the NpF_6^+ abstract F^- to generate a solution species NpF_7. The high ionization potential we have estimated for NpF_6 would be consistent with very low basicity on the part of NpF_7.

REFERENCES

1. V. I. Spitsyn, A. D. Gelman, N. N. Krot, M. P. Mefodiyeva, F. A. Zakharova, Yu. A. Komkov, V. P. Shilov, and I. V. Smirhoma, J. Inorg. Nucl. Chem., 31 2733 (1969).
2. C. Keller and H. Seiffert, Inorg. Nucl. Chem. letters, 5 51 (1969).
3. S. K. Awasthi, L. Martinot, J. Fuger, and G. Duyckaerts, Inorg. Nucl. Chem. letters, 7 145 (1971).
4. F. Trotman - Deckenson ed., "Comprehensive Inorganic Chemistry" vol. 5, Pergamon, Oxford, 1973.
5. J. H. Burns, W. S. Baldwin, and J. R. Stokely, Inorg. Chem., 12 466 (1973).
6. R. D. Peacock and N. Edelstein, J. Inorg. Nucl. Chem., 38 771 (1976).
7. Yu. Y. Drobyshevskii, V. F. Serik and V. B. Sokolov, Dakl. Acad. Nauk. SSSR., 225 1079 (1975)
8. Yu. Y. Drobyshevskii, V. F. Serik and V. B. Sokolov and M. V. Tulskii, Radiokhimiya, 20 238 (1978).
9. R. J. Gillespie and G. J. Schrobilgen, J. Chem. Soc. Chem. Comm. 90 (1974).
10. R. J. Gillespie and G. J. Schrobilgen, Inorg. Chem., 13 1230 (1974).
11. V. B.Sokolov, V. N. Prusakov, A. V. Ryzhkov, Yu. Y Drobyshevskii and S. S. Khoroshev, Dakl. Akad. Nauk. SSSR, 229 884 (1976)
12. N. Bartlett and K. Zuchner, 7the European Symposium on fluorine chemistry. 1980.
13. K. O. Christe, W. W. Wilson, and E. C. Curtis, Inorg. Chem., 22 3056 (1983).

14. K. O. Christe, C. J. Schack, and D. Pilipovich, Inorg. Chem., 11 2205 (1972).

15. F. O. Roberto, Inorg. Nucl. Chem. letters, 8 737 (1972).

16. K. O. Christe, Inorg. Nucl. Chem. letters, 8 741 (1972).

17. M. I. Nikitin, L. N. Sidorov and M. V. Korobov, Int. J. Mass. Spectr. Ion Phys., 37 13 (1981).

Table Content

Table I

Raman vibrational bands asssignment for

$BrF_6^+AuF_6^-$ in BrF_5 solution, in sapphire tube.

Frequencies (cm^{-1})	Assignment	Note
658	$\nu_1(BrF_6^+)$	polarized
598	$\nu_1(AuF_6^-)$	polarized
405	$\nu_5(BrF_6^+)$	-
238	$\nu_5(AuF_6^-)$	-
218		

Figure Captions

Fig. 1. Raman spectrum of $BrF_6^+AuF_6^-$ in BrF_5 solution, in sapphire tube.

Fig. 2. Raman spectrum of $ClF_4^+AuF_6^-$, in quartz capillary.

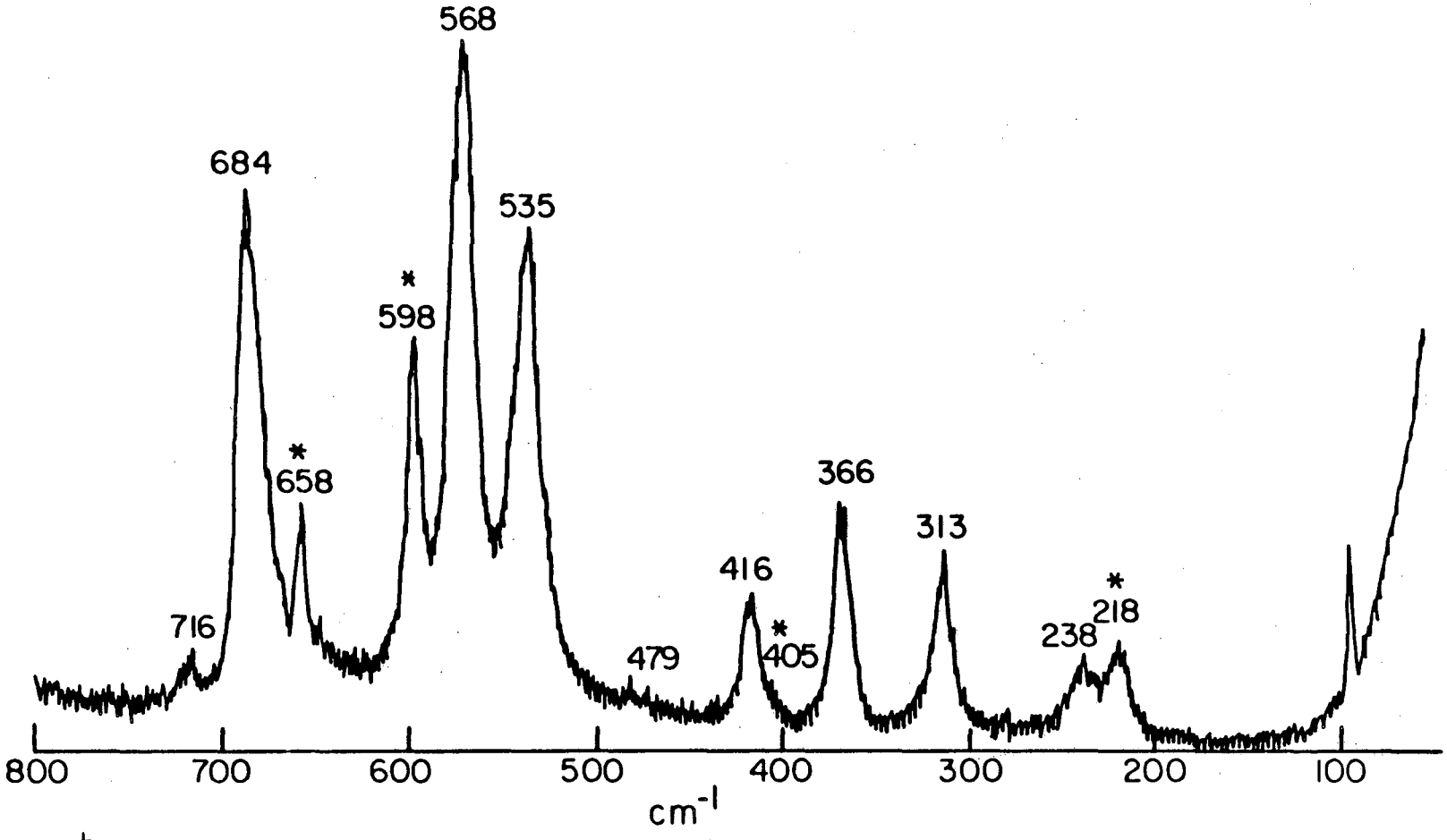
568
684
535
*
598
*
658
366
313
416
*
405
*
218
238
716
479
800
700
600
500
400
300
200
100
cm-1
*BrF6+AuF6- bands
XBL 818-6365

Fig. 1

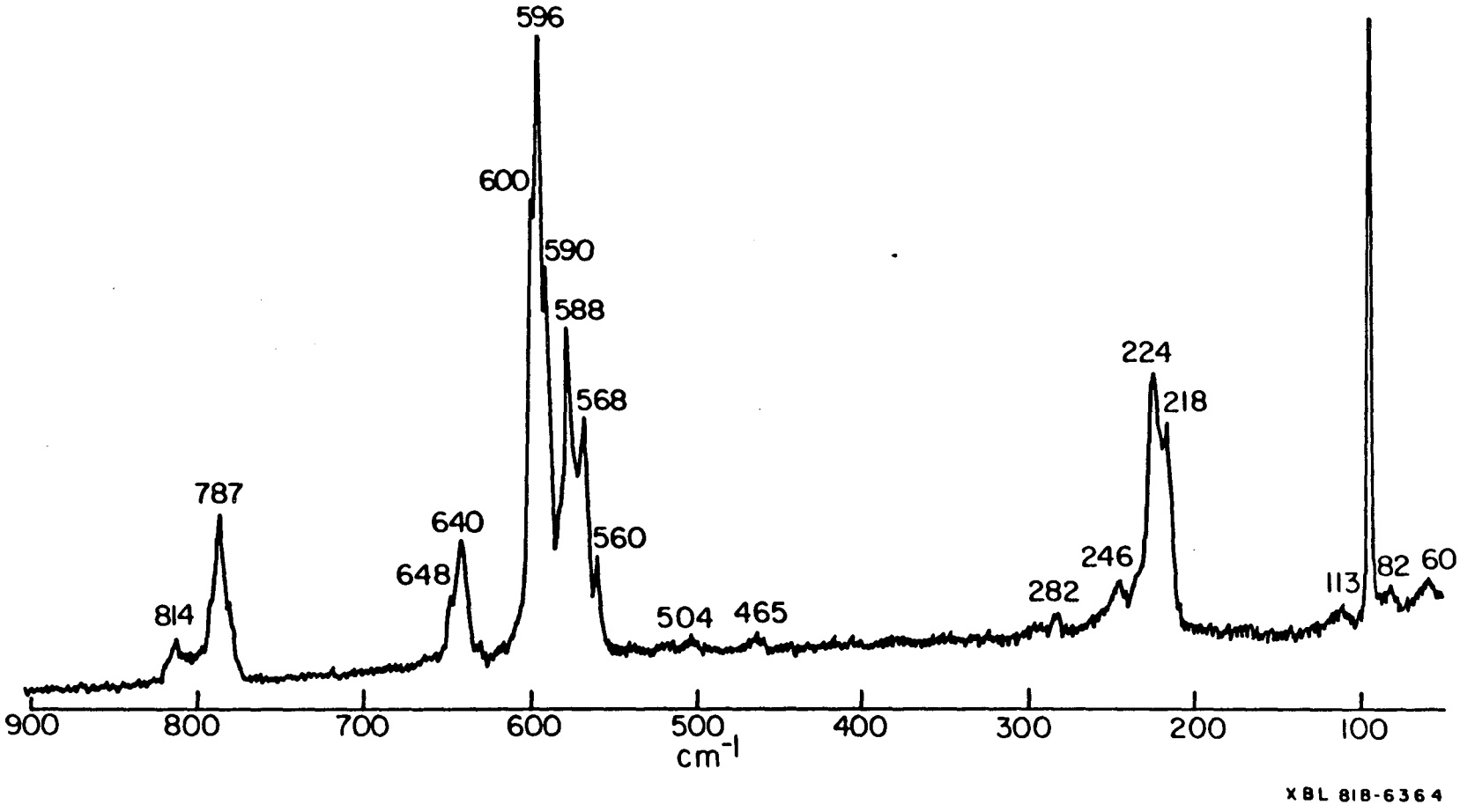
596
600
590
588
568
560
640
648
787
814
504
465
224
218
246
282
113
82
60
900
800
700
600
500
400
300
200
100
cm-1
XBL 818-6364

Fig. 2

ACKNOWLEDGEMENT

To Professor Neil Bartlett I offer my most sincere thanks and gratitude. He led me into the most interesting field of synthetic chemistry and guided me through my graduate years with warmth, patience and kindness. He has been the source of countless fresh ideas and inspiration and encouragement. My appreciation to him is beyond my description.

I am also grateful to Professor Tom O'Donnell for introducing me to vacuum line techniques; to Dr. Rodney Bank from whom I learned to handle radioactive materials; to Dr. Tom Mallouk for his help in thermochemical energy evaluations; to Dr. Klaus Zuchner, Dr. Bernard Desbat and Dr. Tom Richardson for their help and contributions to the various parts of this work.

I have been fortunate in being associated with the group of people in Professor Bartlett's laboratory. My thanks go to Tom Richardson, Lionell Graham, Rich Biagioni, Fran Tanzella, Barry McQuillan, Gene McCarron, Tom Mallouk, Guy Rosenthal, Fujio Okino and Ray Brusasco. Their warm friendship make me feel at home in the laboratory.

Finally, I thank my parents and my wife Julie, for their understanding, patience and support in every aspect, and thanks particularly to Julie, for sharing the highs and lows with me all these years.

This work was supported by U. S. Department of Energy under Contract No. DE-AC03-76SF00098.

This report was done with support from the Department of Energy. Any conclusions or opinions expressed in this report represent solely those of the author(s) and not necessarily those of The Regents of the University of California, the Lawrence Berkeley Laboratory or the Department of Energy.

Reference to a company or product name does not imply approval or recommendation of the product by the University of California or the U.S. Department of Energy to the exclusion of others that may be suitable.

TECHNICAL INFORMATION DEPARTMENT
LAWRENCE BERKELEY LABORATORY
UNIVERSITY OF CALIFORNIA
BERKELEY, CALIFORNIA 94720